GEOLOGICAL SURVEY OF DENMARK AND GREENLAND BULLETIN 13 • 2007

Review of Survey activities 2006

Edited by
Martin Sønderholm and A.K. Higgins

GEOLOGICAL SURVEY OF DENMARK AND GREENLAND
DANISH MINISTRY OF THE ENVIRONMENT

Geological Survey of Denmark and Greenland Bulletin 13

Keywords
Geological Survey of Denmark and Greenland, survey organisations, current research, Denmark, Greenland.

Cover photographs from left to right

1. Study of potentially gold-bearing Archaean supracrustal rocks south-west of the Isua supracrustal belt, southern West Greenland. Photo: Adam A. Garde.
2. Detailed surveying of the coastal zone is an important task during construction of e.g. harbours, bridges and man-made beach resorts. Photo: Merete Binderup.
3. Drilling of the ENRECA-2 well on the Vietnamese island of Phu Quoc. The well encountered a 500 m thick Lower Cretaceous fluvial sandstone unit that is widely distributed in the area including onshore Cambodia. The formation constitutes a potential reservoir for hydrocarbon and freshwater in the area. Photo: Lars Henrik Nielsen.
4. Mapping of hydraulic fractures induced for enhanced treatment of contaminated soil at the Kluzcewo Airport in Poland. The activities were carried out in connection with the FP6 project STRESOIL sponsored by the EU. Photo: Tomasz Kasela.

Frontispiece: facing page
Study of oil seeps in basalts on the south-western shores of Nuussuaq, West Greenland during an excursion in 2004. Petroleum exploration offshore West Greenland is now going into a new phase after the licensing rounds in 2006 and 2007 where seven new licences were awarded. Photo: Martin Sønderholm.

Printers: Schultz Grafisk, Albertslund, Denmark
Manuscripts submitted: 2–19 February 2007
Final versions approved: 14 August 2007
Printed: 12 October 2007

ISSN 1603-9769 (Review of Survey activities)
ISSN 1604-8156 (Geological Survey of Denmark and Greenland Bulletin)
ISBN 978-87-7871-202-8

Available from

Geological Survey of Denmark and Greenland (GEUS), Øster Voldgade 10, DK-1350 Copenhagen K, Denmark
Phone: +45 38 14 20 00, fax: +45 38 14 20 50, e-mail: geus@geus.dk

or

Geografforlaget ApS, Filosofgangen 24,1., DK-5000 Odense C, Denmark
Phone: +45 63 44 16 83, fax: +45 63 44 16 97, e-mail: go@geografforlaget.dk

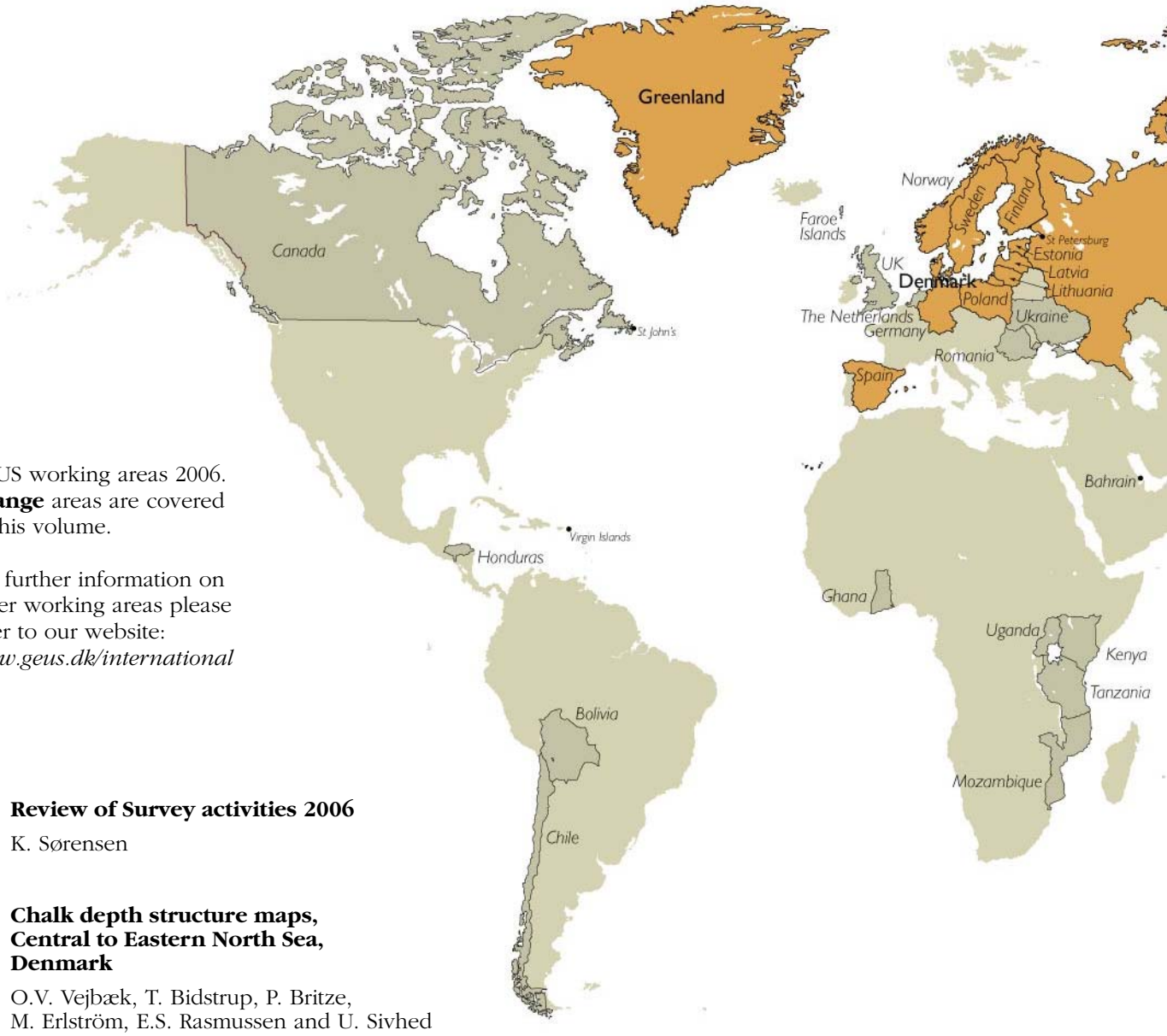

GEUS working areas 2006. **Orange** areas are covered in this volume.

For further information on other working areas please refer to our website: *www.geus.dk/international*

33. **A multi-disciplinary study of Phanerozoic landscape development in West Greenland**

J.M. Bonow, P. Japsen, P.F. Green, R.W. Wilson, J.A. Chalmers, K.E.S. Klint, J.A.M. van Gool, K. Lidmar-Bergström and A.K. Pedersen

37. **Pre-metamorphic hydrothermal alteration with gold in a mid-Archaean island arc, Godthåbsfjord, West Greenland**

A.A. Garde, H. Stendal and B.M. Stensgaard

41. **Gold-hosting supracrustal rocks on Storø, southern West Greenland: lithologies and geological environment**

C. Knudsen, J.A.M. van Gool, C. Østergaard, J.A. Hollis, M. Rink-Jørgensen, M. Persson and K. Szilas

45. ***P–T* history of kimberlite-hosted garnet lherzolites from South-West Greenland**

M.T. Hutchison, L.J. Nielsen and S. Bernstein

49. **Two tectonically significant enclaves in the Nordre Strømfjord shear zone at Ataneq, central West Greenland**

W.E. Glassley, J.A. Korstgård and K. Sørensen

53. **A well-preserved bimodal Archaean volcanic succession in the Tasiusarsuaq terrane, South-West Greenland**

H. Stendal and A. Scherstén

57. **Seismic hazard assessment of Greenland**

P. Voss, S.K. Poulsen, S.B. Simonsen and S. Gregersen

61. **Development of marine landscape maps for the Baltic Sea and the Kattegat using geophysical and hydrographical parameters**

Z.K. Al-Hamdani, J. Reker, J.O. Leth, A. Reijonen, A.T. Kotilainen and G.E. Dinesen

65. **Shallow groundwater quality in Latvia and Denmark**

E. Gosk, I. Levins and L.F. Jørgensen

69. **Bayesian belief networks as a tool for participatory integrated assessment and adaptive groundwater management: the Upper Guadiana Basin, Spain**

H.J. Henriksen, P. Rasmussen, J. Bromley, A. de la Hera Portillo and M.R. Llamas

73. **Cenozoic evolution of the Vietnamese coastal margin**

M.B.W. Fyhn, L.H. Nielsen and L.O. Boldreel

Review of Survey activities 2006

Kai Sørensen
Director

The Geological Survey of Denmark and Greenland (GEUS) has lived through a period of intense unrest during most of 2006. This was a consequence of the decision by the Danish Government in 2005 to carry out a major reorganisation of the Danish research world. The aim was to improve the quality and competitiveness of Danish universities and research organisations (such as GEUS), by means of a fusion of universities and the merging of independent research institutions with the universities. At the conclusion of this process all but three of the major government research institutions were merged with the universities in Århus and Copenhagen, and the Technical University in Lyngby. For many reasons, one being the special tasks that GEUS is responsible for in Greenland, the Government decided that GEUS should continue as one of these three independent national research institutions.

This issue of Review of Survey activities (RoSa) is the fourth published after it was decided to publish an annual research overview illustrating the activities of GEUS in Denmark, Greenland and other countries building on a long-standing tradition of a Greenland review publication. Although only approximately a third of our institution's turnover is related to Greenland, no less than 34 papers out of the 73 published in the four issues of RoSa (including this one) relate to Greenland activities. Greenland thus continues to be a potent measure of scientific productivity at GEUS, and it is deeply satisfying to acknowledge the dedication to the geology of Greenland as one of the major factors that helped secure the independence of the Survey.

Although this issue of Review of Survey activities presents 17 papers providing a panorama of the current research carried out at GEUS, it illustrates only a small part of the wide range of projects undertaken in Denmark and Greenland and other countries in 2006. A factual overview of the activities of GEUS as a whole can be seen on the GEUS website.

In the present volume, three papers deal with various aspects of petroleum exploration in the Danish part of the North Sea. One of these papers links exploration for deep groundwater aquifers onshore Denmark with offshore petroleum exploration. Another paper from Denmark is devoted to recent environmental changes during the Roman Warm Period.

In Greenland, exploration activities for both minerals and petroleum have reached unprecedented highs during 2006. This is reflected by the nine papers dealing with projects related to Greenland. Three papers are concerned with petroleum geological matters; two of these are a result of seismic and provenance studies carried out by GEUS for the Government of Greenland in preparation for the Disko West 2006 Licensing Round. The third paper presents a combination of landscape and fission track analysis to elucidate the Cenozoic uplift of the West Greenland margin. Five papers are related to various aspects of mineral exploration, focussing on gold (two papers), diamonds (one paper) and general mapping of Proterozoic and Archaean primary geological environments with special emphasis on tectonic and mineralising events (two papers). The last article on Greenland deals with seismic hazard assessment, a discipline carried out at GEUS since the incorporation of the seismological service for Denmark and Greenland in 2004.

GEUS is also involved in a wide range of activities outside its core working areas in Denmark and Greenland that are well illustrated by the four last papers in this review. Three papers are related to national implementation of European legislation, such as the Water Framework Directive. The first paper documents a circum-Baltic project on the development of marine landscape maps, and the two following papers deal with various aspects of groundwater management. One of these is related to the establishment of a groundwater monitoring programme in Latvia, while the other deals with stakeholder participation in adaptive and integrated water resource management in Spain. The last paper on the Cenozoic evolution of the Vietnamese offshore region illustrates how the Survey's broad technical expertise has been put to use in developing countries.

Chalk depth structure maps, Central to Eastern North Sea, Denmark

Ole V. Vejbæk, Torben Bidstrup, Peter Britze, Mikael Erlström, Erik S. Rasmussen and Ulf Sivhed

The Upper Cretaceous – Danian chalk may be considered to be the economically most important rock type in Denmark. Onshore it constitutes an important groundwater aquifer and it is also quarried for e.g. building materials and paper production. Offshore the chalk reservoirs contain more than 80% of the oil and gas produced in Denmark (Fig. 1).

During the last few years efforts have therefore been made to map this important succession in the Danish and adjoining areas (Vejbæk *et al*. 2003). The stratigraphic interval mapped comprises the Chalk Group of Cenomanian to Danian ages and its stratigraphically equivalent units (Fig. 2). The north-eastern limit of the Chalk Group is determined by Neogene erosion. The limits of the map to the west and south were mainly determined by the amount of available data.

Data base

The comprehensive data base comprises high-resolution and conventional 2-D and 3-D reflection seismic data as well as published maps (e.g. Britze *et al*. 1995; Hommel 1996; Ottesen *et al*. 1997; Jensen 1998; Kramarskiej 1999; Baldschuhn *et al*. 2001; Stoker 2005). More than 500 deep wells and numerous onshore water wells have provided control for the mapping. This is especially relevant for the mapping where the Top Chalk is immediately overlain by the Neogene (Fig. 3). In these areas in particular, mapping was based on high-resolution seismic data.

Depth conversion

Depth conversion was undertaken by using depth-dependent velocity functions, where the velocity V at depth z is given by:

$$V = V_0 + dV + K \times z$$

where V_0 is the surface velocity, dV is a variation of the surface velocity and K is the gradient of velocity increase with depth (Table 1; e.g. Japsen 1998, 1999). The surface velocity variation is typically mapped on the basis of well data and may reflect lateral facies changes, burial anomalies or excess fluid pressures.

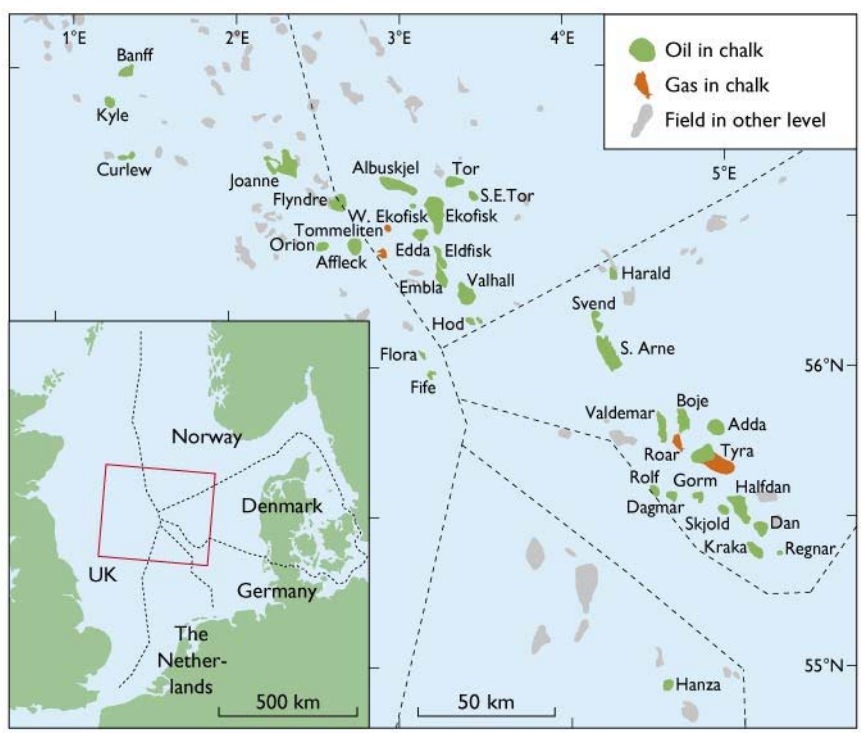

Fig. 1. Hydrocarbon accumulations in the North Sea with chalk fields highlighted.

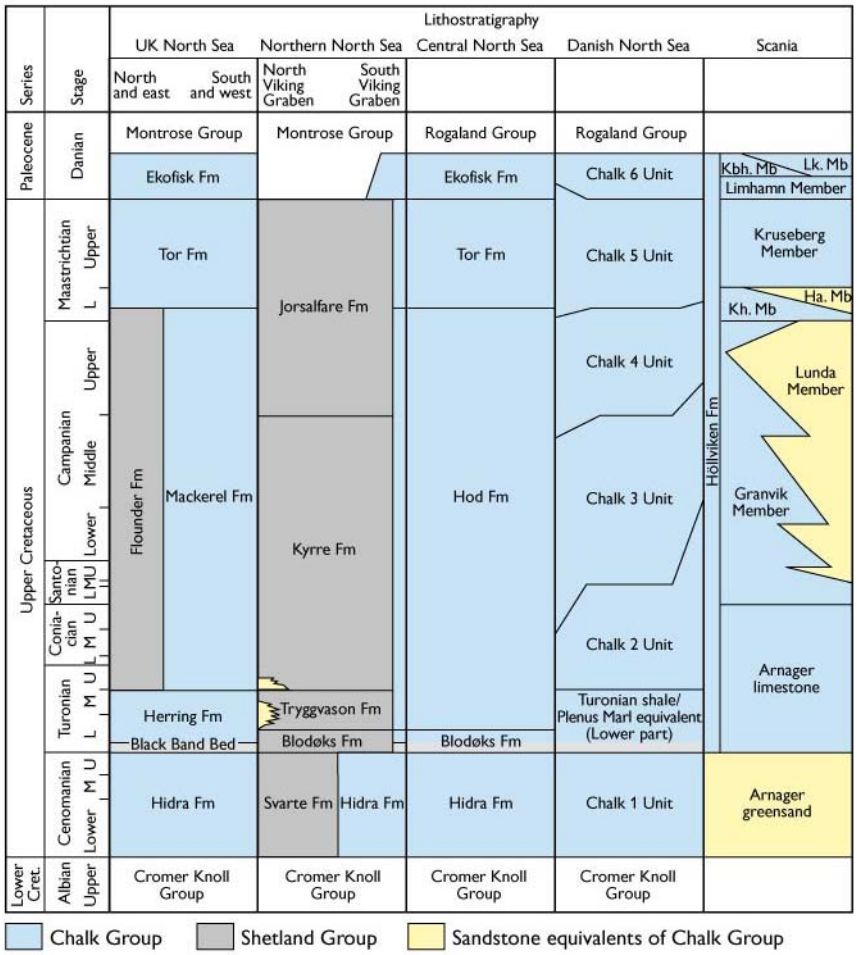

Fig. 2. Lithostratigraphic correlation for the Upper Cretaceous – Danian succession as mapped in this paper. Based on Deegan & Scull (1977), Isaksen & Tonstad (1989), Johnson & Lott (1993) and Schiøler *et al.* (2007) with additions modified from Surlyk *et al.* (2003) and Sivhed *et al.* (1999).
Ha. Mb, Hansa Member;
Kbh. Mb, København Member;
Kh. Mb, Kyrkheddinge Member;
Lk. Mb, Landskrona Member.

Notes about the maps

In some areas where the Neogene lies directly on the Top Chalk seismic horizon, the erosional truncation of the Chalk Group is negligible. This occurs around Copenhagen, in northern Sjælland and in south-western Scania, where minor outliers of Selandian deposits document the former extent of the Chalk Group. The occurrence of Palaeogene sediments offshore Poland also indicates that erosion of the Chalk Group is generally not very deep in the western Baltic outside the main inversion zones (Fig. 3).

In Norwegian waters, however, extensive Neogene erosion has occurred. The erosion in these areas is sufficiently deep for Lower Cretaceous deposits to subcrop the base of the Neogene. Outside these areas the Chalk Group generally has a larger areal extent than the Lower Cretaceous. (Fig. 3).

A general increase in thickness of the Chalk Group is found west of the Sorgenfrei–Tornquist inversion zone. A north-eastward increase in thickness is also found in the areas unaffected by Neogene erosion offshore southern Norway, suggesting the presence of similar depocentres on the flanks of inversion zones. Thus, inversion may also have occurred in the south-western coastal areas of Norway.

The Cenozoic velocity model consists of a single layer onshore Denmark and two layers offshore. The division between the two layers is taken at the 'near Top Middle Miocene marker' that corresponds approximately to the top of the over-pressured section (Upper and Lower Post Chalk Group in Table 1). The parameters for these layers were taken from Britze *et al.* (1995) and Japsen (1999, 2000) who derived a similar but segmented model for the Chalk Group. Since the parameters are based on a large well data base from the entire North Sea (e.g. Japsen 2000), they are applicable to most of the North Sea.

Table 1. Parameters for depth conversion

Unit	V_0 (m/sec)	K (sec^{-1})	Source
Upper Post Chalk Group	1725	0.4	Britze *et al.* 1995
Lower Post Chalk Group	1517.2	0.6	Japsen *et al.* 1999
Chalk z < 900 m	1550	1.3	Japsen 2000
Chalk 900 m < z < 1471	920	2	Japsen 2000
Chalk 1471 m < z < 2250	1950	1.3	Japsen 2000
Chalk 2250 m < z < 2875	2625	1	Japsen 2000

Facing page:
Fig. 3. Simplified structure maps of the Chalk Group and equivalent deposits. **A**, depth to top Chalk Group; **B**, depth to base Chalk Group and **C**, isopach. Grey shadings in A and C indicate where the Lower Cretaceous subcrops Quaternary sediments (i.e. where the Chalk Group has been totally removed by erosion). **Cph**, Copenhagen. PDF versions of the maps with more detail are available from *www.geus.dk/publications/bull/nr13/index-uk.htm*

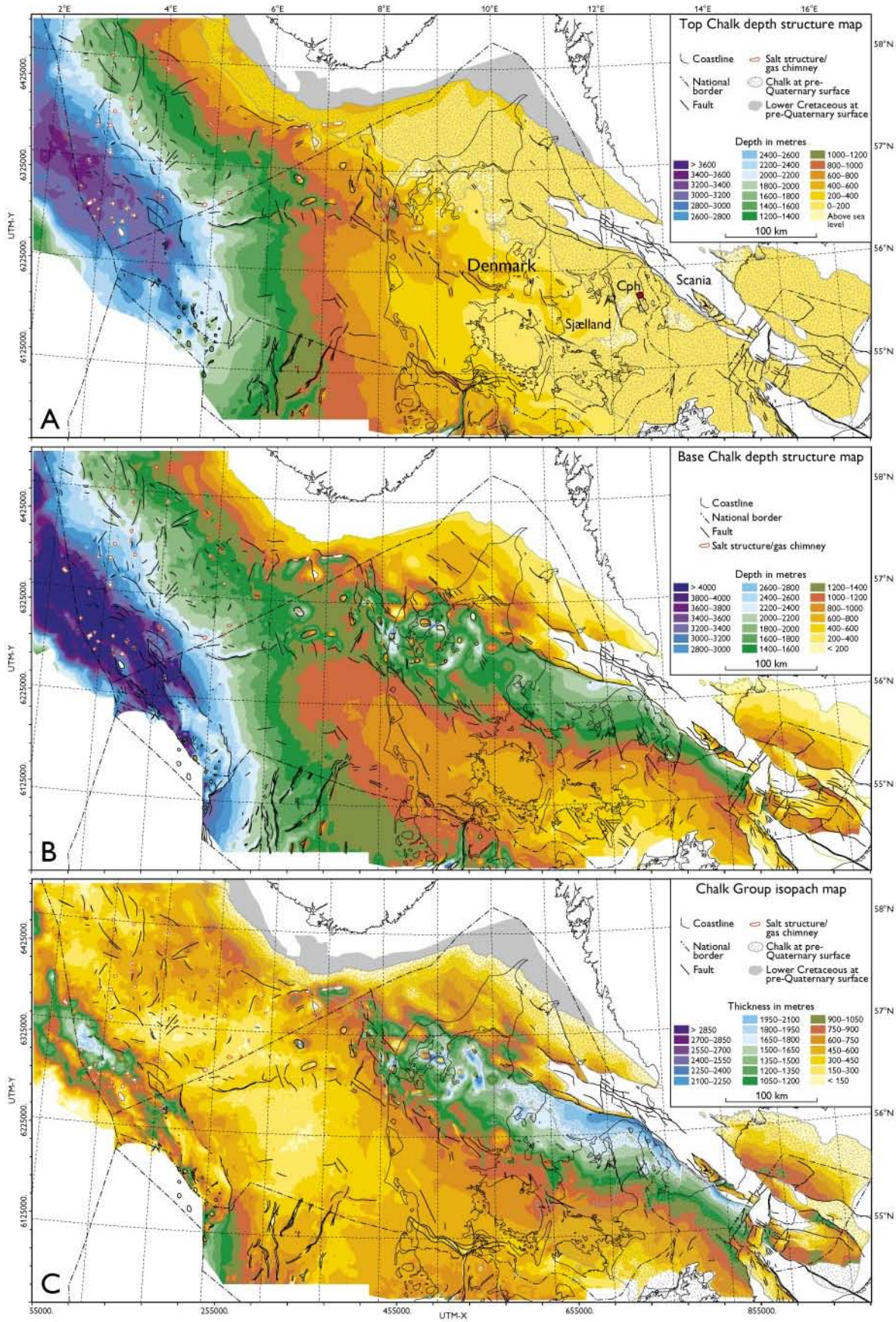
Top Chalk depth structure map
Coastline
National border
Fault
Salt structure/ gas chimney
Chalk at pre-Quaternary surface
Lower Cretaceous at pre-Quaternary surface
Depth in metres
> 3600
3400–3600
3200–3400
3000–3200
2800–3000
2600–2800
2400–2600
2200–2400
2000–2200
1800–2000
1600–1800
1400–1600
1200–1400
1000–1200
800–1000
600–800
400–600
200–400
0–200
Above sea level
100 km
Denmark
Cph
Scania
Sjælland
A
Base Chalk depth structure map
Coastline
National border
Fault
Salt structure/gas chimney
Depth in metres
> 4000
3800–4000
3600–3800
3400–3600
3200–3400
3000–3200
2800–3000
2600–2800
2400–2600
2200–2400
2000–2200
1800–2000
1600–1800
1400–1600
1200–1400
1000–1200
800–1000
600–800
400–600
200–400
< 200
100 km
B
Chalk Group isopach map
Coastline
National border
Fault
Salt structure/ gas chimney
Chalk at pre-Quaternary surface
Lower Cretaceous at pre-Quaternary surface
Thickness in metres
> 2850
2700–2850
2550–2700
2400–2550
2250–2400
2100–2250
1950–2100
1800–1950
1650–1800
1500–1650
1350–1500
1200–1350
1050–1200
900–1050
750–900
600–750
450–600
300–450
150–300
< 150
100 km
C
58°N
57°N
56°N
55°N
2°E
4°E
6°E
8°E
10°E
12°E
14°E
16°E
6425000.
6325000.
6225000.
6125000.
UTM-Y
55000.
255000.
455000.
655000.
855000.
UTM-X

Hydrocarbon aspects

The Chalk Group in the Central Graben area is an important reservoir and migration path for oil and gas. It is the most important oil-producing interval in Denmark and is also a major contributor to oil and gas production in Norway and the Netherlands, while production from the Chalk Group is still insignificant in the UK sector (Fig. 1). Traps within the Chalk Group range from inversion-generated anticlines (e.g. the Valhall, Roar, Tyra and South Arne fields), over salt domes with some degree of inversion overprint (e.g. the Dan, Ekofisk and Svend fields) to salt diapirs (e.g. the Skjold and Harald fields). Stratigraphic traps may also play a major role (e.g. the Halfdan and Adda fields). These traps owe their existence to a combination of over-pressuring and early hydrocarbon invasion to preserve the quality of their reservoirs despite the great depths to which they have been buried (e.g. Anderson 1999; Vejbæk in press). Their position directly above the main Upper Jurassic source rock also seems to be a necessary condition for their existence (e.g. Anderson 1999; Surlyk *et al.* 2003), since the generally very low permeability of the chalk precludes long-distance migration and even keeps accumulations in hydrodynamic dis-equilibrium (e.g. Dennis *et al.* 2005; Vejbæk *et al.* 2005).

References

Anderson, J.K. 1999: The capabilities and challenges of the seismic method in chalk exploration. In: Fleet, A.J. & Boldy, S.A.R. (eds): Petroleum geology of Northwest Europe. Proceedings of the 5th conference, 939–947. London: Geological Society.

Baldschuhn, R., Binot, F., Fleig, S. & Kockel, F. 2001: Geotektonischer Atlas von Nordwest-Deutschland und dem deutschen Nordsee-Sektor. Geologisches Jahrbuch Reihe A **153**, 88 pp. + 3 CD-ROMs.

Britze, P., Japsen, P. & Andersen, C. 1995: The Danish Central Graben: Top Chalk and the Post Chalk Group. Two-way travel time and depth and interval velocity, 1:200 000. Geological Survey of Denmark Map Series **47**, 5 pp. + 3 maps.

Deegan, C.E. & Scull, B.J. 1977: A proposed standard lithostratigraphic nomenclature for the Central and Northern North Sea. Report of the Institute of Geological Sciences **77/25**, 35 pp. (also published as Norwegian Petroleum Directorate Bulletin **1**).

Dennis, H., Bergmo, P. & Holt, T. 2005: Tilted oil-water contacts: modelling effects of aquifer heterogeneity. In: Doré, A.G. & Vining, B.A. (eds): Petroleum geology: North-West Europe and global perspectives. Proceedings of the 6th petroleum geology conference, 145–158. London: Geological Society.

Hommel, V. 1996: Structural evolution of the Rønne–Kolobrzeg Graben area. Unpublished M.Sc. thesis, 82 pp. University of Copenhagen, Denmark.

Isaksen, D. & Tonstad, V. 1989: A revised Cretaceous and Tertiary lithostratigraphic nomenclature for the Norwegian North Sea. Norwegian Petroleum Directorate Bulletin **5**, 59 pp.

Japsen, P. 1998: Regional velocity-depth anomalies, North Sea Chalk; a record of overpressure and Neogene uplift and erosion. American Association of Petroleum Geologists Bulletin **82**, 2031–2074.

Japsen, P. 1999: Overpressured Cenozoic shale mapped from velocity anomalies relative to a baseline for marine shale, North Sea. Petroleum Geoscience **5**, 321–336.

Japsen, P. 2000: Fra kridthav til Vesterhav, Nordsøbassinets udvikling vurderet ud fra seismiske hastigheder. Geologisk Tidskrift **2002/2**, 36 pp.

Jensen, S.K. 1998: Structural development of the Sorgenfrei–Tornquist Zone and adjacent areas, Norwegian North Sea Sector. Unpublished M.Sc. thesis, 88 pp. University of Aarhus, Denmark.

Johnson, H. & Lott, G.K. 1993: Cretaceous of the Central and Northern North Sea. In: Knox, R.W. O'B. & Cordey, W.G. (eds): Lithostratigraphic nomenclature of the UK North Sea, **2**, 169 pp. Nottingham: British Geological Survey.

Kramarskiej, R. (ed.) 1999: Geological map of the Baltic Sea bottom without Quaternary deposits, 1: 500 000. Gdansk-Warszawa: Panstwowy Instytut Geologiczny.

Ottesen, D., Bøe, R., Longva, O., Olsen, H. A., Rise, L., Skilbrei, J. R. & Thorsnes, T. 1997: Geologisk atlas – Skagerrak. Atlas over kvartære avleiringer, bunnsedimenter, berggrunn og batymetri i norsk sektor av Skagerrak. Norges Geologiske Undersøkelse Rapport **96.138**, 55 pp.

Schiøler, P. *et al.* 2007: Lithostratigraphy of the Palaeogene – Lower Neogene succession of the Danish North Sea. Geological Survey of Denmark and Greenland Bulletin **12**, 77 pp.

Sivhed, U., Wikman, H. & Erlström, M. 1999: Beskrivning till berggrundskartorna 1C Trelleborg NV och SO samt 2C Malmö SV, SO, NV och NO. (SGU Serie Af 191, 192, 193, 194, 196, 198, skala 1:50 000). Uppsala: Sveriges Geologiska Undersökning, 143 pp.

Stoker, S. 2005: Chalk play of the UK Central Graben, 11 pp. Department of Trade and Industry Workshop, Aberdeen, 23 November, 2005. Poster (available on: http://www.og-mrp.com/dissemination/workshops/ukcs/Posters/UKCS_Chalk_Play_BGS.pdf).

Surlyk, F., Dons, T., Clausen, C.K. & Higham, J. 2003: Upper Cretaceous. In: Evans, D. *et al.* (eds.): The millennium atlas: petroleum geology of the central and northern North Sea, 213–233. London: Geological Society.

Vejbæk, O. in press: On dis-equilibirium compaction as the cause for the Cretaceous–Paleogene over-pressures in the Danish North Sea. American Association of Petroleum Geologists Bulletin.

Vejbæk, O.V., Bidstrup, T., Britze, P., Erlström, M., Rasmussen, E.S. & Sivhed, U. 2003: Chalk structure maps of the Central and Eastern North Sea. Danmarks og Grønlands Geologiske Undersøgelse Rapport **2003/106**, 55 pp.

Vejbæk, O.V., Frykman, P., Bech, N. & Nielsen, C.M. 2005: The history of hydrocarbon filling of Danish Chalk field. In: Doré, A.G. & Vining, B.A. (eds): Petroleum geology: North-West Europe and global perspectives. Proceedings of the 6th petroleum geology conference, 1331–1346. London: Geological Society.

Authors' addresses

O.V.V., T.B., P.B. & E.S.R., *Geological Survey of Denmark and Greenland, Øster Voldgade 10, DK-1350 Copenhagen K, Denmark*. E-mail: *ov@geus.dk*

M.E. & U.S., *Sveriges Geologiska Undersökning, Kiliansgatan 10, S-223 50, Lund, Sweden*.

Are Carboniferous coals from the Danish North Sea oil-prone?

Henrik I. Petersen and Hans P. Nytoft

The Central Graben in the North Sea is a mature petroleum province with Upper Jurassic – lowermost Cretaceous marine shale of the Kimmeridge Clay Formation and equivalents as the principal source rock, and Upper Cretaceous chalk as the main reservoirs. However, increasing oil prices and developments in drilling technologies have made deeper plays depending on older source rocks increasingly attractive. In recent years exploration activities have therefore also been directed towards deeper clastic plays where Palaeozoic deposits may act as petroleum source rocks. Carboniferous coaly sections are the most obvious source rock candidates. The gasfields of the major gas province in the southern North Sea and North-West Europe are sourced from the thick Upper Carboniferous Coal Measures, which contain hundreds of coal seams (Drozdzewski 1993; Lokhorst 1998; Gautier 2003). North of the gas province Upper Carboni-ferous coal-bearing strata occur onshore in northern England and in Scotland, but offshore in the North Sea area they have been removed by

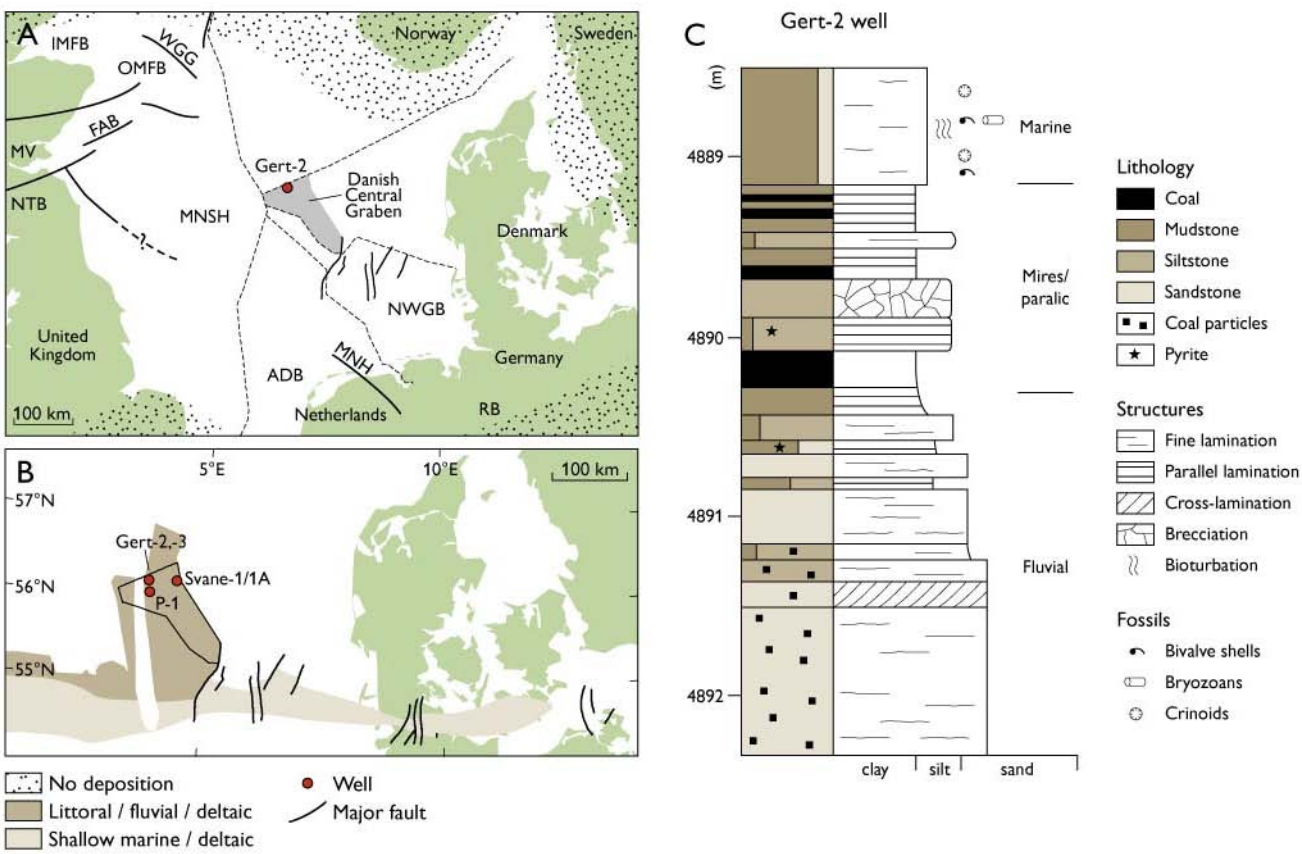

Fig. 1. **A**: Simplified map showing Carboniferous basins in the North Sea area. The Danish Central Graben is also shown (grey area). **ADB**, Anglo-Dutch Basin; **FAB**, Forth Approaches Basin; **IMFB**, Inner Moray Firth Basin; **MNH**, Mid Netherlands High; **MNSH**, Mid North Sea High; **MV**, Midland Vally; **NTB**, Northumberland/Tweed Basin; **NWGB**, North-west German Basin; **OMFB**, Outer Moray Firth Basin; **RB**, Ruhr Basin; **WGG**, Witch Ground Graben. Based on Ziegler (1990), Besly (1998) and Bruce & Stemmerik (2003). **B**: Present-day distribution of Lower Carboniferous littoral/fluvial/deltaic and shallow marine/deltaic deposits in the southern North Sea area. The positions of the Gert-2, Gert-3, P-1 and Svane-1 wells are shown. Modified from Lokhorst (1998). **C**: Sedimentological log of the coal-bearing interval of the Gert-2 well. The coaly interval is underlain by fluvial sediments and overlain by fossiliferous marine mudstones of the so-called Marine Unit. Slightly modified from Petersen & Nytoft (2007).

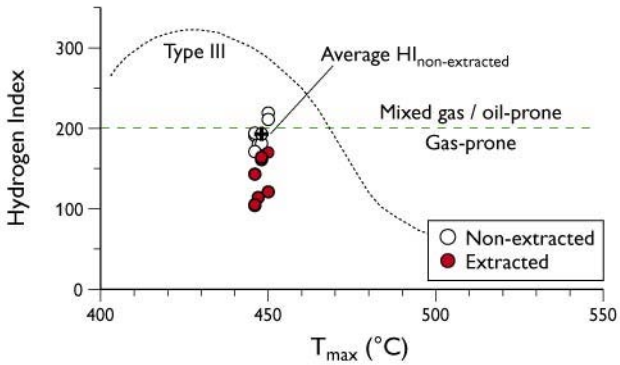

Fig. 2. Hydrogen Index versus T_{max} plot of non-extracted and solvent extracted coal samples from the Gert-2 well. The average Hydrogen Index of the non-extracted coals is also shown.

erosion. However, Lower Carboniferous strata are present offshore and have been drilled in the Witch Ground Graben and in the north-eastern part of the Forth Approaches Basin (Fig. 1A), where most of the Lower Carboniferous sediments are assigned to the sandstone/shale-dominated Tayport Formation and to the coal-bearing Firth Coal Formation (Bruce & Stemmerik 2003). Highly oil-prone Lower Carboniferous lacustrine oil shales occur onshore in the Midland Valley, Scotland, but they have only been drilled by a single well offshore and seem not to be regionally distributed (Parnell 1988).

In the southern part of the Norwegian and UK Central Graben and in the Danish Central Graben a total of only nine wells have encountered Lower Carboniferous strata, and while they may have a widespread occurrence (Fig. 1B; Bruce & Stemmerik 2003) their distribution is poorly constrained in this area. The nearly 6000 m deep Svane-1/1A well (Fig. 1B) in the Tail End Graben encountered gas and condensate at depths of 5400–5900 m, which based on carbon isotope values may have a Carboniferous source (Ohm *et al.* 2006). In the light of this the source rock potential of the Lower Carboniferous coals in the Gert-2 well (Fig. 1C) has recently been assessed (Petersen & Nytoft 2007).

Lower Carboniferous strata in the Danish Central Graben

In the Danish Central Graben, Lower Carboniferous strata were drilled by the Gert-2, Gert-3 and P-1 wells (Fig. 1B). The depth to the Lower Carboniferous ranges from 3289 m in the P-1 well to 4840 m in the Gert-2 well. Whereas the P-1 well reached Caledonian basement after penetrating about 67 m of Carboniferous sediments, the Gert-2 well drilled 192 m of Carboniferous strata before drilling terminated at about 5000 m depth within the Carboniferous. The drilled Carboniferous section in the Gert-2 well is principally non-marine (Fluvial Unit) and contains a coaly interval at about 4890 m (Fig. 1C) that constitutes a transition to marine shales and shoreface and tidally influenced sandstones of the Marine Unit (Petersen & Nytoft 2007). The coals overlie a fluvial fining-upward succession and are overlain by fossiliferous marine shales (Fig. 1C). The coals formed in peat-forming coastal plain mires as shown by high sulphur contents (average 5.3 wt%) and the presence of framboidal pyrite (Petersen & Nytoft 2007). High contents of vitrinite (65–82 vol.%), derived from degradation of higher land plant woody material, indicate waterlogged, oxygen-deficient conditions in the precursor mires. Although the proportion of more oil-prone liptinite constituents is generally small (4–8 vol.%), the paralic peat-forming conditions may be favourable for the oil generation potential of the resulting coals (Petersen 2006). This raises the question: are the coals encountered in the Gert-2 well oil- or gas-prone?

Source rock quality and hydrocarbon generation capacity

The average Tmax of the coals is 448°C, which corresponds to a vitrinite reflectance of ~0.95%R_o indicating that the coals are at the threshold of, or slightly within, the so-called 'effective oil window' (in which efficient oil expulsion occurs; Sykes 2001; Petersen 2006). In addition the Hydrogen Index (HI) values of the coals are very close to their HI_{max} values. During initial maturation the HI of coals increases to a maximum value, which is considered to be a better estimate of the generation potential of coal (Sykes & Snowdon 2002; Petersen 2006). Thus, at first glance HI values from 171–219 mg HC/g TOC may suggest some potential for liquid petroleum formation (Fig. 2). The type of generated petroleum is, however, determined by the paraffinicity of the organic matter, i.e. the proportion and length of hydrogen-bearing carbon chains (aliphatic chains) in the kerogen structure. The ability to generate and expel typical waxy terrestrial crude oil requires the presence of long-chain aliphatics with more than ~20–25 carbon atoms (Isaksen *et al.* 1998; Killops *et al.* 1998). Fourier transform infrared spectroscopy (FTIR) of the Gert-2 coals clearly reveals a response in the aliphatic stretching region, but the response can mainly be assigned to isolated CH_2 compounds, which are of no importance to the liquid petroleum generation potential (Petersen & Nytoft 2006). Quantification of the proportion of long-chain aliphatics in the kerogen structure of the Gert-2 coals by comprehensive chemical treatment (so-called ruthenium tetroxide catalysed oxidation; see Petersen & Nytoft 2006, 2007) demonstrates a negligible or extremely low amount of aliphatic chains with more than 18 carbon atoms. The dominance of shorter aliphatic chains strongly indicates that the coals are gas- and condensate-prone.

Carboniferous coals are inherently gas-prone

The above results are in line with the findings of Petersen & Nytoft (2006), who showed that Carboniferous coals in general contain very minor proportions of long-chain aliphatics in the range $C_{19–35}$ and are therefore inherently poorly suited to generate oil. Thus, for Carboniferous coals only an effective gas/condensate window exists.

Of the total amount of aliphatic chains in the range $C_{12–35}$, Carboniferous coals contain on average about 20% in the $C_{19–35}$ range (Fig. 3A). In contrast, Jurassic coals from the Søgne Basin in the North Sea contain about 26%, while Cenozoic coals contain on average as much as 55% (Fig. 3A). The significantly higher proportion of long-chain ali-phatics in the youngest coals seems to be related to the high amount of organic de-trital groundmass (Fig. 3B). The groundmass consists of detrital vitrinitic and liptinitic organic matter that can be positively correlated to the long-chain ali-phatics in the kerogen structure (Petersen & Nytoft 2006). The oil-proneness of the Cenozoic coals thus seems to be related to the evolution of more diversified plant communities, including the appearance of angiosperms in the Late Cretaceous.

Limited expulsion efficiency and implications for enhanced gas-proneness

In agreement with the kerogen structure the generated hydrocarbons from the Lower Carboniferous Gert-2 coals are dominated by shorter-chain aliphatics. These do not facilitate expulsion (Isaksen *et al.* 1998), and the generated hydrocarbons remain trapped in the coals. This is sustained by a pronounced difference in the HI of the non-extracted coals and the HI of the extracted coals: upon extraction the HI is on average reduced by 30% (Fig. 2; Petersen &

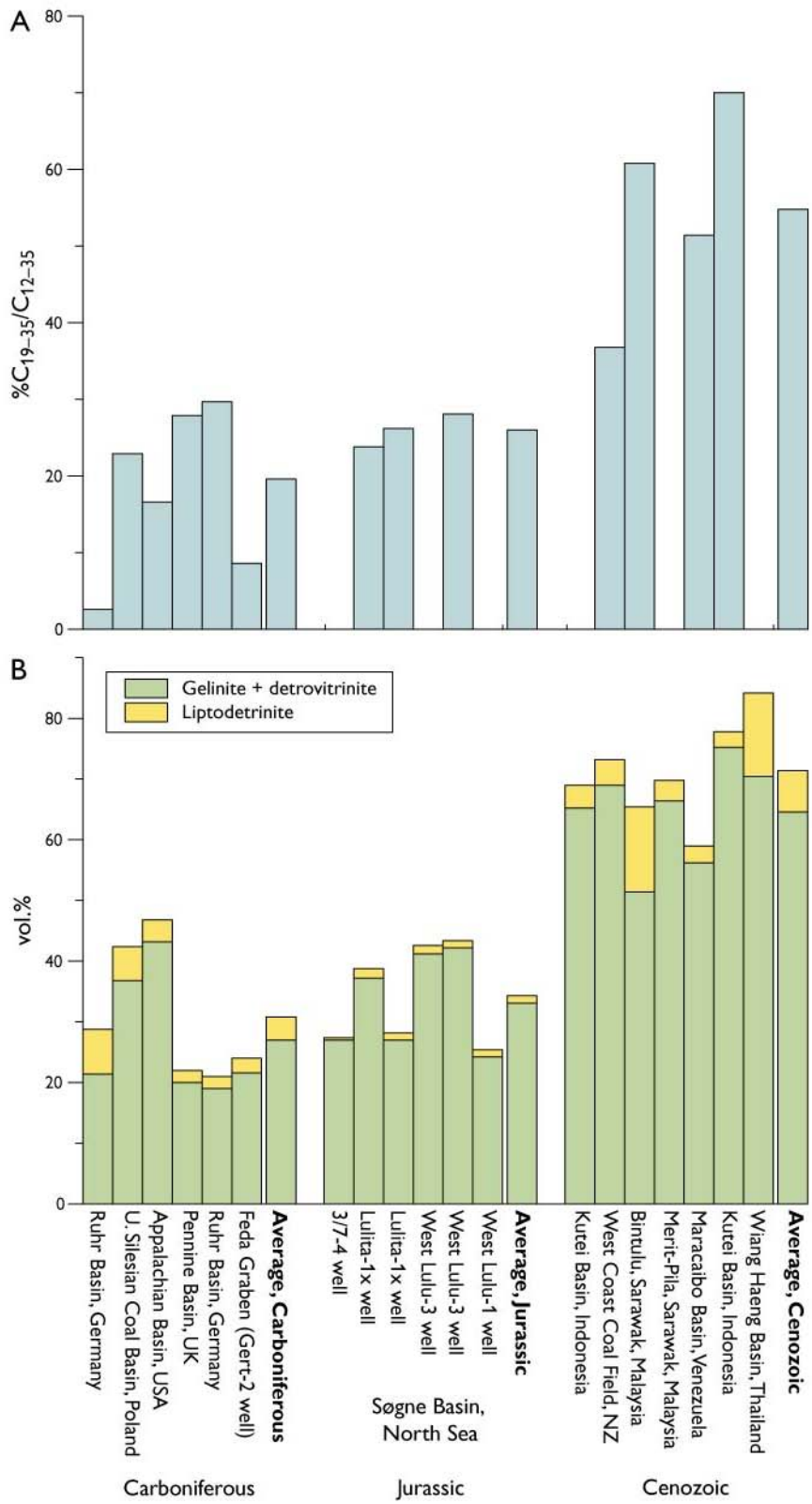

Fig. 3. **A**: The proportion (%) of $C_{19–35}$ long-chain aliphatics of the total amount of $C_{12–35}$ aliphatics in a number of Carboniferous, Jurassic and Cenozoic coals. **B**: The proportion (vol.%) of groundmass composed of detrital vitrinite and liptinite in a number of Carboniferous, Jurassic and Cenozoic coals.

Nytoft 2007). Hence, the measured HI values of the Gert-2 coals are strongly influenced by the trapped petroleum in the coals. The limited (or lack of) expulsion maintains a low saturate/aromatic hydrocarbon ratio of the trapped petroleum, which according to Pepper & Dodd (1995) is less thermally stable than expelled oil that is dominated by saturated (aliphatic) hydrocarbons. For source rocks with HI values below 300 mg HC/g TOC, intra-source rock cracking of hydrocarbons commences from 115–145°C (Pepper & Dodd 1995). The average HI of the Gert-2 coals is 193 mg HC/g TOC, and the vitrinite reflectance values suggest burial temperatures of 124–132°C, implying that intra-source rock oil-to-gas cracking of the trapped hydrocarbons may enhance the gas-proneness of the coals. Observation of pyrolytic carbon in the coals may provide direct evidence for gas generation (Petersen & Nytoft 2007).

Concluding remarks

As is the case with other Carboniferous coals, the drilled Lower Carboniferous coals encountered in the Gert-2 well, located at the northern margin of the Danish Central Graben, are gas-prone. The gas-proneness is inherited from the coaly organic matter, which generally contains a small amount of oil-prone kerogen due to the lack of long-chain aliphatics. Limited expulsion efficiency maintains a low saturate/aromatic ratio of the generated and trapped petroleum. The thermally less stable petroleum mixture promotes intra-source rock oil-to-gas cracking of the trapped hydrocarbons in the coals, which enhances their gas-proneness. The thin coaly section, present in the Gert-2 well, has no economic significance. However, provided that the Lower Carboniferous coaly section is regionally distributed and the section elsewhere is thicker with a larger number of coal seams and/or thick sections of coaly shale, it can potentially be a gas source for deep plays in the Danish Central Graben and adjacent areas. This is supported by the encountered gas in the Svane-1/1A well (Ohm *et al.* 2006).

Acknowledgements

The study was part of a larger project financially supported by the Danish Natural Science Research Council (grant 21-04-0605).

References

Besly, B.M. 1998: Carboniferous. In: Glennie, K.W. (ed.): Petroleum geology of the North Sea: basic concepts and recent advances, 104–136. Oxford: Blackwell Science Ltd.

Bruce, D.R.S. & Stemmerik, L. 2003: Carboniferous. In: Evans, D., Graham, C., Armour, A. & Bathurst, P. (eds): The millennium atlas: petroleum geology of the central and northern North Sea, 83–89. Bath: Geological Society of London.

Drozdzewski, G. 1993: The Ruhr coal basin (Germany): structural evolution of an autochthonous foreland basin. International Journal of Coal Geology **23**, 231–250.

Gautier, D.L. 2003: Carboniferous-Rotliegend total petroleum system description and assessment results summary. U.S. Geological Survey Bulletin **2211**, 24 pp.

Isaksen, G.H., Curry, D.J., Yeakel, J.D. & Jenssen, A.I. 1998: Controls on the oil and gas potential of humic coals. Organic Geochemistry **29**, 23–44.

Killops, S.D., Funnell, R.H., Suggate, R.P., Sykes, R., Peters, K.E., Walters, C., Woolhouse, A.D., Weston, R.J. & Boudou, J.-P. 1998: Predicting generation and expulsion of paraffinic oil from vitrinite-rich coals. Organic Geochemistry **29**, 1–21.

Lokhorst, A. (ed.) 1998: NW European gas atlas – composition and isotope ratios of natural gases. Utrecht: Netherlands Institute of Applied Geoscience (CD-ROM).

Ohm, S.E., Karlsen, D.A., Roberts, A., Johannessen, E. & Høiland, O. 2006: The Paleocene sandy Siri fairway: an efficient 'pipeline' draining the prolific Central Graben? Journal of Petroleum Geology **29**, 53–82.

Parnell, J. 1988: Lacustrine petroleum source rocks in the Dinantian Oil Shale Group, Scotland: a review. In: Fleet, A.J., Kelts, K. & Talbot, M.R. (eds): Lacustrine petroleum source rocks. Geological Society Special Publication (London) **40**, 235–246.

Pepper, A.S. & Dodd, T.A. 1995: Simple kinetic models of petroleum formation. Part II: oil-gas cracking. Marine and Petroleum Geology **12**, 321–340.

Petersen, H.I. 2006: The petroleum generation potential and effective oil window of humic coals related to coal composition and age. International Journal of Coal Geology **67**, 221–248.

Petersen, H.I. & Nytoft, H.P. 2006: Oil generation capacity of coals as a function of coal age and aliphatic structure. Organic Geochemistry **37**, 558–583.

Petersen, H.I. & Nytoft, H.P. 2007: Assessment of the petroleum generation potential of Lower Carboniferous coals, North Sea: evidence for inherently gas-prone source rocks. Petroleum Geoscience **13**, 271–285.

Sykes, R. 2001: Depositional and rank controls on the petroleum potential of coaly source rocks. In: Hill, K.C. & Bernecker, T. (eds): Eastern Australasian Basins Symposium, a refocused energy perspective for the future. Petroleum Exploration Society of Australia Special Publication **1**, 591–601.

Sykes, R. & Snowdon, L.R. 2002: Guidelines for assessing the petroleum potential of coaly source rocks using Rock-Eval pyrolysis. Organic Geochemistry **33**, 1441–1455.

Ziegler, P.A. 1990: Geological atlas of western and central Europe, 2nd edition, 239 pp. Mijdrecht: Shell International Petroleum.

Authors' address

Geological Survey of Denmark and Greenland, Øster Voldgade 10, DK-1350 Copenhagen K, Denmark. E-mail: *hip@geus.dk*

Prediction of reservoir sand in Miocene deltaic deposits in Denmark based on high-resolution seismic data

Erik S. Rasmussen, Thomas Vangkilde-Pedersen and Peter Scharling

Intense investigations of deep aquifers in Jylland, western Denmark, during the last seven years have resulted in detailed mapping of Miocene sand-rich deposits laid down in fluvial channels, delta lobes, shoreface and spit complexes (Fig. 1; Rasmussen 2004). Detailed sedimentological and palynological studies of outcrops and cores, and interpretation of high-resolution seismic data, have resulted in a well-founded sequence-stratigraphic and lithostratigraphic scheme (Fig. 1) suitable for prediction of the distribution of sand.

The Miocene succession onshore Denmark is divided into three sand-rich deltaic units: the Ribe and Bastrup sands and the Odderup Formation (Fig. 2). Prodeltaic clayey deposits of the Vejle Fjord and Arnum Formations interfinger with the sand-rich deposits. Most of the middle and upper Miocene in Denmark is composed of clayey sediments referred to the Hodde and Gram Formations (Fig. 2).

This paper presents examples of seismic reflection patterns that have proved to correlate with sand-rich deposits from lower Miocene deltaic deposits and that could be applied in future exploration for aquifers and as analogues for oil- and gas-bearing sands in wave-dominated deltas.

Geology

During the Early Miocene, the eastern North Sea Basin was filled by siliciclastic sediments sourced from the Fennoscandian Shield. The sediment supply was high due to tectonic uplift of the Fennoscandian Shield (Ziegler 1990; Rasmussen 2004). The North Sea was located in the high-latitude belt of westerly winds, which resulted in a long fetch, and the tidal range is interpreted to be micro- to meso-tidal. Regressions and transgressions during the Early Miocene were strongly controlled by eustatic sea-level changes (Friis *et al.* 1998; Rasmussen 2004; Rasmussen & Dybkjær 2005).

During the early Miocene, two phases of shoreline progradation occurred. Sand deposited adjacent to the delta mouth or in association with topographic highs was immediately redistributed and deposited either as spit complexes or as barrier islands in the down-drift areas of delta lobes. These sand-rich successions are commonly around 20 m thick; however, delta lobes prograding into topographic lows, i.e. deep water, are characterised by up to 70 m thick successions of clean sand. The delta front sediments were deposited either as mass-flow sediments or current-derived deposits. During sea-level fall, incision of the delta plain took place. These incised valleys were successively filled with thick, sand-rich fluvial deposits during the succeeding sea-level rise.

Fig. 1. Map of Jylland showing distribution of Lower Miocene environments (from Rasmussen 2004). Insert map shows position of seismic sections and boreholes used in this study.

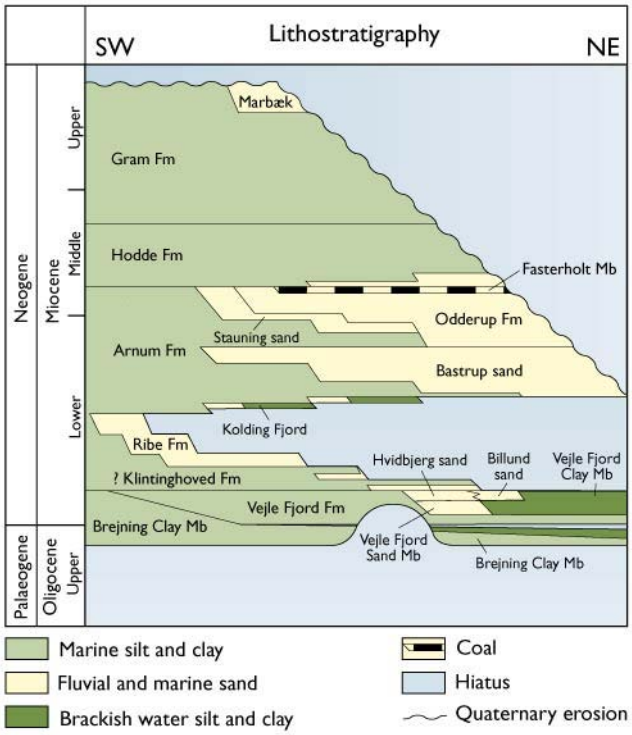

Fig. 2. Lithostratigraphy of the Danish Miocene sediments (modified from Rasmussen 2004).

Seismic data acquisition

Mapping of aquifers in Denmark has previously been dominated by electric and electromagnetic methods, as the high cost of conventional, shallow, onshore reflection seismic surveys was a factor that limited its use. Recently, however, the technique of landstreamer high-resolution seismic data has provided considerable savings of manpower and increased productivity compared to using traditionally planted geophones and cable lay-outs. The mapping of deeper units is also possible now. The landstreamer technique also facilitates short geophone spacing and differential spacing of geophones along the spread without increasing time- or manpower consumption.

The use of landstreamers for acquisition of shallow seismic data has increased throughout the world in recent years. The landstreamers are commonly used together with relatively weak sources such as a pipegun or sledgehammer (e.g. van der Veen & Green 1998; van der Veen *et al.* 2001) resulting in a relatively limited penetration depth (typically a few hundred metres). Since the year 2000, more than 1000 km of high-resolution seismic data have been acquired to map deep aquifers in Denmark. The acquisition setup used has included high-frequency seismic vibrators (3.5 T and 6.5 T) as the energy source. Under normal conditions the landstreamer setup has provided very high data quality with reflections from *c.* 20–50 m down to more than 1 km with a vertical resolution of 5–10 m. The coverage, especially in the central and western parts of Jylland, provides unique opportunities for interpretation and correlation.

The design of the seismic landstreamers has developed from a 150 m, 60-channel streamer with 2.5 m spacing used

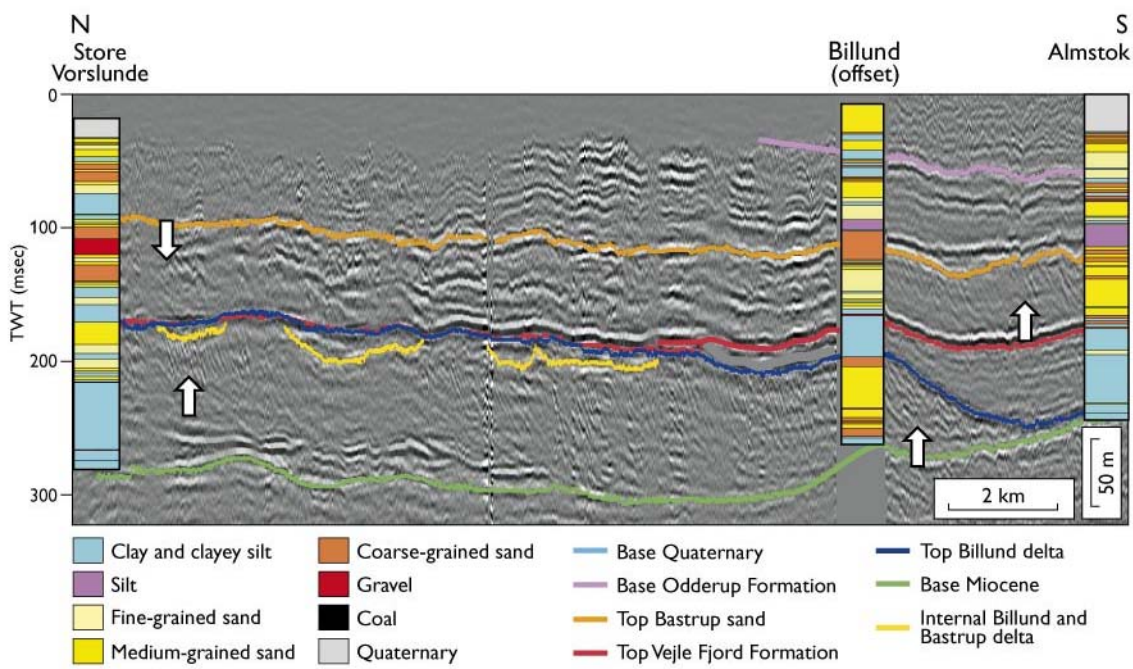

Fig. 3. Seismic section with boreholes from the Billund area illustrating two prograding deltaic sand-rich units (Billund sand and Bastrup sand). The grain size of the penetrated succession is indicated by different colours. Note that the parallel clinoformal seismic reflection pattern (arrows) always correlates with sand. Seismic data courtesy of COWI A/S and Rambøll A/S.

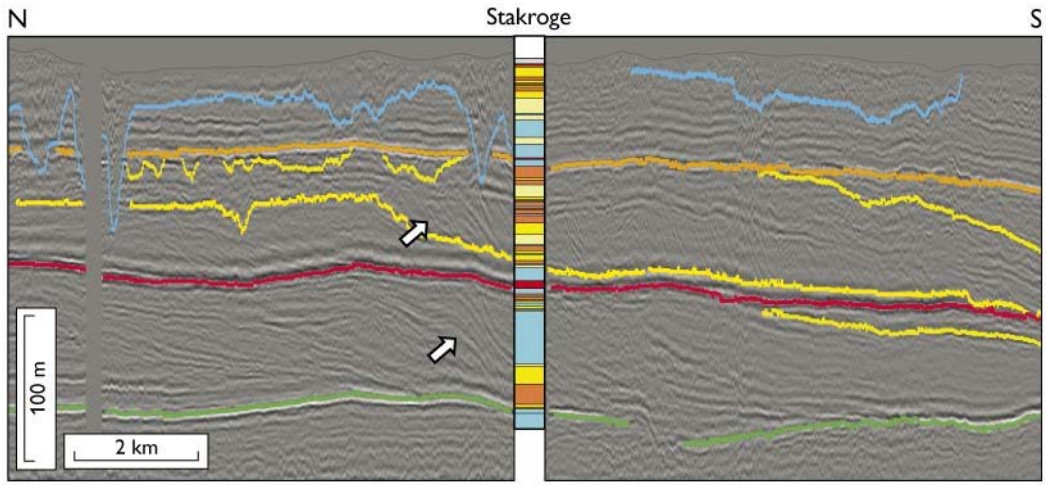

Fig. 4. Seismic section from Sønder Omme. Note the close relationship between the parallel clinoformal reflection pattern and the sand as indicated by the arrows. Note especially the lower delta where only the toe of the delta front has been penetrated by the Stakroge borehole. Seismic data courtesy of Rambøll A/S. See Fig. 3 for legend.

in 2000 to the current 200–220 m streamers with 96–102 channels and differential geophone spacings of 1.25, 2.5 and 5 m (Vangkilde-Pedersen *et al.* 2003, 2006). The differential geophone spacing along the streamers, with the shortest spacing close to the vibrator, has greatly improved the quality and resolution of the near-surface data. In the same period, both the vibrator sweeps and processing of the data have also been optimised. During the first couple of years a simple standard processing sequence was applied to the data, but in recent years the processing sequence has been significantly improved.

Examples of Lower Miocene reservoir sand

Delta front sand. Thick delta front sands occur in association with progradation into deep water that is normally associated with structurally confined areas. Delta lobes deposited during a relative sea-level fall are especially sand-rich. These deposits are characterised by a parallel clinoform reflection pattern (Figs 3, 4) in which the dip of the clinoforms range from 7° to 10°. The thickness of sand associated with this reflection pattern has never been recorded as less than 20 m and thicknesses of up to 50 m have been found at Billund (Fig. 3); the thickness may be more than 70 m within the Brande lobe, north of Billund. The grain size is commonly medium to coarse sand, but gravel may occur in connection with mass-flow deposits on the delta front or in association with channels and shoreface deposits in the upper part of the delta. Delta sand laid down during a sea-level fall is particularly clean and homogenous.

Fluvial point-bar sand. Delta deposits of the Lower Miocene Bastrup sand are often capped by fluvial sediments that have been protected during the succeeding transgression. The fluvial channels are expressed by a concave-up structure filled with a shingled seismic reflection pattern probably representing point-bar deposits (Fig. 5). From seismic and borehole data, the point-bar deposits comprise up to 20 m thick, fining-upwards successions composed of coarse- to fine-grained sand that are commonly capped by coal.

Incised valley sand. Well-defined, large, concave-upward erosional surfaces are found especially in the proximal parts of the deltas. The infills of these features on the seismic lines are often characterised by a transparent seismic reflection pattern (Fig. 6). From outcrop and borehole data the valleys are known to be filled typically by coarse-grained sand and gravel that were deposited in braided river systems. The thickness and lateral distribution of the fill vary within the delta complexes.

Future perspectives

The application of seismic data in the search for aquifers in Denmark by recognition of different seismic reflection pat-

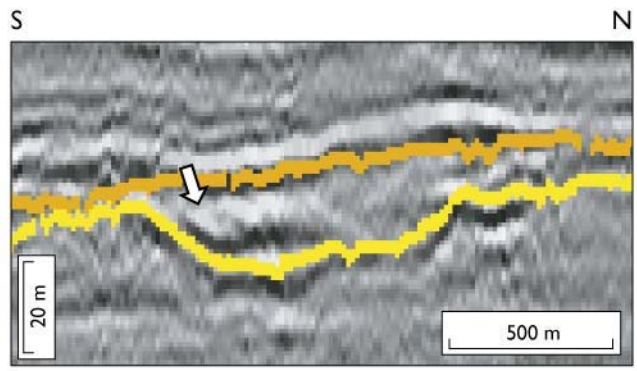

Fig. 5. Seismic section showing shingled, seismic reflection pattern (arrow) within a channel structure. Similar structures have been found on 3D seismic data from Canada (Posamentier 2005) and represent lateral accretion of a point bar. Seismic data courtesy of COWI A/S.

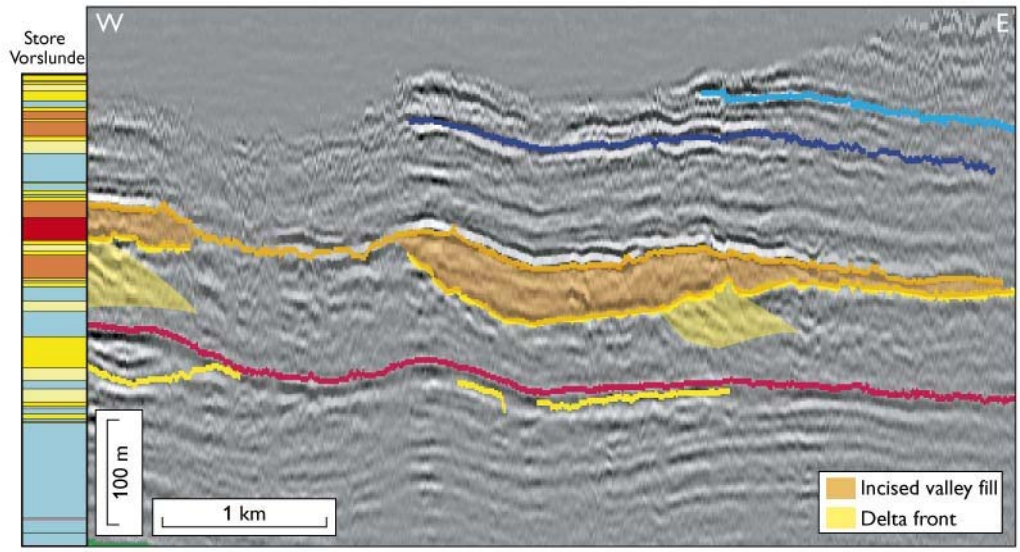

Fig. 6. Seismic section showing 2 km wide and 20 m deep erosional features on top of clinoforms interpreted as a fluvial valley fill. These features are often filled with coarse-grained sand or gravel deposits. Seismic data courtesy of COWI A/S.

terns and morphological features, e.g. the geometry of clinoforms, has proved to be useful in the prediction of sand-rich sediments in Miocene deposits. Sand-rich sediments in front of a delta complex are normally associated with clinoform reflection patterns. A shingled seismic reflection pattern within channels characterises sand-rich, point-bar deposits. Distinct erosional features, with a transparent reflection pattern, capping delta foresets commonly indicate fluvial sand-rich sediments. A detailed mapping of the Miocene delta complexes and the construction of a three-dimensional model of delta lobes will be essential for developing future hydrogeological models.

Furthermore, the connection between the observed seismic facies and sand-rich environments may also be applied as a tool for prediction of Jurassic hydrocarbon reservoir sands in the North Sea area.

Acknowledgements

The Carlsberg Foundation and the counties of Vejle, Ringkøbing and Ribe are thanked for financial support of the study of the Miocene succession in Denmark.

References

Friis, H., Mikkelsen, J. & Sandersen, P. 1998: Depositional environment of the Vejle Fjord Formation of the Upper Oligocene – Lower Miocene of Denmark: A back island/barrier-protected depositional complex. Sedimentary Geology **17**, 221–244.

Posamentier, H.W. 2005: Application of 3D seismic visualization techniques for seismic stratigraphy, seismic geomorphology and depositional systems analysis: examples from fluvial to deep-marine depositional environments. In: Doré, A.G. & Vining, B.A. (eds): Petroleum geology: North-West Europe and global perspectives – Proceedings of the 6th petroleum geology conference, 1563–1576. London: Geological Society.

Rasmussen, E.S. 2004: Stratigraphy and depositional evolution of the uppermost Oligocene – Miocene succession in western Denmark. Bulletin of the Geological Society of Denmark **51**, 89–109.

Rasmussen, E.S. & Dybkjær, K. 2005: Sequence stratigraphy of the Upper Oligocene – Lower Miocene of eastern Jylland, Denmark: role of structural relief and variable sediment supply in controlling sequence development. Sedimentology **52**, 25–63.

van der Veen, M. & Green, A.G. 1998: Landstreamer for shallow seismic data acquisition: valuation of gimbal-mounted geophones. Geophysics **63**, 1408–1413.

van der Veen, M., Spitzer, R., Green, A.G. & Wild, P. 2001: Design and application of a towed landstreamer for cost-effective 2D and pseudo-3D shallow seismic data acquisition. Geophysics **66**, 482–500.

Vangkilde-Pedersen, T., Skjellerup, P., Ringgaard, J. & Jensen, J.F. 2003: Pulled array seismic (PAS) – a new method for shallow reflection seismic data acquisition. 65th EAGE Conference & Exhibition, Stavanger, Norway, 2–5 June 2003. Extended abstracts, 201 only.

Vangkilde-Pedersen, T., Dahl, J.F. & Ringgaard, J. 2006: Five years of experience with landstreamer vibroseis and comparison with conventional seismic data acquisition. Proceedings of the 19th Annual SAGEEP Symposium on the Application of Geophysics to Engineering and Environmental Problems, Seattle, USA, 1086–1093.

Ziegler, P. 1990: Geological atlas of western and central Europe, 2nd edition, 239 pp, Mijdrecht: Shell International Petroleum.

Authors' address

Geological Survey of Denmark and Greenland, Øster Voldgade 10, DK-1350 Copenhagen K, Denmark. E-mail: *esr@geus.dk*

Environmental change in Danish marine waters during the Roman Warm Period inferred from mollusc data

Peter Rasmussen, Kaj Strand Petersen and David B. Ryves

Modern geological research into the late and postglacial history of the inner Danish waters (i.e. Kattegat, Bælthavet and Øresund, plus the adjoining fjords and estuaries) began at the turn of the last century. Since then most investigations have focused on the timing of the initial marine inundation of the area, the early to mid-Holocene changes in land–sea configuration and sea level changes during the mid-Holocene Littorina period. Research on the late Holocene marine environment has received less emphasis, undoubtedly due to problems in finding continuous marine sediment records, as sedimentation in large areas of the Danish waters seems to have been characterised by complex spatial and temporal patterns of deposition and non-deposition (e.g. Lykke-Andersen *et al.* 1993).

In an ongoing project we aim to explore the continuous development of Danish coastal environments over the last 9000 years using a variety of proxy data, including molluscs, diatoms, foraminifera, algal pigments, plant macrofossils and physical properties of sediments. The project spans both environmental and cultural history, and addresses the important links between them, as the nature of the coastal environment has exerted major influences on cultural and societal expression and activity from Mesolithic to modern times. This paper presents some of the first results from the project concerning environmental changes in the Roman Warm Period (*c.* 2000–1600 years B.P.) as shown by changes in molluscan faunas at two coring sites in Horsens Fjord and Tempelkrog in southern Isefjord (Fig. 1).

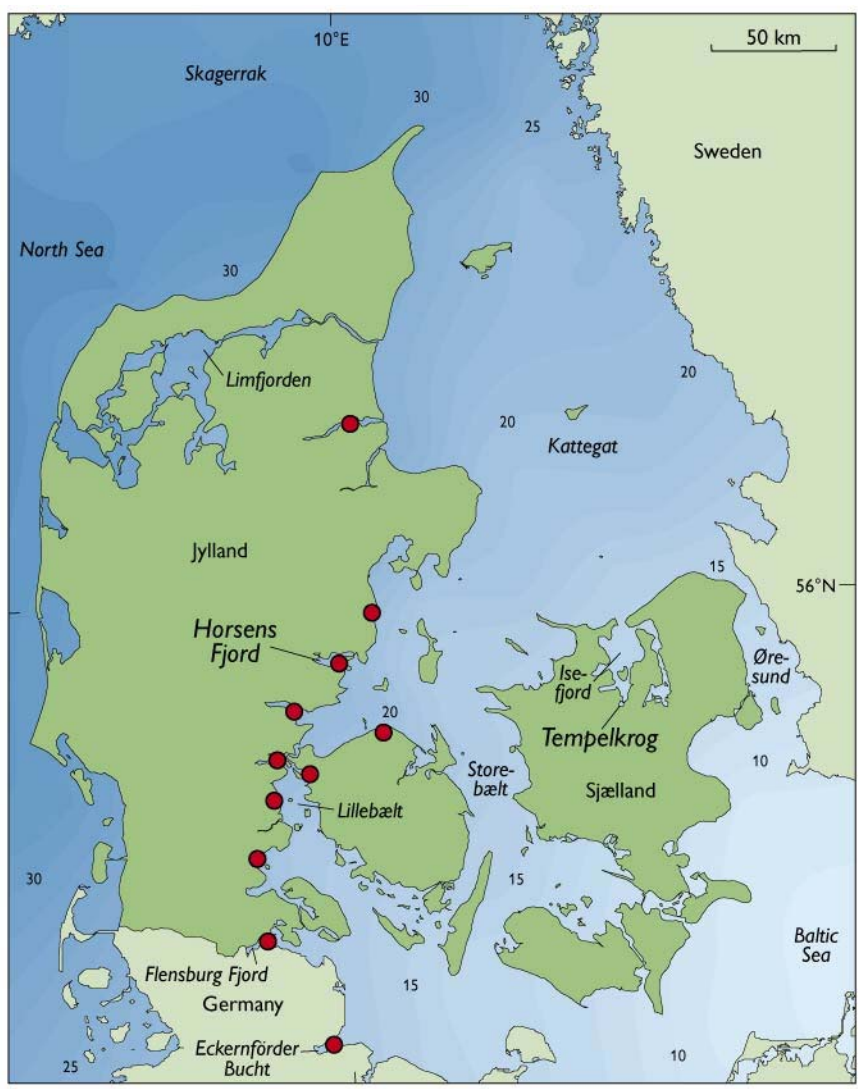

Fig. 1. Map of Denmark showing the location of the two study sites Horsens Fjord and Tempelkrog in Isefjord and the present day sea surface salinities (psu; annual mean) in the Danish waters. The red dots indicate fjords and estuaries with Iron Age shell middens. (modified from Dahl *et al.* 2003). Bælthavet includes Storebælt and Lillebælt and the sea between the islands south of Fyn and Sjælland.

Hydrography

The present-day circulation pattern in the inner Danish waters is dominated by a two-layer estuarine flow, driven by outflow of low-salinity surface water from the Baltic Sea and

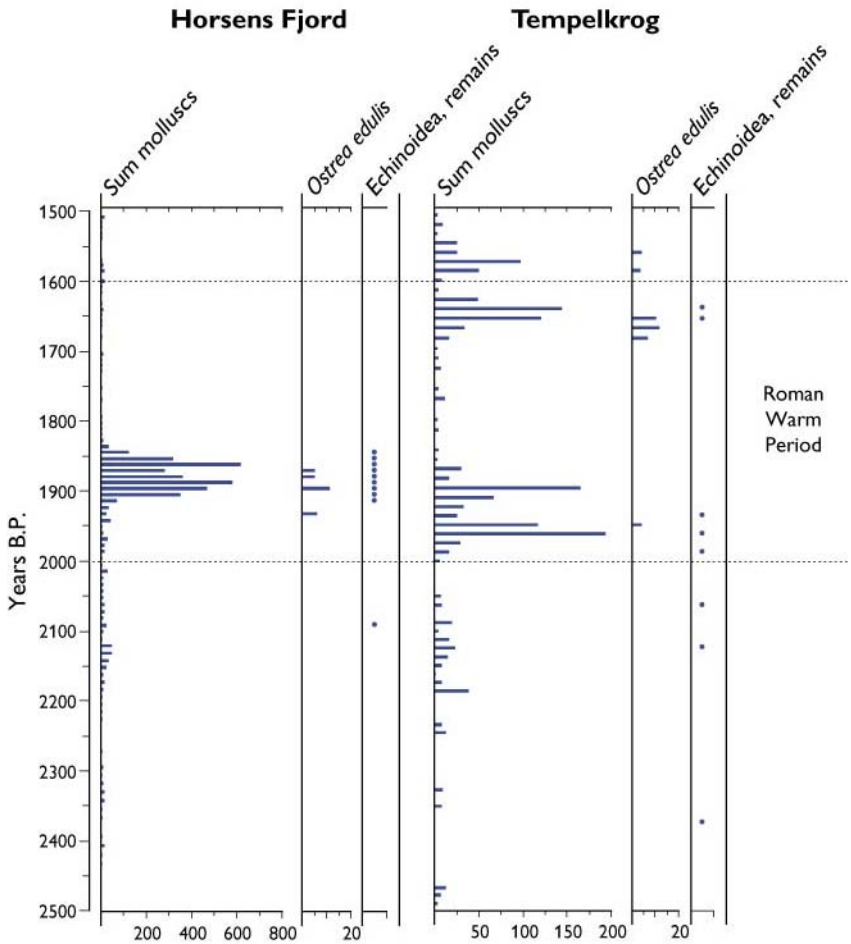

Fig. 2. Summary stratigraphic, macrofaunal data from two sediment cores from Horsens Fjord and Tempelkrog. Abundances of molluscs are expressed as specimens per 100 ml of fresh sediment. Remains of echinoids are shown as present/not-present. The dotted lines delimit the Roman Warm Period. Note the change of x-axis scale.

inflow of high-salinity bottom water from the North Sea and Skagerrak. Due to high inflows of freshwater to the Baltic Sea from rivers there is a strong surface-salinity gradient from west to east: from >30 psu (practical salinity units, equivalent to ppt) in Skagerrak decreasing eastwards to <5 psu in the Baltic Sea (Fig. 1; Al-Hamdani *et al.* 2007 – this volume). There is also a strong salinity stratification (a halocline) within the water column, with a wedge of higher salinity, North Sea-derived water underlying less dense, less saline surface water.

Material and methods

Two sediment core lengths of 6 m and 13.5 m were extracted from respectively Horsens Fjord and Tempelkrog, both at a water depth of around 5 m and both consisting of homogeneous clay-gyttja. The two sediment records were Accelerator Mass Spectrometry (AMS) ^{14}C-dated using terrestrial plant material, thus avoiding marine-derived material which suffers from uncertain reservoir and hard-water effects that can cause serious dating problems in Danish fjord and marine waters (Heier-Nielsen *et al.* 1995). The Horsens Fjord and Tempelkrog sediment cores were subsampled at intervals of 1 cm and 2 cm, respectively, which is equivalent to a resolution of 10–15 years in both records for the time period discussed in this paper. Molluscs were extracted from the cores by wet-sieving of known sediment volumes through a sieve with a mesh size of 0.1 mm. Macrofaunal specimens were identified and counted and species numbers were calculated for 100 ml of sediment (Fig. 2).

Results and discussion

Molluscan faunas

Based on analogies with their present-day ecological requirements in relation to salinity, temperature, depth and substrate, Quaternary molluscs are useful tools as indicators of environmental and climatic changes through time. Changes in surface salinity (and temperature) have often been linked with fluctuations in different marine populations, for example stocks of fish and molluscs, which tolerate only certain ranges of salinity and temperature. In the transitional area between the Skagerrak and the Baltic Sea, the salinity gradient seems to be the main limiting factor in the geographic distribution of mollusc species (Sorgenfrei 1958; Petersen 2004).

Fig. 3. Section of an Iron Age shell midden at Horsens Fjord. The Iron Age middens are mainly composed of shells, charcoal and pot boilers (stones used in cooking) and are interpreted as specialised coastal sites used for gathering and processing of shellfish (Poulsen 1978). Mollusc analysis from North German middens suggests that they are seasonal sites used in the late summer or autumn (Anger 1973). Photograph courtesy of Karen Løkkegaard Poulsen.

The summary stratigraphic, macrofauna data from Horsens Fjord and Tempelkrog during the period 2500 to 1500 years B.P. are shown in Fig. 2. At both sites there is a distinct increase in mollusc abundance at the beginning of the Roman Warm Period between *c*. 2000 and 1850 years B.P. and at Tempelkrog again at the end of the Roman Warm Period. At Horsens, this increase is mainly due to *Mytilus edulis* (blue mussel), *Rissoa albella, R. albella var. sarci, Bittium reticulatum, Cerastoderma edule* (common cockle) and *Mysella bidentata*, and at Tempelkrog, *Hydrobia ulvae*, *H. ventrosa, H. neglecta* and *Rissoa albella*. At both sites, this increase in mollusc abundance is accompanied by the appearance of *Ostrea edulis* (European flat oyster) and a more steady presence of remains of echinoids (sea urchins), both indicating more saline conditions than in the period before or after (Fig. 2). *Ostrea edulis* needs at least 25 psu in order to reproduce (Jensen & Spärck 1934) and is not present in the inner Danish waters today, except for the western part of Limfjorden which is connected to the North Sea. Furthermore, the reproductive success of *Ostrea edulis* is very sensitive to temperature with optimal conditions around 20–22°C (Spärck 1924). Echinoids are generally stenohaline and therefore disappear when the water becomes brackish (*c*. 10 psu). In addition, other mollusc species, which also indicate an increase in salinity to >25 psu, appear at Horsens Fjord, although with low abundance. These include *Parvicardium scabrum, Abra nitida, Rissoa violacea, Gari fervensis, Velutina velutina, Odostomia umbilicaris* and *Abra prismatica* (Sorgenfrei 1958).

The two study sites are located 120 km apart and the similar pattern in macrofaunal assemblages, with an increase in mollusc abundance and the appearance of a suite of almost fully marine taxa at various times during the Roman Warm Period, thus testifies to a widespread change to more saline and productive conditions across the inner Danish waters. The fairly regular presence of *Ostrea edulis* (see below) may also suggest an increase in sea surface temperature during this period. The reason for two (or three) 'episodes' with changes in faunal compositon at Tempelkrog and only one at Horsens Fjord is unclear but could be a result of spatial or temporal differences in substrate, local current conditions or post-mortem (taphonomic) processes.

Sea and society

Inferences of higher salinity and productivity during the Roman Warm Period from the palaeoenvironmental data are also supported by an independent line of evidence from the archaeological record. Large shell middens dated to the centuries around 2000 years B.P., and predominantely composed of *Mytilus edulis, Cerastoderma edule, Littorina littorea* (common periwinkle) and to a lesser extent *Ostrea edulis*, are recorded along several Danish and North German fjords (Figs 1, 3; Anger 1973; Harck 1973; Poulsen 1978; Petersen 1985). The synchroneity between the inferred changes in the marine environment and the appearance of these Iron Age shell middens strongly suggest a causal connection between the two, implying that people responded to the increased productivity in the marine environment by a comprehensive and targeted gathering and processing of shellfish.

Outlook

The evidence of salinity increase in the inner Danish waters during the Roman Warm Period only seems to be explicable by the more frequent inflow of high-salinity North Sea water, which travelled through the Danish straits and further east into the Baltic Sea. This scenario is supported by the presence of *Ostrea edulis* in Iron Age shell middens as far into the Baltic as the head of Flensburg Fjord and Eckernförder Bucht

(North Germany; Anger 1973; Harck 1973); this is only possible through a combination of a more frequent input of high-salinity water and a higher rate of water exchange than today. The increased inflow of North Sea water seems to have penetrated as far as the central Baltic Sea where diatom and isotopic data also suggest a salinity rise during the Roman Warm Period (Emeis *et al.* 2003). Diatom-based sea-surface salinity reconstructions from southern Skagerrak also indicate higher salinity during the period (Hebbeln *et al.* 2006), in good agreement with our results from the Danish waters and evidence from the Gotland Basin (Emeis *et al.* 2003).

Future work

Work is ongoing to analyse the other proxy records from the two sites over the last 9000 years to provide additional independent environmental information and to test the inferences made from the subfossil mollusc data. For instance, a model to relate fossil diatom assemblage composition to past surface-water salinity is being developed using a large range of contemporary samples from the western Baltic Sea, Limfjorden and coastal brackish lakes and fjords (the MOLTEN project: http://craticula.ncl.ac.uk/Molten/jsp/; Ryves *et al.* 2004). Coastal sediments contain important natural archives of past environmental changes and palaeoecological techniques can provide a powerful means of revealing the natural variability of the marine environment and the links between environmental and socio-cultural changes over time. Furthermore, this approach can establish the nature of environmental conditions in nearshore marine areas prior to the impact of modern society on coastal regions. It is especially important to establish ecological baseline conditions before realistic goals for environmental management of coasts can be set.

Acknowledgements

The ongoing research project *Denmark's coastal environment over the last 9000 years: linking cultural and hydrographic change* is co-financed by the Danish Research Council for the Humanities (FKK) and the Danish Natural Science Research Council (FNU), whose support is gratefully acknowledged. Additional funding for the project has been provided by Loughborough University, UK. Karen Løkkegaard Poulsen is thanked for information about Iron Age shell middens.

References

Al-Hamdani, Z.K., Reker, J., Leth, J.O., Reijonen, A., Kotilainen, A.T. & Dinesen, G.E. 2007: Development of marine landscape maps for the Baltic Sea and the Kattegat using geophysical and hydrographical parameters. Geological Survey of Denmark and Greenland Bulletin **13**, 61–64.

Anger, K. 1973: Untersuchungen an eisenzeitlichen Muschelhaufen an der Flensburger Förde. Offa **30**, 55–59.

Dahl, K., Lundsteen, S. & Helmig, S.A. 2003: Stenrev – havets oaser, 104 pp. Copenhagen: Gads Forlag.

Emeis, K.-C., Struck, U., Blanz, T., Kohly, A. & Voss, M. 2003: Salinity changes in the Baltic Sea (NW Europe) over the last 10 000 years. The Holocene **13**, 411–421.

Harck, O. 1973: Eisenzeitliche Muschelhaufen an der schleswigschen Ost- und Westküste. Offa **30**, 40–54.

Hebbeln, D., Knudsen, K.-L., Gyllencreutz, R., Kristensen, P., Klitgaard-Kristensen, D., Backman, J., Scheurle, C., Jiang, H., Gil, I., Smelror, M., Jones, P.D. & Sejrup, H.-P. 2006: Late Holocene coastal hydrographic and climate changes in the eastern North Sea. The Holocene **16**, 987–1001.

Heier-Nielsen, S., Heinemeier, J., Nielsen, H.L. & Rud, N. 1995: Recent reservoir ages for Danish fjords and marine waters. Radiocarbon **37**, 875–882.

Jensen, A.S. & Spärck, R. 1934: Bløddyr II. Saltvandsmuslinger. Danmarks Fauna **40**, 208 pp.

Lykke-Andersen, H., Knudsen, K.L. & Christiansen, C. 1993: The Quaternary of the Kattegat area, Scandinavia: a review. Boreas **22**, 269–281.

Petersen, K.S. 1985: Det sydfynske arkipelag. Dets geologiske udvikling med særlig hensyntagen til havniveauændringer og den marine molluskfauna. In: Skaarup, J. (ed.): Yngre Stenalder på øerne syd for Fyn, 15–27. Rudkøbing: Langelands Museum.

Petersen, K.S. 2004: Late Quaternary environmental changes recorded in the Danish marine molluscan faunas. Geological Survey of Denmark and Greenland Bulletin **3**, 268 pp.

Poulsen, K.L. 1978: Eisenzeitliche Muschelhaufen in Dänemark. Offa **35**, 64–85.

Ryves, D.B., Clarke, A.L., Appleby, P.G., Amsinck, S.L., Jeppesen, E., Landkildehus, F. & Anderson, N.J. 2004: Reconstructing the salinity and environment of the Limfjord and Vejlerne nature reserve, Denmark, using a diatom model for brackish lakes and fjords. Canadian Journal of Fisheries and Aquatic Sciences **61**, 1988–2006.

Sorgenfrei, T. 1958: Molluscan assemblages from the marine middle Miocene of South Jutland and their environments. Danmarks Geologiske Undersøgelse II. Række **29**, 356–503.

Spärck, R. 1924: Undersøgelser over Østersens (*Ostrea edulis*) Biologi i Limfjorden, særlig med Henblik paa Temperaturens Indflydelse paa Kønsskiftet, 82 pp. København: Centraltrykkeriet.

Authors' addresses

P.R. & K.S.P., *Geological Survey of Denmark and Greenland, Øster Voldgade 10, DK-1350 Copenhagen K, Denmark.* E-mail: *per@geus.dk*

D.B.R., *Department of Geography, Loughborough University, Loughborough, Leicestershire, LE11 3TU, UK.*

Petroleum systems and structures offshore central West Greenland: implications for hydrocarbon prospectivity

Ulrik Gregersen, Torben Bidstrup, Jørgen A. Bojesen-Koefoed, Flemming G. Christiansen, Finn Dalhoff and Martin Sønderholm

A detailed geophysical mapping project has been carried out by the Geological Survey of Denmark and Greenland (GEUS) in the offshore region south-west and west of Disko and Nuussuaq, central West Greenland as part of the preparations for the Disko West Licensing Round in 2006 (Fig. 1). The main purpose of the study was to evaluate the prospectivity of this almost 100 000 km^2 large region, and to increase knowledge of basin evolution and the structural development. Results of the work, including a new structural elements map of the region and highlights of particular interest for hydrocarbon exploration of this area, are summarised below.

Evidence of live petroleum systems has been recognised in the onshore areas since the beginning of the 1990s when seeps of five different oil types were demonstrated (Bojesen-Koefoed *et al.* 1999). Oil seeps suggesting widely distributed marine source rocks of Mesozoic age are particularly promising for the exploration potential (Bojesen-Koefoed *et al.* 2004, 2007). Furthermore, possible DHIs (Direct Hydrocarbon Indicators) such as gas-clouds, pock marks, bright spots and flat events have been interpreted in the offshore region (Skaarup *et al.* 2000; Gregersen & Bidstrup in press).

The evaluation of the region (Fig. 1) is based on all public and proprietary seismic data together with public domain magnetic and gravity data. The seismic data (a total of *c.* 28 000 line km) are tied to the two existing offshore exploration wells in the region (Hellefisk-1 and Ikermiut-1). The study also incorporates information on sediments and volcanic rocks from onshore Disko and Nuussuaq (Fig. 2).

Ten seismic horizons ranging from 'mid-Cretaceous' to 'Base Quaternary' (Fig. 2) have been interpreted regionally. Large correlation distances to wells, varying data quality and a thick cover of basalt in the north-eastern part of the region, add uncertainty in the regional interpretation, especially for the deeper horizons such as the 'mid-Cretaceous' equivalent to Santonian sandstone interval drilled in Qulleq-1 far south.

Based on the seismic interpretation (Fig. 3) structural elements maps, horizon-depth maps and isopach maps have been produced; these maps, together with general stratigraphic knowledge on potential reservoirs, seals and source rocks (Fig. 2), provide important information for discussions of critical play elements including kitchens and structures. The existence of many large structures combined with the evidence of live petroleum systems has spurred the recent major interest for hydrocarbon exploration in the region.

Structural development and basin evolution

A number of deep basins with Cretaceous and Cenozoic sedimentary successions have been recognised offshore West Greenland since the 1970s (e.g. Chalmers *et al.* 2001). In Early to mid-Cretaceous times a number of major structural complexes and basins developed in the region (Figs 1, 3), mainly as a result of extensional faulting. These include the

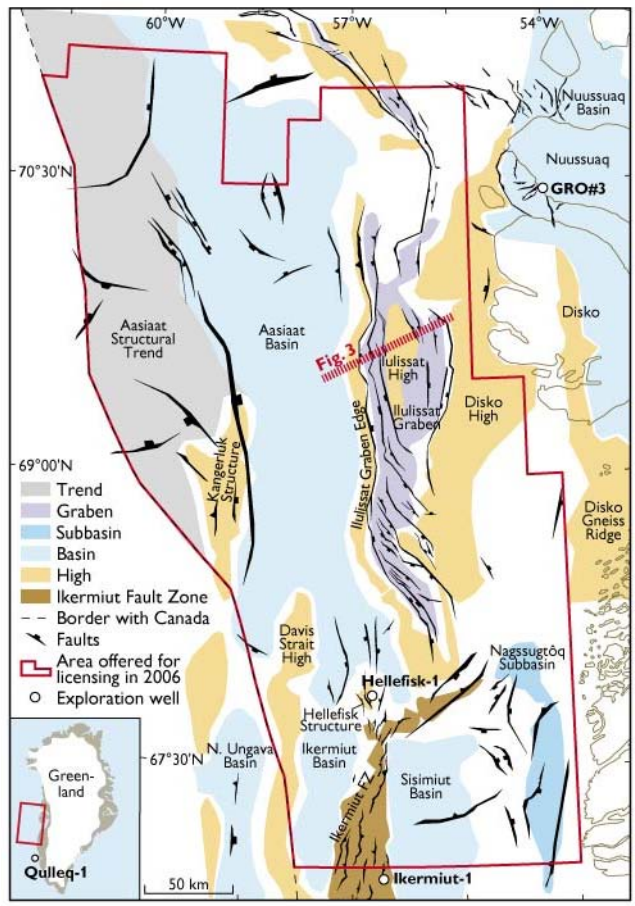

Fig. 1. Structural elements offshore the Disko–Nuussuaq region, central West Greenland. The position of the seismic example in Fig. 3 is shown.

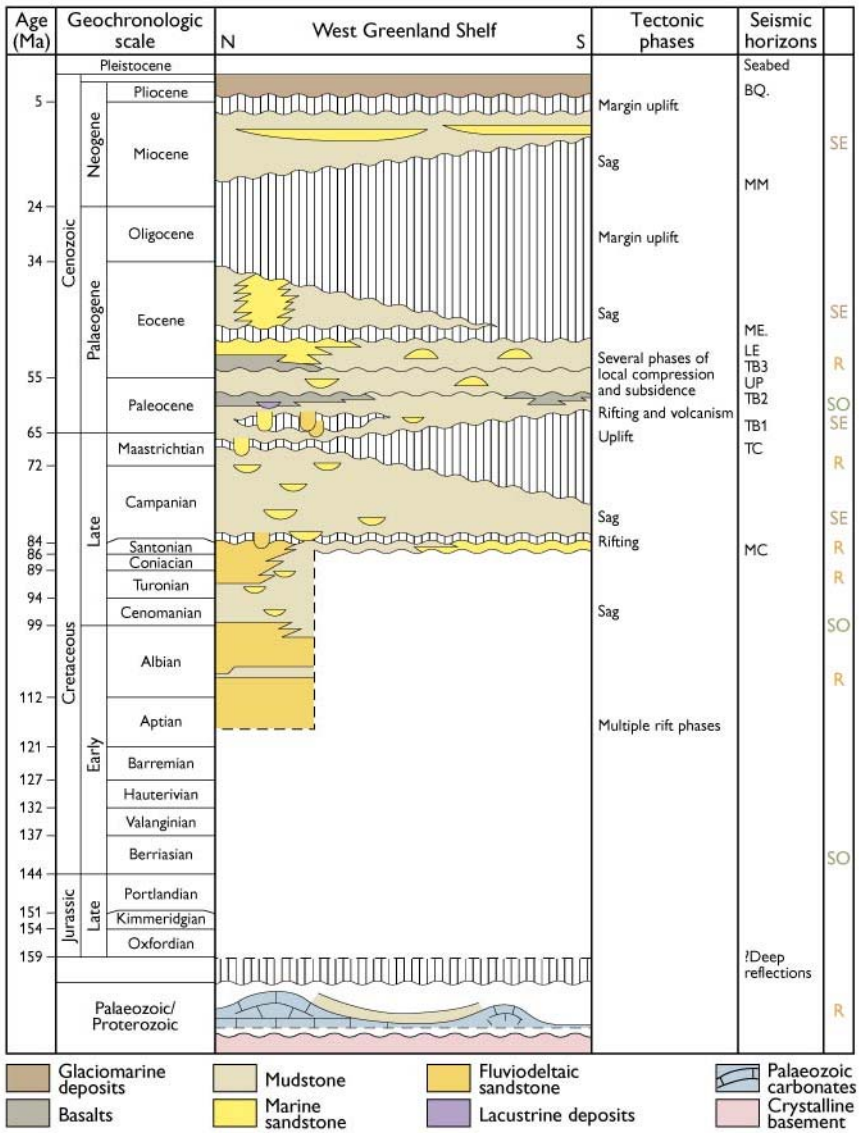

Fig. 2. Simplified stratigraphic scheme with lithology from present coastal areas of Disko and Nuussuaq (north), and from offshore West Greenland wells towards the south. The main phases of tectonism and subsidence are listed. The main interpreted seismic horizons are Seabed, Base Quaternary (**BQ**), mid-Miocene (**MM**), Lower Eocene (**LE**), Top Basalt 3 (**TB3**), Upper Paleocene (**UP**), Top Basalt 2 (**TB2**), Top Basalt 1/Base Basalt 2 (**TB1**), Top Cretaceous (**TC**), mid-Cretaceous (**MC**) and unspecified deep reflections. The most likely intervals with source rocks (**SO**), reservoir sands (**R**) and seals (**SE**) are also indicated.

Aasiaat Structural Trend, the Kangerluk Structure, the Aasiaat Basin, the Sisimiut Basin and the Nagssugtôq Subbasin (Fig. 1). Deep-seated fault-bounded basins locally showing anticlinal structures are occasionally observed below the interpreted 'mid-Cretaceous' seismic horizon. Seabed sampling has shown the presence of Ordovician carbonate strata on the Davis Strait High (Dalhoff *et al.* 2006). Together with reworked Jurassic or older palynomorphs observed in the Qulleq-1 well farther south (Nøhr-Hansen *et al.* 2000) these suggest the possibility of pre-Cretaceous strata in the deepest parts of these basins. Based on outcrop studies, regional Cretaceous sand-prone units are expected to be present in the offshore region, both as deltaic and shallow-marine deposits and as turbidite deposits (Fig. 2).

During the Late Cretaceous a new rifting episode was initiated and was characterised by normal faulting, subsidence and syn-rift sedimentation including deposition of a thick mudstone succession of Campanian–Maastrichtian age (Dam *et al.* 2000). This phase lasted into Early Paleocene times resulting in repeated erosion and filling of subaerial valley and submarine canyons and formation

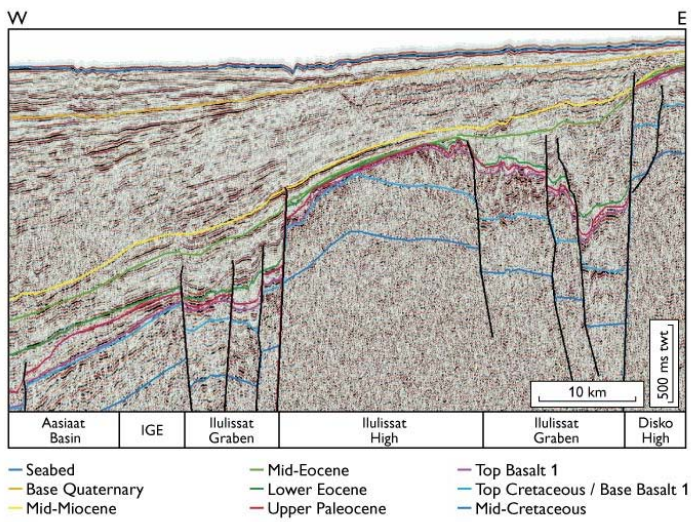

Fig. 3. Seismic section (GGUi95-17) through eastern parts of the study region, showing main structural elements. The main structural elements are from west to east: The easternmost parts of the Aasiaat Basin, the Ilulissat Graben Edge (**IGE**), the Ilulissat Graben on both sides of the Ilulissat High, and the westernmost part of the Disko High. Note the amplitude anomalies above the Ilulissat High (see Fig. 1 for location).

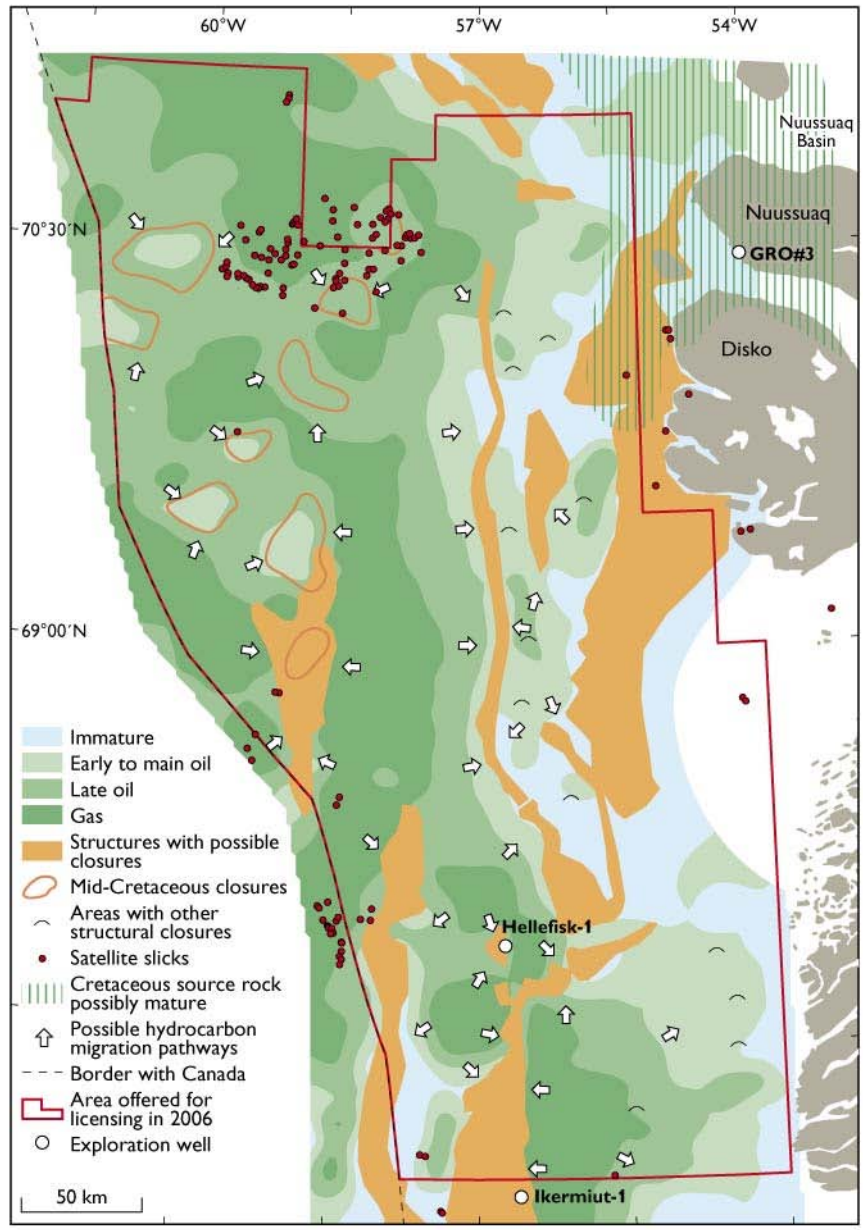

Fig. 4. Simplified prospectivity map. Cretaceous to Palaeogene structures and major mid-Cretaceous 4-way dip closures to the west, possible hydrocarbon migration pathways and mid-Cretaceous hydrocarbon generation areas (maturity levels – early to main oil: ~0.5 – >1% R_o; late oil: ~1 – >1.3% R_o; gas: >1.3% R_o).

of regional unconformities (Dam & Sønderholm 1998; Dam 2002).

A zircon age provenance study of sandstone units in outcrops and offshore exploration wells indicates that most of the sand units show local age signatures characteristic of the Greenland shield to the east. However, a Grenville age component of probable Canadian derivation also seems to be present in the deep-water deposits of the Nuussuaq Basin and in the Qulleq-1 well suggesting a long-shore transport component (Scherstén & Sønderholm 2007 – this volume).

During the Paleocene–Eocene a major episode of volcanic eruption took place, and some hundreds of metres of thick basalts cover part of the offshore region (Fig. 3). The basalts may reach thicknesses of more than 2 km in the north-eastern offshore part of the study region. However, the current mapping suggests that the volcanic succession is thinner and less widely distributed than suggested in previous publications and maps (e.g. Chalmers *et al.* 1993; Chalmers & Pulvertaft 2001; Skaarup 2002). Strike-slip movements during the Late Paleocene and Early Eocene caused local transpression of structures primarily along the Ikermiut Fault Zone, and locally in the basins and structures farther north, contemporaneous with subsidence in the Ikermiut Basin region. Transtensional and extensional movements farther to the north-east, subsequent to the extrusion of the Paleocene basalts, resulted in the development of the more than 200 km long Ilulissat Graben (Fig. 1).

During the Eocene, and especially during the late Miocene to Pliocene, the offshore basins subsided rapidly, and large sedimentary wedges prograded towards the west and south, possibly as a consequence of Neogene uplift in the present onshore areas to the east (Fig. 3; Dalhoff *et al.* 2003; Japsen *et al.* 2005; Bonow *et al.* 2007 – this volume).

Petroleum systems and prospectivity

Based on seismic interpretation, depth conversion using seismic velocities, sonic log data from the wells and the thermal maturity gradient from selected wells, the most likely source rock intervals (mid-Cretaceous and Lower Paleocene) seem to be mature in large parts of the region (Fig. 4), though seismic interpretation is difficult.

In particular the Aasiaat Basin, the Aasiaat Structural Trend, the North Ungava Basin, the Ikermiut Basin, the Sisimiut Basin and the Ilulissat Graben (Fig. 1) may have adequate dimensions and depths to have potential as kitchens for hydrocarbon generation, with the potential also depending on factors such as source rocks being present in sufficient quality and quantity. This study indicates that the interpreted

source rock intervals possibly came into the oil window after mid-Miocene time, subsequent to the formation of the main structural closures providing a favourable timing for charging.

In the interpreted Cretaceous and Cenozoic sections, amplitude anomalies are locally observed and may be interpreted as DHIs (such as e.g. bright spots above the Ilulissat High in Fig. 3) that could be caused by trapped hydrocarbon. Clusters of DHIs are located especially over or near the supposed Cretaceous kitchen areas, and also locally where satellite slicks have been recorded (Fig. 4), and contribute to an indication of live petroleum systems in the offshore region.

Mapping of the Cretaceous and Palaeogene intervals and structural highs has revealed many structures. Large structural closures can be outlined both in the western part of the region (in the Aasiaat Basin, the Aasiaat Structural Trend and the Kangerluk Structure), in the eastern part of the region (both along the edge and within the Ilulissat Graben) and in the southern part of the region related to the Ikermiut Fault Zone (Fig. 4). The Cretaceous and Palaeogene structural closures are situated close to supposed kitchen areas (Fig. 4), and together with the oil seeps and reservoir quality sandstones known onshore and their supposed offshore equivalents, these elements indicate that the offshore area west and south of Disko could potentially be prospective.

Acknowledgements

The geophysical study was supported by the Bureau of Minerals and Petroleum, Government of Greenland. TGS-NOPEC and NUNAOIL A/S are thanked for permission to publish the structural maps that incorporate proprietary seismic and satellite slick data.

References

Bojesen-Koefoed, J.A., Christiansen, F.G., Nytoft, H.P. & Pedersen, A.K. 1999: Oil seepage onshore West Greenland: evidence of multiple source rocks and oil mixing. In: Fleet, A.J. & Boldy, S.A.R. (eds): Petroleum geology of Northwest Europe: proceedings of the 5th conference, 305–314. London: Geological Society.

Bojesen-Koefoed, J.A., Nytoft, H.P. & Christiansen, F.G. 2004: Age of oils in West Greenland: Was there a Mesozoic seaway between Greenland and Canada? Geological Survey of Denmark and Greenland Bulletin **4**, 49–52.

Bojesen-Koefoed, J.A., Bidstrup, T., Christiansen, F.G., Dalhoff, F., Gregersen, U., Nytoft, H.P., Nøhr-Hansen, H., Pedersen, A.K. & Sønderholm, M. 2007: Petroleum seepages at Asuk, Disko, West Greenland – implications for regional petroleum exploration. Journal of Petroleum Geology **30**, 219–236.

Bonow, J.M., Japsen, P., Green, P.F., Wilson, R.F., Chalmers, J.A., Klint, K.E., van Gool, J.A.M., Lidmar-Bergström, K. & Pedersen, A.K. 2007: A multi-disciplinary study of Phanerozoic landscape development in West Greenland. Geological Survey of Denmark and Greenland Bulletin **13**, 41–44.

Chalmers, J.A. & Pulvertaft, T.C.R. 2001: Development of the continental margins of the Labrador Sea – a review. In: Wilson, R.C.L. *et al.* (eds): Non-volcanic rifting of continental margins: a comparison of evidence from land and sea. Geological Society Special Publication (London) **187**, 79–107.

Chalmers, J.A., Pulvertaft, T.C.R., Christiansen, F.G., Larsen, H.C., Laursen, K.H. & Ottesen, T.G. 1993: The southern West Greenland continental margin: rifting history, basin development, and petroleum potential. In: Parker, J.R. (ed.): Petroleum geology of NW Europe: proceedings of the 4th conference, 915–931. London: Geological Society.

Chalmers, J.A., Christiansen, F.G., Sønderholm, M., Olsen, J.C., Myklebust, R. & Schønwandt, H.K. 2001: Geological information base growing on North Atlantic rift basins. Data developed for Greenland licensing. Offshore **61**(11), 87–89, 100.

Dalhoff, F., Chalmers, J.A., Gregersen, U., Nøhr-Hansen, H., Rasmussen, J.A. & Sheldon, E. 2003: Mapping and facies analysis of Paleocene–Mid-Eocene seismic sequences, offshore southern West Greenland. Marine and Petroleum Geology **20**, 935–986.

Dalhoff, F., Larsen, L.M., Ineson, J.R., Stouge, S., Bojesen-Koefoed, J.A., Lassen, S., Kuijpers, A., Rasmussen, J.A. & Nøhr-Hansen, H. 2006: Continental crust in the Davis Strait: new evidence from seabed sampling. Geological Survey of Denmark and Greenland Bulletin **10**, 33–36.

Dam, G. 2002: Sedimentology of magmatically and structurally controlled outburst valleys along rifted volcanic margins; examples from the Nuussuaq Basin, West Greenland. Sedimentology **49**, 505–532.

Dam, G. & Sønderholm, M. 1998: Sedimentological evolution of a fault-controlled Early Paleocene incised-valley system, Nuussuaq Basin, West Greenland. In: Shanley, K.W. & McCabe, P.J. (eds): Relative role of eustasy, climate, and tectonism in continental rocks. Society for Sedimentary Geology (SEPM) Special Publication **59**, 109–121.

Dam, G., Nøhr-Hansen, H., Pedersen, G.K. & Sønderholm, M. 2000: Sedimentary and structural evidence of a new early Campanian rift phase in the Nuussuaq Basin, West Greenland. Cretaceous Research **21**, 127–154.

Gregersen, U. & Bidstrup, T. in press: Structures and hydrocarbon prospectivity in the northern Davis Strait area, offshore West Greenland. Petroleum Geoscience.

Japsen, P., Green, P.F. & Chalmers, J.A. 2005: Separation of Palaeogene and Neogene uplift on Nuussuaq, West Greenland. Journal of the Geological Society (London) **162**, 299–314.

Nøhr-Hansen, H., Piasecki, S., Rasmussen, J.A. & Sheldon, E. 2000: Biostratigraphy of well 6354/4-1 (Qulleq-1), West Greenland. Danmarks og Grønlands Geologiske Undersøgelse Rapport **2000/101**, 81 pp.

Scherstén, A. & Sønderholm, M. 2007: Provenance of Cretaceous and Paleocene sandstones in the West Greenland basins based on detrital zircon dating. Geological Survey of Denmark and Greenland Bulletin **13**, 37–41.

Skaarup, N. 2002: Evidence for continental crust in the offshore Palaeogene volcanic province, central West Greenland. Geology of Greenland Survey Bulletin **191**, 97–102.

Skaarup, N., Chalmers, J.A. & White, D. 2000: An AVO study of a possible new hydrocarbon play, offshore central West Greenland. American Association of Petroleum Geologists Bulletin **84**, 174–182.

Authors' address

Geological Survey of Denmark and Greenland, Øster Voldgade 10, DK-1350 Copenhagen K, Denmark. E-mail: *ug@geus.dk*

Provenance of Cretaceous and Paleocene sandstones in the West Greenland basins based on detrital zircon dating

Anders Scherstén and Martin Sønderholm

The extensive and very deep ?Jurassic/Cretaceous–Palaeogene sedimentary basins offshore West Greenland have a significant petroleum exploration potential. This is particularly true for the offshore region west of Disko and Nuussuaq where a live petroleum system has been documented for many years. At present, stratigraphic knowledge in this area is almost non-existent and analogue studies from onshore areas and offshore exploration wells to the south are therefore crucial to understanding the distribution and quality of possible reservoir rocks in the Disko–Nuussuaq offshore area.

One of the main risk parameters in petroleum exploration in this region is the presence of an adequate reservoir rock. Tectonostratigraphic considerations suggest that several sand-prone stratigraphic levels are probably present, but their provenance and reservoir quality are at present poorly known both onshore and offshore.

A sediment provenance study including zircon provenance U-Pb dating and whole-rock geochemical analysis was therefore initiated by the Geological Survey of Denmark and Greenland (GEUS) in preparation for the Disko West Licensing Round 2006 (Scherstén *et al.* 2007). The main aims of this study were to:

1. Characterise the source areas and dispersal patterns for the various sandstone units of Cretaceous–Paleocene age in the Nuussuaq Basin and compare these with sandstone units in selected West Greenland offshore exploration wells (Figs 1, 2), employing advanced zircon provenance U-Pb dating using laser ablation inductively coupled plasma mass spectrometry (LA-ICP-MS; cf. Frei *et al.* 2006).
2. Detect possible changes in sediment source with time, e.g. local versus regional sources.

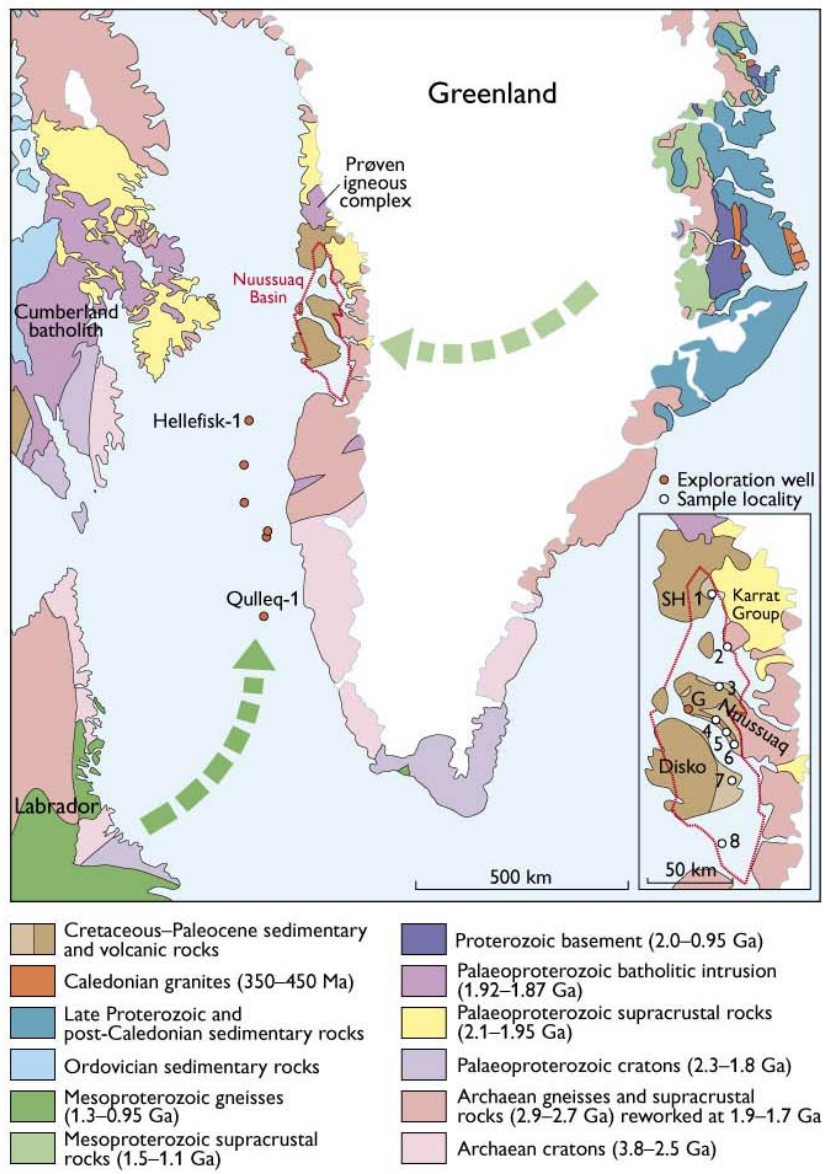

Fig. 1. Simplified geological map of eastern Canada and Greenland (modified from Escher & Pulvertaft 1995 and St-Onge *et al.* 2006). Greenland is shown in a Paleocene pre-drift position (from Oakey 2005, p. 222). Arrows indicate possible source of Grenvillian age components in West Greenland zircon samples. Inset shows sampled localities in the Nuussuaq Basin; **1**, Itsaku on Svartenhuk Halvø (**SH**); **2**, Upernivik Ø; **3**, Ikorfat; **4**, Paatuut; **5**, Kingittoq; **6**, Atanikerluk; **7**, Pingu and **8**, Grønne Ejland. Sampled wells are GRO#3 (**G**), Hellefisk-1 and Qulleq-1.

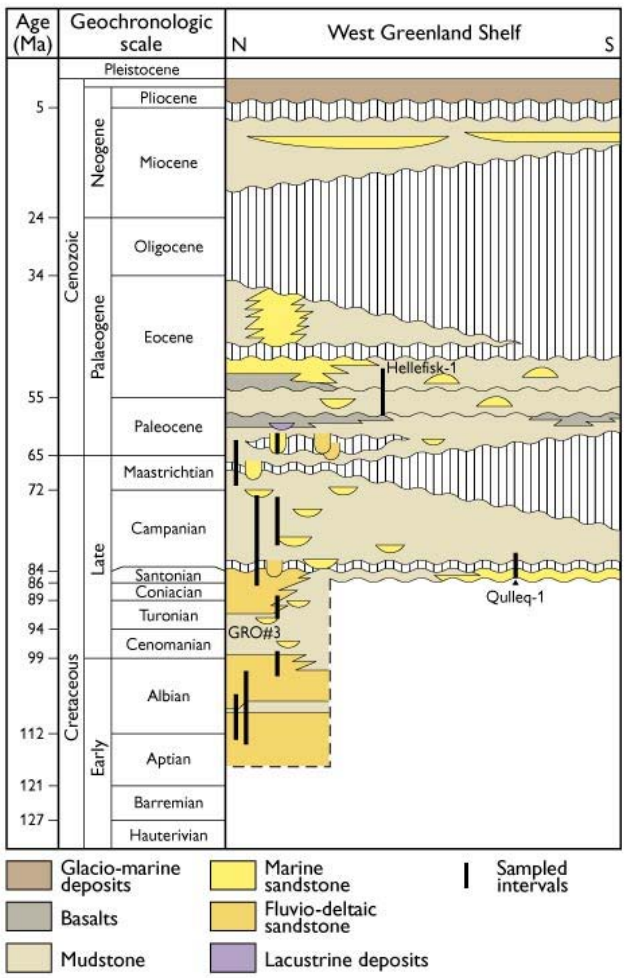

Fig. 2. Simplified stratigraphic scheme of the Nuussuaq Basin and West Greenland offshore region showing stratigraphic distribution of analysed samples.

Zircon as a provenance tool is receiving increasing attention and has proven to be a powerful indicator of clastic sediment sources, a tracer of the Earth's oldest materials, and a tracer of continental crust-forming processes (Froude *et al.* 1983; Williams & Claesson 1987; Dodson *et al.* 1988; Fedo *et al.* 2003; Hawkesworth & Kemp 2006). Zircon is common in continental rocks and it is assumed that its distribution in sediments will normally represent the source rocks. Although there are several complications, the sediment zircon U-Pb age frequency should in general terms mirror the relative proportions of different source materials. This assumption is particularly important if exotic components can be identified, as their frequency will provide an estimate of the exotic influx: it may also be essential in tracing sediment paths that affect the detrital compositions and subsequent diagenetic history of possible hydrocarbon reservoir rocks.

Cretaceous sediment provenance

It is assumed that the age structure of the North Atlantic cratons surrounding the study area is well enough known to constrain the origin of the source components that contributed to the sediments. Archaean gneisses that range from 3850 to 2600 Ma (Hollis *et al.* 2006) dominate southern West Greenland. Important peaks occur at 3600, 3100, 2900 and 2700 Ma. Farther north, the Archaean basement was reworked during the Nagssugtoqidian/Rinkian orogeny, which adds an age peak centred at 1900–1750 Ma (Figs 1, 3; Connelly *et al.* 2000).

As part of this study, 4262 grains were dated from 65 sediment samples from eight localities in the Nuussuaq Basin and three exploration wells (Fig. 1; Scherstén *et al.* 2007). Data that are >10% discordant were filtered out as they are more likely to be disturbed by common Pb contamination, ancient Pb-loss and mixed domains. The remaining 2735 grains display a relative age distribution that is dominated by age peaks between ~2500–3200 Ma (Fig. 3). There is also a peak at ~3600 Ma, which constitutes several samples suggesting that 3600 Ma age components are perhaps more abundant than those from the well-known Godthåbsfjord area (Friend & Nutman 2005; Hollis *et al.* 2006). A ~1900

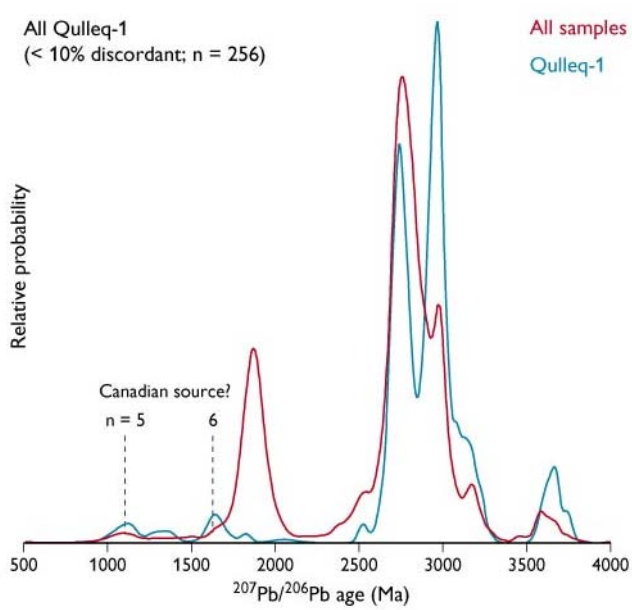

Fig. 3. Relative $^{207}Pb/^{206}Pb$ age distribution of 2735 <10% discordant zircon grains from the Cretaceous–Palaeogene sediments in this study (red curve). The relative probability reflects the likelihood of finding any given age, although the ~1900 Ma peak is overrepresented due to sampling bias. Zircon ages from the Qulleq-1 well show small but significant peaks at ~1600–1700 and ~1100 Ma (n is the number of grains that are within error of 1600 and 1100 Ma, respectively). These appear to be coupled and may have been either derived from East Greenland or the Canadian Shield. See text for further discussion.

Ma peak is also distinct, but is probably overrepresented due to sampling bias through the many samples taken at Itsaku where this age component is strongly represented in comparison to the sediments farther south (see discussion below). The 1900 Ma peak is slightly asymmetric with a tail towards younger ages and an age component around 1600–1700 Ma. The overall age distribution is in excellent agreement with a source from the West Greenland crystalline basement; and the zircon data support the existing depositional models indicating that a major deltaic system drained into the Nuussuaq Basin from the east-south-east during Cretaceous–Paleocene time (Pedersen & Pulvertaft 1992).

A small but significant peak at ~1100 Ma suggests a distal component that is not readily explained by derivation from the West Greenland crystalline basement as described above. This component seems to be associated with the 1600–1700 Ma occurrence noted above (Fig. 3). Two possible sources can explain the dual peaks: from East Greenland or Labrador (Fig. 1). If an East Greenland origin is favoured, it would be anticipated that this signature would also be associated with Caledonian ages between 380 and 480 Ma, which have not yet been identified (Figs 1, 3). Given the large number of grains analysed, it would be expected that even a very small contribution would have been detected suggesting Labrador as the most likely source for the 1100 Ma peak. A southern, Labrador source for the 1100 Ma component in the Qulleq-1 well is corroborated by the absence of the 1900 Ma peak that is ubiquitous in the Nuussuaq Basin to the north (Fig. 4). The samples from the Qulleq-1 well are dominated by Archaean ages without contributions from rocks reworked during the Nagssugtoqidian/Rinkian orogenic event.

In the Nuussuaq Basin the 1100 Ma component is very rare in the onshore, deltaic facies and occurs almost exclusively in the deep-water deposits in accordance with a longshore transport component from the south as the source of this component. However, current data from turbidite channel units on western Nuussuaq show transport directions towards the south (Dam & Sønderholm 1994). It is not possible to explain this apparent discrepancy based on the present database. More data including the other offshore wells will be needed to elucidate the possible interconnections and transport paths in the West Greenland offshore basins.

Paleocene point source provenance on Svartenhuk Halvø

A set of samples was collected on Itsaku on Svartenhuk Halvø where a major hiatus separates an Upper Albian to Lower Cenomanian deltaic succession from an Upper Campanian to Paleocene marine turbidite succession. The detrital zircon age

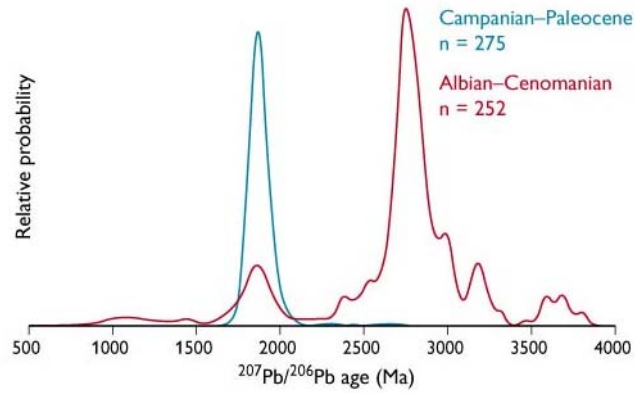

Fig. 4. Relative probability diagram for $^{207}Pb/^{206}Pb$ ages for zircon from Upper Albian – Cenomanian deltaic sediments (red) and Upper Campanian/Maastrichtian – Paleocene marine sediments (blue) on Itsaku, Svartenhuk Halvø. The deltaic deposits display a pattern that is typical for the sediments in the Nuussuaq Basin, whereas the constrained pattern of the overlying marine deposits is unique and seems to require a single point source.

distribution in the deltaic succession is typical for the Nuussuaq Basin and dominated by a distinct peak at ~2800 Ma; this is flanked by scattered peaks between 2400 and 3200 Ma (Fig. 4), as well as significant peaks at 3600–3800 Ma representing Eoarchaean components. A 1900 Ma peak is another typical feature of the Nuussuaq Basin sediments, whereas the occurrences of 1100 and 1600–1700 Ma peaks are more intermittent (see above). The overall pattern is in good agreement with that of the general West Greenland Cretaceous population and deltaic deposition from the east-south-east.

The zircon age distribution of the overlying turbidite succession is in stark contrast to the lower section (Fig. 4). Here, the zircon population forms a single, well-defined ~1900 Ma peak with an apparent normal distribution indicative of a single point source with respect to zircon. The only known source that fits this distribution is the 1869 ± 9 Ma Prøven igneous complex (Fig. 1; Thrane *et al.* 2005). Assuming the Prøven igneous complex forms a single source to the upper part of the succession, a Tukey's biweight mean of 1872 ± 4 Ma (n = 275) can be calculated, which is in excellent agreement with the Prøven igneous complex. A few grains scatter towards 2700 Ma, which likely reflects inherited components, in accordance with its derivation from lower continental crust (Thrane *et al.* 2005).

Trace element systematics in zircon may provide further constraints on zircon origin in provenance studies (Hoskin & Ireland 2000). However, several hurdles need to be overcome. For instance, many features are shared intimately between zircon that are derived from widely different sources (Hoskin & Ireland 2000), and in a detrital population each grain has

to be treated separately, as a common age does not necessarily imply the same source rock, and by inference, the same crystallisation processes or conditions. Nevertheless, it is assumed here that zircon from the upper part of the section represents one population that was derived from the Prøven igneous complex. Trace element abundances were determined for 138 zircon grains from this part of the section and contrasted against Archaean (n = 424) zircon grains from other stratigraphic levels. As expected, there are no systematic variations with age, which would require an age dependent systematic change in zircon crystallisation processes. Titanium in zircon thermometry (Watson *et al.* 2006) enables calculation of zircon crystallisation temperatures. The upper zircon population yields a mean temperature of 845 ± 19°C (± $2\sigma_{mean}$; n = 93; GJ-1 standard reproducibility 668 ± 30°C 2σ n = 17), which is similar to zircon saturation temperatures of 790– 880°C (n = 4) calculated from bulk rock data and the independently estimated intrusion temperature of the Prøven igneous complex (Thrane *et al.* 2005). The Prøven igneous complex is inferred to have been derived from a lower continental crust source as reflected by significantly negative Eu-anomalies from a plagioclase residue (Eu/Eu* ~0.45; Thrane *et al.* 2005). This appears to be reflected by the zircon population, which has a mean of 0.23 ± 0.03 (± $2\sigma_{mean}$; n = 93; GJ-1 standard reproducibility 0.96 ± 0.06 2σ n = 23). The values contrast with the average Archaean population (Eu/Eu* = 0.49 ± 0.03 $2\sigma_{mean}$; n = 257), which is assumed to be dominated by rocks such as tonalite–trondhjemite–granodiorite (TTG) suites that have Eu/Eu* ~1.0. Thus, the zircon population of the Upper Campanian to Paleocene marine turbidite succession seems to form a single population that is in accordance with derivation from the Prøven igneous complex. This implies a major change in depositional transport direction compared to the underlying Lower Cretaceous deltaic deposits from a south-eastern and eastern source to a northern source.

Acknowledgement

The project was supported by the Bureau of Minerals and Petroleum, Government of Greenland.

References

Connelly, J.N., van Gool, J.A.M. & Mengel, F.C. 2000: Temporal evolution of a deeply eroded orogen: the Nagssugtoqidian Orogen, West Greenland. Canadian Journal of Earth Sciences **37**, 1121–1142.

Dam, G. & Sønderholm, M. 1994: Lowstand slope channels of the Itilli succession (Maastrichtian – lower Paleocene), Nuussuaq, West Greenland. Sedimentary Geology **94**, 49–71.

Dodson, M.H., Compston, W., Williams, I.S. & Wilson, J.F. 1988: A search for ancient detrital zircons in Zimbabwean sediments. Journal of the Geological Society (London) **145**, 977–983.

Escher, J. & Pulvertaft, T.C.R. 1995: Geological map of Greenland, 1 : 2 500 000. Copenhagen: Geological Survey of Greenland.

Fedo, C.M., Sircombe, K.N. & Rainbird, R.H. 2003: Detrital zircon analysis of the sedimentary record. In: Hanchar, J.M. & Hoskin, P.W.O. (eds): Zircon. Reviews in Mineralogy and Geochemistry **53**, 277–303.

Frei D., Hollis J.A., Gerdes A., Harlov D., Karlsson C., Vasquez P., Franz G., Johansson L. & Knudsen, C. 2006: Advanced *in-situ* trace element and geochronological microanalysis of geomaterials by laser ablation techniques. Geological Survey of Denmark and Greenland Bulletin **10**, 25–28.

Friend, C. & Nutman, A. 2005: New pieces to the Archaean terrane jigsaw puzzle in the Nuuk region, southern West Greenland: steps in transforming a simple insight into a complex regional tectonothermal model. Journal of the Geological Society (London) **162**, 147–162.

Froude, D.O., Ireland, T.R., Kinny, P.D., Williams, I.S., Compston, W., Williams, I.R. & Myers, J.S. 1983: Ion microprobe identification of 4000–4200 Myr-old terrestrial zircons. Nature **304**, 616–618.

Hawkesworth, C.J. & Kemp, A.I.S. 2006: Evolution of the continental crust. Nature **443**, 811–817.

Hollis, J.A., Frei, D., van Gool, J.A.M., Garde, A.A. & Persson, M. 2006: Using zircon geochronology to resolve the Archaean geology of southern West Greenland. Geological Survey of Denmark and Greenland Bulletin **10**, 49–52.

Hoskin, P.W.O. & Ireland, T.R. 2000: Rare earth element chemistry of zircon and its use as a provenance indicator. Geology **28**, 627–630.

Oakey, G.N. 2005: Cenozoic evolution and lithosphere dynamics of the Baffin Bay – Nares Strait region of Arctic Canada and Greenland, 233 pp. Amsterdam: Vrije Universiteit.

Pedersen, G.K. & Pulvertaft, T.C.R. 1992: The nonmarine Cretaceous of the West Greenland Basin, onshore West Greenland. Cretaceous Research **13**, 263–272.

Scherstén, A., Sønderholm, M. & Steenfelt, A. 2007: Provenance of West Greenland Cretaceous and Paleocene sandstones and stream sediment samples based on U-Pb dating of detrital zircon: data and results. Danmarks og Grønlands Geologiske Undersøgelse Rapport **2007/21**, 121 pp.

St-Onge, M. (compiler), van Gool, J.A.M., Garde, A.A. & Scott, D.J. 2006: Correlations of Archaean to Mesoproterozoic units and structures across Baffin Bay, Davis Strait and the Labrador Sea: Kangerlussuaq workshop 2005 report and literature review. Danmarks og Grønlands Geologiske Undersøgelse Rapport **2006/6**, 20–57.

Thrane, K., Baker, J., Connelly, J. & Nutman, A. 2005: Age, petrogenesis and metamorphism of the syn-collisional Prøven igneous complex, West Greenland. Contributions to Mineralogy and Petrology **149**, 541–555.

Watson, E.B., Wark, D.A. & Thomas, J.B. 2006: Crystallisation thermometers for zircon and rutile. Contributions to Mineralogy and Petrology **151**, 413–433.

Williams, I.S. & Claesson, S. 1987: Isotopic evidence for the Precambrian provenance and Caledonian metamorphism of high grade paragneisses from the Seve Nappes, Scandinavian Caledonides: II. Ion microprobe zircon U-Th-Pb. Contributions to Mineralogy and Petrology **97**, 205–217.

Authors' address

Geological Survey of Denmark and Greenland, Øster Voldgade 10, DK-1350 Copenhagen K, Denmark. E-mail: *asch@geus.dk*

A multi-disciplinary study of Phanerozoic landscape development in West Greenland

Johan M. Bonow, Peter Japsen, Paul F. Green, Robert W. Wilson, James A. Chalmers, Knud Erik S. Klint, Jeroen A.M. van Gool, Karna Lidmar-Bergström and Asger Ken Pedersen

The western margin of the Greenland craton has been much less stable in the Phanerozoic than previously thought. This new insight has come from close integration of independent data sets: geomorphological analysis of large-scale landscapes, apatite fission track analysis (AFTA), onshore and offshore stratigraphy and analysis of onshore fault and fracture systems. Each data set records specific and unique parts of the event chronology and is equally important to establish a consistent model. A key area for understanding the Mesozoic–Cenozoic landscape evolution and into the present is the uplifted part of the Nuussuaq Basin, where remnants of planation surfaces cut across the Cretaceous to Eocene sedimentary and volcanic rocks. Our integrated analysis concluded that the West Greenland mountains were formed by late Neogene tectonic uplift (Fig. 1) and also provided new insight into early Phanerozoic development. To understand our model, we present the different methods and the results that can be deduced from them.

Basic concepts

The mapping of volcanic and sedimentary successions within the Nuussuaq Basin is crucial for understanding the late Mesozoic–Palaeogene landscape development (e.g. Dam *et al.* 1998; Chalmers *et al.* 1999; Dalhoff *et al.* 2003). Especially important for the landscape analysis is the availability of maps showing vertical geological sections (Pedersen *et al.* 2006). Exploration for hydrocarbons has resulted in many seismic data, and several deep wells have been drilled both onshore and offshore (e.g. Chalmers *et al.* 1999; Piasecki 2003).

Landscape analysis aims at setting up a relative tectonic event chronology through identification and mapping of both extensive baselevel governed surfaces and re-exposed surfaces. These palaeosurfaces, formed by erosion in climates or tectonic settings different from the present, cut across bedrock of different ages and can be arranged in chronological order based on (1) stratigraphical relationships with cover rocks, (2) geometrical relationships between different palaeosurfaces, and (3) analysis of the detailed forms of the large-scale landscapes, reflecting climatic-driven formation processes. The baselevel is fundamental, as lowering of baselevel (an uplift event) causes valley incision and initiation of surface formation while raising baselevel (subsidence) causes palaeosurfaces to be preserved below cover rocks (Bonow 2005; Bonow *et al.* 2006a, b).

AFTA is a method for defining the temperature history of rock samples, based on analysis of radiation damage features ('fission tracks') produced by spontaneous fission of ^{238}U atoms within apatite crystals. Tracks are produced continu-

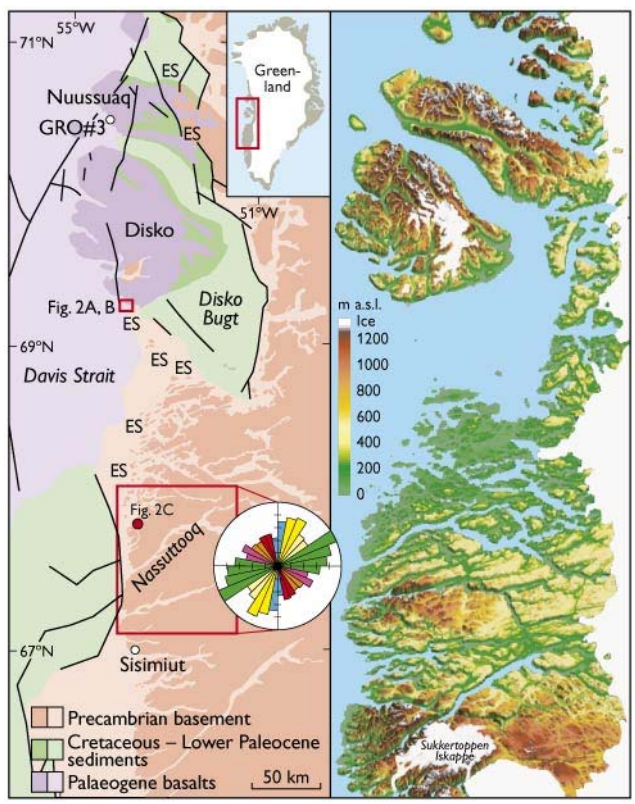

Fig. 1. **Left**: Study area with Precambrian basement and cover rocks that are crucial for determining the relative age of palaeosurfaces. The rose diagram summarises the regional lineament patterns, based on field mapping in the framed area (cf. Wilson *et al.* 2006). The relationship between lineaments onshore and offshore allows for a relative event chronology; colouring refers to timing (cf. Fig. 3). Position of GRO#3 well indicated. **ES**, etch surface of Late Mesozoic – Paleocene age. Note its position close to cover rocks. Modified from Bonow *et al.* (2006a). **Right**: Topography. A regionally developed Oligocene–Miocene planation surface was differentially uplifted on separate tectonic blocks in the Neogene. Today it is close to the summit level and has been tilted in different directions.

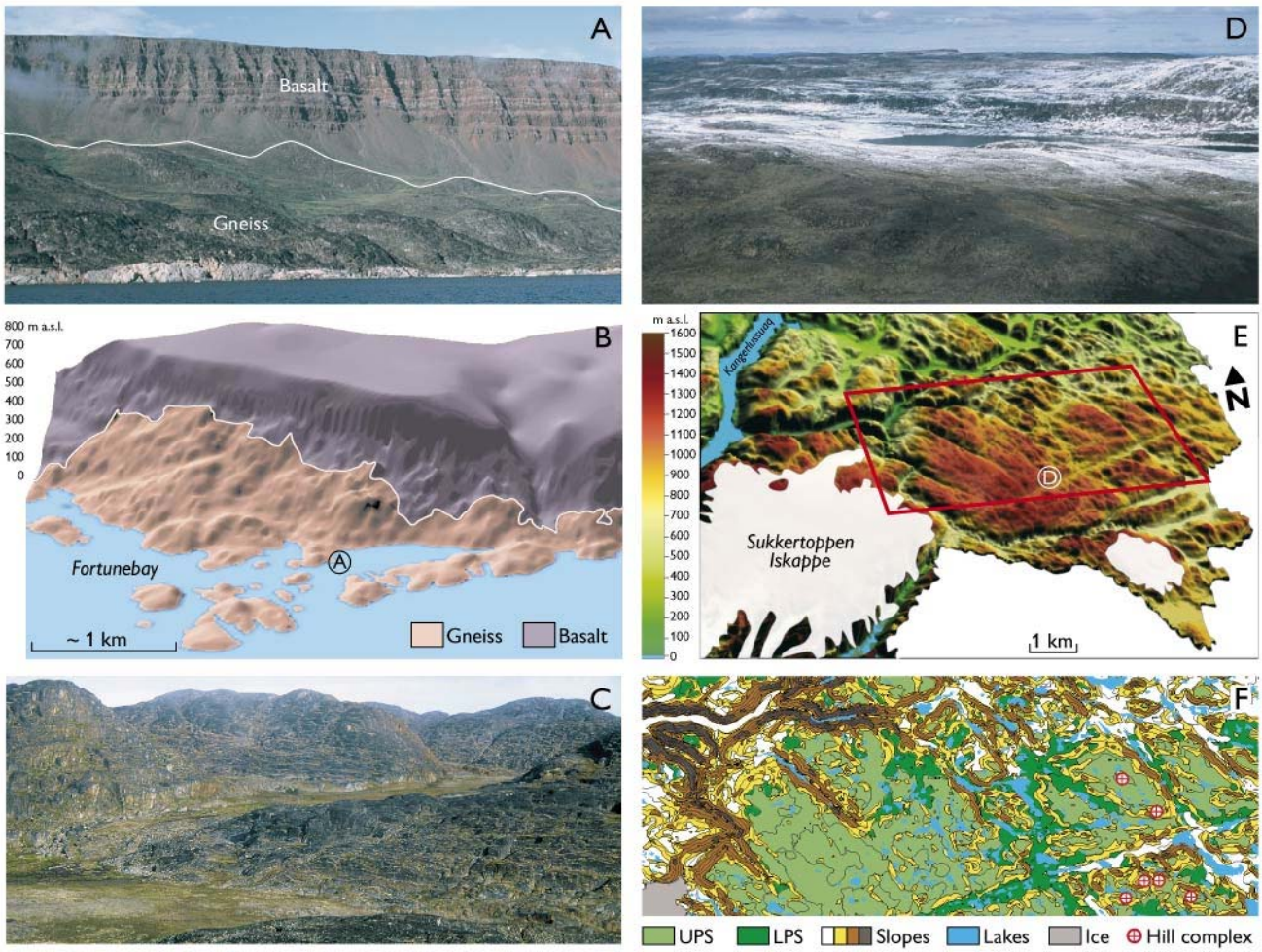

Fig. 2. Views of the etch surface (ES) and the upper and lower planation surfaces (UPS and LPS) formed in basement rocks. **A**: The re-exposed ES at Fortunebay, southern Disko. The white line shows the approximate border between Paleocene basalt and gneiss. Area location in Fig. 1. Photo location in B. **B**: 3D model of the Fortunebay area. Note the Oligocene–Miocene planation surface at high elevation across the basalt. Modified from Bonow (2005). **C**: The stripped ES at Nassuttooq. Location in Fig 1. **D**: The Oligocene–Miocene UPS east of Sukkertoppen Iskappe cuts across Precambrian basement. Location in E. **E**: 3D model showing the well-preserved UPS east of Sukkertoppen Iskappe. Red frame indicates position of map in F. **F**: Map showing UPS and LPS. Hill complexes rising above the UPS may be part of a sub-Ordovician peneplain. Modified from Bonow *et al.* (2006a).

ously over geological time, but are shortened at a rate that depends on the prevailing temperature, until at temperatures higher than *c.* 120°C tracks are totally erased ('annealing'). Fission track age and track length data provide the basis for estimating the time at which a sample began to cool from a palaeo-thermal maximum as well as the magnitude of the maximum palaeotemperature. Cooling can be interpreted as either change of heat-flow within the crust or erosion of overlying rocks (e.g. Green *et al.* 2002).

Structural analysis of faults and fracture systems aims to establish a relative chronology of tectonic movements that have changed the stress field, as a change will lead to the formation of a new set of faults and possibly the reactivation of older ones. Structural analysis of the area between Nuussuaq and Sisimiut forms the basis for a regional model, explaining different tectonic movements through time (Wilson *et al.* 2006).

Key results

Geology. The Cretaceous–Palaeogene sedimentary and volcanic successions within the Nuussuaq Basin record deep incision of valleys in the Maastrichtian and early Paleocene (e.g. Dam *et al.* 1998), subsidence during volcanism, and deposition of marine sediments within the volcanic succession now at high elevation (Piasecki *et al.* 1992), which are evidence that both uplift and subsidence of kilometre scale took place during and after rifting (Chalmers *et al.* 1999). During the Palaeogene the basalts offshore (and probably onshore, Japsen *et al.* 2006a) became buried below sediments. Seismic sections west of Nuussuaq show that Palaeogene and younger sequences have been tilted seawards and truncated at a late date (Chalmers 2000).

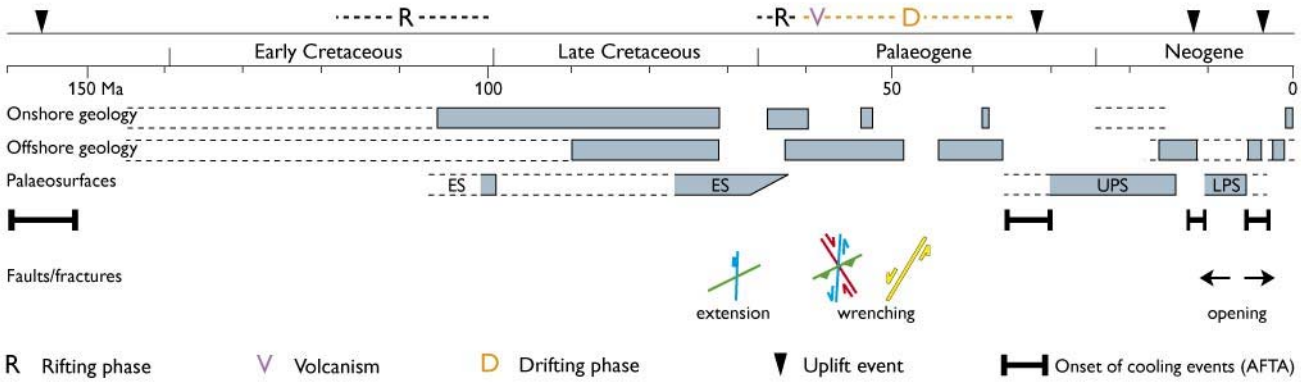

Fig. 3. Event chronology for central West Greenland based on data from the separate disciplines. Integration of these data sets shows that the western margin of the Greenland craton has been less stable than previously thought. Shaded intervals indicate the proven age of geological units, onshore and offshore, and the estimated time required for formation of palaeosurfaces. Horizontal arrows indicate extensional reactivation and opening of vertical fault and fracture systems. The associated intervals indicated by stippled lines illustrate the probable geological age range and uncertainties in dating palaeo-surfaces. **ES**, etch surfaces; **UPS**, upper planation surface; **LPS**, lower planation surface. Data from Piasecki *et al.* (1992); Dam *et al.* (1998); Chalmers *et al.* (1999); Chalmers (2000); Dalhoff *et al.* (2003); Piasecki (2003); Bonow (2005); Japsen *et al.* (2005, 2006a); Bonow *et al.* (2006a, b, c); Pedersen *et al.* (2006) and Wilson *et al.* (2006).

Geomorphology. Three different palaeosurfaces in the Precambrian basement have been identified in West Greenland, viz. a surface formed by deep weathering and stripping of the weathering mantle (etch surface, ES), and an upper and lower planation surface (UPS and LPS; Bonow 2005; Bonow *et al.* 2006a, b). The ES is characterised by distinct hills (Fig. 2A) and received its final shape in part prior to the deposition of Upper Cretaceous deltaic sediments and in part prior to the extrusion of Palaeogene basalts (Fig. 2B). The ES can mainly be identified at low elevations and close to cover rocks (Figs 1, 2C). The UPS has low relative relief compared to the ES (Fig. 2D) and must be younger as it cuts across both mid-Eocene basalts and the etch surface. The UPS forms the summits of differentially tilted, fault-bounded tectonic blocks. A planation surface cannot be formed as an inclined plain because any tilt would cause valleys to incise and the relief to rejuvenate towards the baselevel (Bonow *et al.* 2006b, fig. 6). The LPS was formed in response to lowered baselevel (uplift) and became incised into the UPS (Fig. 2E). Furthermore, summits of distinct hill complexes above the UPS (Fig. 2F) may relate to a sub-Ordovician palaeosurface because remnants of Lower Palaeozoic rocks suggest that West Greenland may have had a long-lasting Palaeozoic cover (Bonow *et al.* 2006a). Consequently, erosion of Precambrian basement rocks has been limited since the early Palaeozoic, but this does not exclude deposition and subsequent removal of thick sequences of Phanerozoic cover rock as indicated by AFTA data.

Table 1. Onset of cooling episodes determined from AFTA data

Stratigraphic age	Onset of cooling, Ma
Cambrian / Early Ordovician	560–500
Late Devonian / Carboniferous	370–355
Triassic	230–220
Late Jurassic	160–150
Eocene–Oligocene	36–30
Late Miocene	11–10
Miocene–Pliocene	7–2

From Japsen *et al.* (2006a) and supplementary data herein.

Thermochronology. AFTA data from Cretaceous sedimentary rocks define three major Cenozoic cooling episodes, while basement samples define major Triassic and Jurassic cooling episodes (related to rifting?), and also earlier (Palaeozoic) episodes (Table 1). The deepest samples in the 3 km deep GRO#3 well on Nuussuaq are totally annealed (Fig. 1; Japsen *et al.* 2005). The progressive development of fission tracks can therefore be followed through the sedimentary section, giving a rare opportunity to resolve the details of the late Cenozoic cooling history. Oligocene cooling involved both exhumation and a decrease in basal heat flow, while Miocene and Pliocene cooling episodes were dominantly related to exhumation. The two latest cooling events constrain the cooling events into the present.

Faults and fractures. Analysis of regional lineament trends shows five main systems that fit a two-stage model (Wilson *et al.* 2006). A system of N–S- and NNW–SSE-trending normal faults reflects the fault patterns in the Davis Strait during the Late Cretaceous to Paleocene. This system was overprinted and reactivated by strike-slip faults associated with a later NNE–SSW-trending sinistral wrench system that reflects the development of the Ungava transform system during the Eocene.

The model and future implementation

Our model shows where in time independent constrained data exist and time-frames for uncertainties and lack of data (Fig. 3). The model shows that each discipline has long periods of no data, but when combined only few periods have no data representation at all. In particular, landscape analysis and AFTA data complement each other, because palaeosurfaces show that rock was exposed at the landsurface, whereas AFTA data indicate when and by how much a palaeosurface has been buried. This approach shows that the present summits were buried below up to 1 km of rocks prior to Eocene–Oligocene uplift, and that the UPS formed during the Oligocene–Miocene due to stable baselevel conditions. Similarly, uplift in the late Miocene resulted in valley incision (the LPS) and tilting of the UPS. Final uplift in the ?Pliocene resulted in the present-day mountains. Late uplift reactivated and opened the fault and fracture systems, thus facilitating both weathering and the development of a coastal escarpment (Bonow *et al.* 2006c). Our model is also used in ongoing uplift studies in South-West Greenland (Japsen *et al.* 2006b).

The integration of data from geomorphology, thermochronology, geology and fault/fracture patterns to show that the present landscape of West Greenland is the result of tectonic movements throughout the Phanerozoic with significant movements also in the Neogene and even into the present (Fig. 3). The approach presented here may be applied to understand landscape development along other passive continental margins.

Acknowledgements

This work was supported by the Carlsberg Foundation, the Bureau of Minerals and Petroleum, the Danish Natural Science Research Council, the Swedish Research Council, Arktisk Station, Stiftelsen Margit Althins stipendiefond, Svenska Sällskapet för Antropologi och Geografi and John Söderbergs stiftelse.

References

Bonow, J.M. 2005: Re-exposed basement landforms in the Disko region, West Greenland – disregarded data for estimation of glacial erosion and uplift modelling. Geomorphology **72**, 106–127.

Bonow, J.M., Lidmar-Bergström, K. & Japsen, P. 2006a: Palaeosurfaces in central West Greenland as reference for identification of tectonic movements and estimation of erosion. Global and Planetary Change **50**, 161–183.

Bonow, J.M., Japsen, P., Lidmar-Bergström, K., Chalmers, J.A. & Pedersen, A.K. 2006b: Cenozoic uplift of Nuussuaq and Disko, West Greenland – elevated erosion surfaces as uplift markers of a passive margin. Geomorphology **80**, 325–337.

Bonow, J.M., Klint, K.E.S. & Japsen, P. 2006c: The Nordre Isortoq Escarpment. Field report summer 2005. Danmarks og Grønlands Geologiske Undersøgelse Rapport **2006/13**, 68 pp.

Chalmers, J.A. 2000: Offshore evidence for Neogene uplift in central West Greenland. Global and Planetary Change **24**, 311–318.

Chalmers, J.A., Pulvertaft, C., Marcussen, C. & Pedersen, A.K. 1999: New insight into the structure of the Nuussuaq Basin, central West Greenland. Marine and Petroleum Geology **16**, 197–224.

Dalhoff, F., Chalmers, J.A., Gregersen, U., Nøhr-Hansen, H., Rasmussen, J.A. & Sheldon, E. 2003: Mapping and facies analysis of Paleocene – mid-Eocene seismic sequences, offshore southern West Greenland. Marine and Petroleum Geology **20**, 935–986.

Dam, G., Larsen, M. & Sønderholm, M. 1998: Sedimentary response to mantle plumes: implications from Paleocene onshore successions, West and East Greenland. Geology **26**, 207–210.

Green, P.F., Duddy, I.R. & Hegarty, K.A. 2002: Quantifying exhumation from apatite fission-track analysis and vitrinite reflectance data: precision, accuracy and latest results from the Atlantic margin of NW Europe. In: Doré, A.G. *et al.* (eds): Exhumation of the North Atlantic margin: timing, mechanisms and implications for petroleum exploration. Geological Society Special Publication (London) **196**, 331–354.

Japsen, P., Green, P.F. & Chalmers, J.A. 2005: Separation of Palaeogene and Neogene uplift on Nuussuaq, West Greenland. Journal of the Geological Society (London) **162**, 299–314.

Japsen, P., Bonow, J.M., Green, P.F., Chalmers, J.A. & Lidmar-Bergström, K. 2006a: Elevated, passive continental margins: long-term highs or Neogene uplifts? New evidence from West Greenland. Earth and Planetary Science Letters **248**, 315–324.

Japsen, P., Bonow, J.M., Peulvast, J.-P. & Wilson, R.W. 2006b: Uplift, erosion and fault reactivation in southern West and South Greenland. Field report summer 2006. Danmarks og Grønlands Geologiske Undersøgelse Rapport **2006/63**, 77 pp.

Pedersen, A.K., Larsen, L.M., Pedersen, G.K. & Dueholm, K.S. 2006: Five slices through the Nuussuaq Basin, West Greenland. Geological Survey of Denmark and Greenland Bulletin **10**, 53–56.

Piasecki, S. 2003: Neogene dinoflagellate cysts from Davis Strait, offshore West Greenland. Marine and Petroleum Geology **20**, 1075–1088.

Piasecki, S., Larsen, L.M., Pedersen, A.K. & Pedersen, G.K. 1992: Palynostratigraphy of the lower Tertiary volcanics and marine clastic sediments in the southern part of the West Greenland basin: implications for the timing and duration of the volcanism. Rapport Grønlands Geologiske Undersøgelse **154**, 13–31.

Wilson, R.W., Klint, K.E.S., van Gool, J.A.M., McCaffrey, K.J.W., Holdsworth, R.E. & Chalmers, J.A. 2006: Faults and fractures in central West Greenland: on-shore expression of continental break-up and sea-floor spreading in the Labrador – Baffin Bay Sea. Geological Survey of Denmark and Greenland Bulletin **11**, 185–204.

Authors' addresses

J.M.B., P.J., J.A.C., K.E.S.K. & J.A.M.v.G., *Geological Survey of Denmark and Greenland, Øster Voldgade 10, DK-1350 Copenhagen K, Denmark.*

E-mail: *jbon@geus.dk*

P.F.G., *Geotrack International, 37 Melville Road, Brunswick West, Victoria 3055, Australia.*

R.W.W., *Reactivation Research Group, Department of Earth Sciences, University of Durham, Durham, DH1 3LE, UK.*

K.L.-B., *Department of Physical Geography and Quaternary Geology, Stockholm University, SE-106 91 Stockholm, Sweden.*

A.K.P., *Geological Museum, University of Copenhagen, Øster Voldgade 5–7, DK-1350 Copenhagen K, Denmark.*

Pre-metamorphic hydrothermal alteration with gold in a mid-Archaean island arc, Godthåbsfjord, West Greenland

Adam A. Garde, Henrik Stendal and Bo Møller Stensgaard

Recently discovered volcaniclastic rocks of andesitic composition form major parts of the mid-Archaean, amphibolite facies supracrustal belts at Qussuk, on Bjørneøen and on part of Storø in western Godthåbsfjord (Fig. 1). These rocks are interpreted as an island arc that represents the onset of the magmatic accretion of the Akia terrane 3070 Ma ago; this terrane is the north-westernmost of several Archaean tectono-stratigraphic terranes in the Nuuk region, which were all amalgamated by 2720 Ma (cf. Hollis *et al.* 2006). The presence of the arc in the Akia terrane points to similarities between high-grade orthogneiss-amphibolite associations in West Greenland and lower-grade granite-greenstone terrains of other Archaean cratons e.g. in Canada and Western Australia. Volcaniclastic rocks belonging to the ancient arc have been subject to intense synvolcanic, hydrothermal alteration associated with gold-copper mineralisation especially in parts of the Qussuk area. Another important gold prospect occurs on central Storø, which is currently being explored by NunaMinerals A/S (Knudsen *et al.* 2007 – this volume). This contribution presents new field observations from some of the best preserved parts of the ancient arc at Qussuk and on Bjørneøen, while it remains unclear if the volcano-sedimentary associations and their gold mineralisation at Qussuk, Bjørneøen and the nearby Storø share a common mid-Archaean geological history.

The age and setting of the ancient arc

The eastern Akia terrane comprises *c.* 3060–3000 Ma tonalitic to trondhjemitic orthogneisses, isoclinally folded panels derived from the older andesitic arc, and granites mobilised from the orthogneisses during a late-kinematic thermal event at *c.* 2980 Ma which also led to granulite facies *P-T* conditions west of Qussuk and Bjørneøen (Garde 1997, 2007; Garde *et al.* 2000). Andesitic metavolcanic and volcano-sedimentary rocks were first reported from the eastern Akia terrane by Garde (1997) and Smith (1998). However, volcanic textures are mostly very poorly preserved, and it was not appreciated then, how widespread the andesitic arc is, and that it forms large parts of the supracrustal belts exposed at Qussuk and on Bjørneøen.

Recent age determinations of volcanic zircon grains from central Bjørneøen show that the age of the andesitic arc is 3071 ± 1 Ma (sample 479827, Garde 2007). The arc is thus marginally older than its orthogneiss host, in agreement with recently observed intrusive contacts into the supracrustal belt (Fig. 2). Similar field relationships in the adjacent Qussuk area further document that the orthogneiss precursors intruded into the arc. However, zircon from volcaniclastic rocks here, on strike with those on Bjørneøen, yields metamorphic ages of 2990–2970 Ma which coincide with the thermal maximum and associated fluid movement; only a few zircon cores approach the true volcanic age of *c.* 3070 Ma

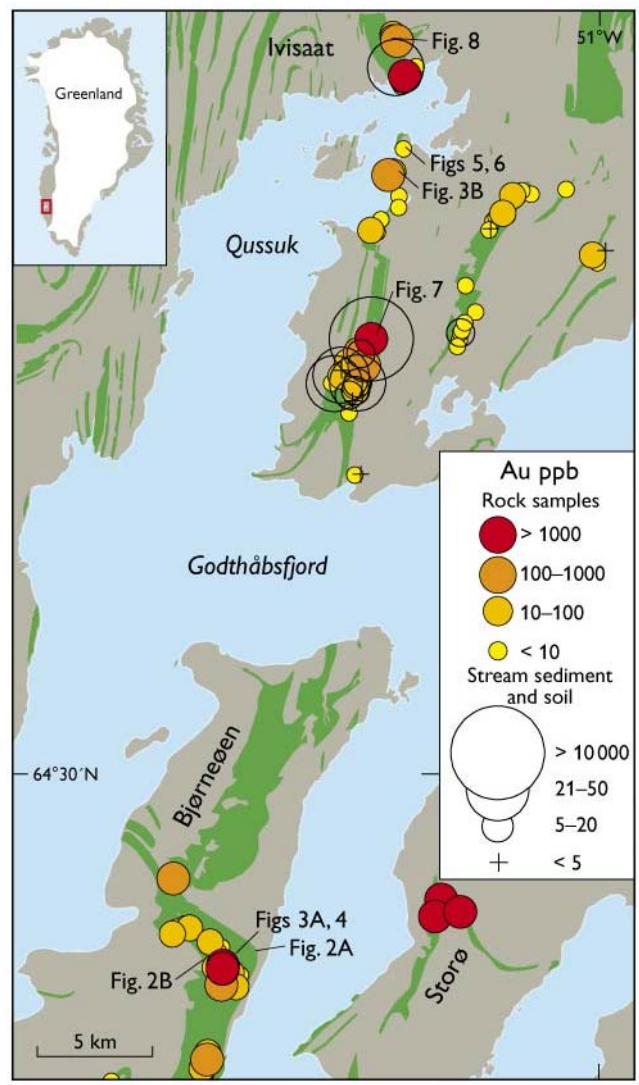

Fig. 1. Simplified map of north-western Godthåbsfjord with supracrustal belts (green), gold anomalies, and locations of Figs 2–8. Modified from Hollis (2005).

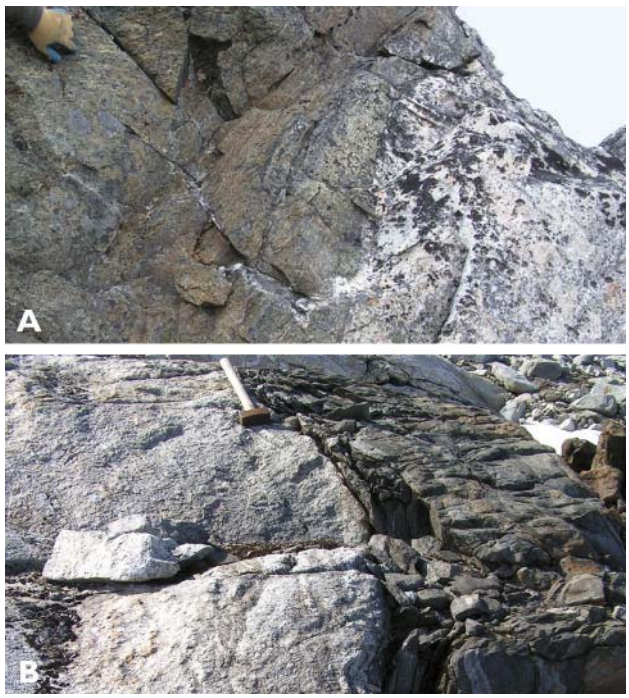

Fig. 2. Intrusive contacts at the footwall (**A**) and hanging wall (**B**) of the supracrustal belt on central Bjørneøen (see Fig. 1 for locations).

(Garde 2007). Zircon grains from yet another volcano-sedimentary rock on central Bjørneøen (Fig. 3A) yielded a range of 2908–2742 Ma ages with a cluster around 2825 Ma (sample 479745, Hollis 2005 p. 55). The 2825 Ma cluster was interpreted as the depositional age, and a complex tectonic model for central Bjørneøen was proposed with thrust-stacking of supracrustal rocks and orthogneisses of different ages and origins at the eastern margin of the Akia terrane. However, further field observations in 2006 uncovered that this sample locality lies within the same volcaniclastic sequence as the sample dated at 3071 Ma. With the established intrusive contacts of orthogneisses dated at *c.* 3065–3050 Ma (Fig. 2; Hollis 2005 pp. 30–39), this tectonic model is no longer tenable, as the supracrustal belt is older than the orthogneisses and its contacts are not tectonic. Furthermore, a duplicate sample collected at the locality of Fig. 3A by the first author in 2006 yielded a metamorphic U-Pb zircon age of 2986 ± 3.6 Ma (13 stubby, very indistinctly zoned zircon grains with Th/U <0.01; unpublished ion probe data, May 2007). Hence, the zircon grains allegedly extracted from sample 479745 seem to have been incorrectly labelled during the sample preparation.

Volcaniclastic and volcano-sedimentary rocks

The relict volcano-sedimentary arc has been intensely deformed and metamorphosed at middle to upper amphibolite grade and now mostly consists of monotonous, fine-grained, schistose andesitic rocks besides intrusive bodies of mafic–ultramafic rocks. However, small pockets of low-strain rocks with distinct volcaniclastic textures are locally well preserved on central Bjørneøen and in the Qussuk area, particularly in the cores of fold hinges. Andesitic rocks containing volcanic clasts with fiamme textures have been identified on central Bjørneøen and north-eastern Qussuk (Fig. 3), as well as rare, more or less undeformed volcano-sedimentary deposits a few tens of metres across with well-preserved sedimentary structures (Fig. 4). The recognition of the volcaniclastic environments is important, because they document widespread explosive volcanism and hence shallow subaqueous or subaerial volcanic activity in an island arc. Unfortunately, it has not been possible to reconstruct individual volcanic edifices due to the general poor state of preservation.

Synvolcanic hydrothermal alteration

Hydrothermally altered aluminous and siliceous rocks, commonly associated with disseminated iron sulphides and gold mineralisation, occur in several parts of the relict arc (Hollis 2005; Garde 2007). Unequivocal evidence that the hydrothermal alteration took place in unconsolidated volcaniclastic rocks prior to deformation and metamorphism was found

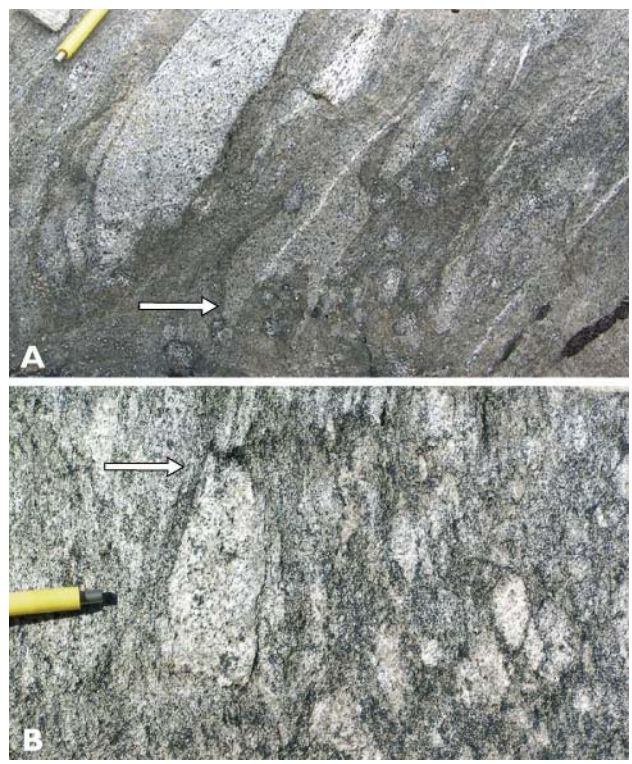

Fig. 3. Volcaniclastic rocks on central Bjørneøen (**A**) and at north-eastern Qussuk (**B**) with fiamme textures. Pen 8 mm thick. For locations see Fig. 1.

Fig. 4. Graded volcano-sedimentary rock with early brittle/ductile deformation. Central Bjørneøen (see Fig. 1 for location).

Fig. 5. Bedded metatuff at north-eastern Qussuk (see Fig. 1 for location) showing a primary contact between mafic and intermediate beds (red arrow) and a narrow rusty hydrothermal alteration zone along primary bedding contact (blue arrow).

in 2006 within the hinge zone of a large fold on the north-eastern coast of Qussuk (Fig. 1). The lower part of Fig. 5 displays several nearly undeformed beds of fine- to coarse-grained tuff (or tuffite) with granitic-pegmatitic partial melt veins. The thickest bed displays right way-up graded bedding. The contact to the overlying bed is rusty weathering and contains sporadic iron sulphides and small garnets (<5 mm), and has clearly been affected by hydrothermal activity. The very localised alteration furthermore indicates that the percolating fluid used the unconsolidated bedding contact as a convenient passageway.

There are many other examples of rocks with more widespread and more intense alteration. Most of these are also intensely deformed and difficult to recognise as hydrothermally altered, but exceptions do occur. Figure 6 shows smooth, grey metatuff hosting an irregular, interfingering, vein-like system of coarser, rusty weathering and crumbling metatuff. This is hydrothermally altered and now contains abundant quartz, biotite, garnet and iron sulphide.

Rusty weathering and variably gold-mineralised rocks, altered by synvolcanic, hydrothermal fluids and now rich in quartz, biotite, garnet and commonly sillimanite, also occur east and north of Qussuk in tracts up to several kilometres long, which have previously been mapped as aluminous metasedimentary rocks. Figure 7 shows a football-sized enclave of unaltered and undeformed amphibolitic metatuff, which is preserved inside a lens several metres across of garnet-rich rock (hydrothermally altered and metamorphosed tuff). The most intensely altered andesitic rocks now consist of massive sillimanite-fuchsite quartzite, from which most major and trace elements have been leached out except Si, Al and Ti, and very immobile elements such as Ga, Zr and rare-earth elements. Such rocks form the top of Ivisaat mountain north of Qussuk (Fig. 8), where they form a layer *c.* 5–10 m thick in the core of an isoclinal fold, surrounded by garnet-rich and sulphidic, less altered andesitic metavolcanic rocks with widespread gold mineralisation in the ppb range (the authors' unpublished data). This very specific type of hydro-

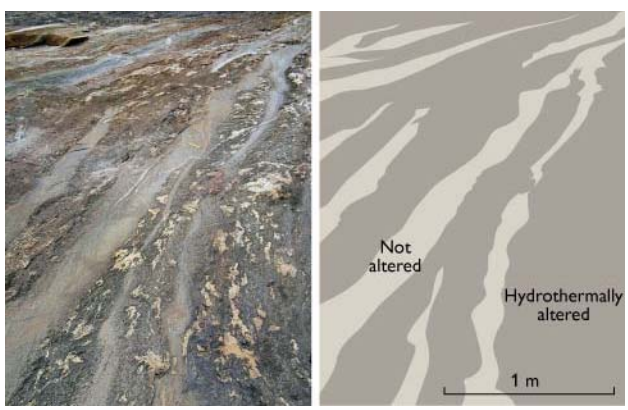

Fig. 6. Interfingering system of early hydrothermal alteration in andesitic (meta)tuff at north-eastern Qussuk (see Fig. 1 for location). Glacial striations have produced a faint oblique 'foliation' visible in the lower left of the exposure.

Fig. 7. Enclave of unaltered and undeformed metavolcanic amphibolite (arrow), surrounded by a lens of hydrothermally altered, now garnet-rich rock of similar origin. Peninsula east of Qussuk (see Fig. 1 for location). Hammershaft is *c.* 85 cm long.

Fig. 8. Folded sillimanite-fuchsite quartzite with disseminated iron sulphides, an intensely hydrothermally altered and metamorphosed rock of andesitic origin. Ivisaat mountain north of Qussuk (see Fig. 1 for location). Hammershaft is *c*. 45 cm long.

thermal alteration points to acid leaching under low pressure, a process which is very characteristic of epithermal, high-level hydrothermal systems in modern andesitic arcs, which are commonly associated with gold and copper mineralisation (e.g. Sillitoe & Hedenquist 2003). A low-pressure hydrothermal system such as found today near the tops of andesitic arcs is a prerequisite for wholesale leaching by strong acids, because higher pressures prevent the dissociation of their hydrogen ions (Sillitoe & Hedenquist 2003).

Conclusions

The *c*. 3070 Ma andesitic arc in the eastern Akia terrane and its slightly younger intrusive counterparts of tonalitic orthogneisses, combined with previous structural evidence of early crustal shortening in most of the Akia terrane, point to the existence of a convergent plate-tectonic system in the North Atlantic craton, where subduction of oceanic crust and partial melting of the subducted slab occurred at least 3070 Ma ago. The identification of the arc complex substantiates previous ideas that the orthogneisses in the Akia terrane are products of slab melting in a convergent plate-tectonic setting. In a wider context this also implies that the typical Archaean high-grade orthogneiss-amphibolite associations in West Greenland may not represent plate-tectonic environments distinct from the granite-greenstone associations found in most other Archaean cratons, but simply expose deeper sections of the same convergent systems.

The relict arc hosts widespread hydrothermally altered rocks and associated gold (-copper) mineralisation. Newly discovered field relationships show that the hydrothermal systems predated deformation and metamorphism. Furthermore, the peculiar mineralogical composition of the altered rocks combined with their gold mineralisation suggest that the hydrothermal alteration was synvolcanic and epithermal, and characteristic of the arc itself.

References

Garde, A.A. 1997: Accretion and evolution of an Archaean high-grade grey gneiss–amphibolite complex: the Fiskefjord area, southern West Greenland. Geology of Greenland Survey Bulletin **177**, 114 pp.

Garde, A.A. 2007: A mid-Archaean island arc complex in the eastern Akia terrane, Godthåbsfjord, southern West Greenland. Journal of the Geological Society (London) **164**, 565–579.

Garde, A.A., Friend, C.R.L., Nutman, A.P. & Marker, M. 2000: Rapid maturation and stabilisation of middle Archaean continental crust: the Akia terrane, southern West Greenland. Bulletin of the Geological Society of Denmark **47**, 1–27.

Hollis, J.A. (ed.) 2005: Greenstone belts in the central Godthåbsfjord region, southern West Greenland: Geochemistry, geochronology and petrography arising from 2004 field work, and digital map data. Danmarks og Grønlands Geologiske Undersøgelse Rapport **2005/42**, 215 pp.

Hollis, J.A., Frei, D., van Gool, J.A.M., Garde, A.A. & Persson, M. 2006: Using zircon geochronology to resolve the Archaean geology of southern West Greenland. Geological Survey of Denmark and Greenland Bulletin **10**, 49–52.

Knudsen, C., van Gool, J.A.M., Østergaard, C., Hollis, J.A., Rink-Jørgensen, M., Persson, M & Szilas, K. 2007: Gold hosting supracrustal rocks on Storø, West Greenland: petrogenesis and structural setting. Geological Survey of Denmark and Greenland Bulletin **13**, 17–20.

Sillitoe, R.H. & Hedenquist, J.W. 2003: Linkages between volcanotectonic settings, ore-fluid compositions, and epithermal precious metal deposits. In: Simmons, S.F. & Graham, I. (eds): Volcanic, geothermal, and ore-forming fluids; rulers and witnesses of processes within the Earth. Society of Economic Geologists Special Publication **10**, 315–343.

Smith, G.M. 1998: Geology and mineral potential of the Bjørneøen supracrustal belt, Nuukfjord, West Greenland. Unpublished report, Nunaoil A/S, 13 pp. (in archives of Geological Survey of Denmark and Greenland, GEUS Report File 21649).

Author's address

Geological Survey of Denmark and Greenland, Øster Voldgade 10, DK-1350 Copenhagen K, Denmark. E-mail: *aag@geus.dk*

Gold-hosting supracrustal rocks on Storø, southern West Greenland: lithologies and geological environment

Christian Knudsen, Jeroen A.M. van Gool, Claus Østergaard, Julie A. Hollis, Matilde Rink-Jørgensen, Mac Persson and Kristoffer Szilas

A gold prospect on central Storø in the Nuuk region of southern West Greenland is hosted by a sequence of intensely deformed, amphibolite facies supracrustal rocks of late Meso- to Neoarchaean age. The prospect is at present being explored by the Greenlandic mining company NunaMinerals A/S. Amphibolites likely to be derived from basaltic volcanic rocks dominate, and ultrabasic to intermediate rocks are also interpreted to be derived from volcanic rocks. The sequence also contains metasedimentary rocks including quartzites and cordierite-, sillimanite-, garnet- and biotite-bearing aluminous gneisses. The metasediments contain detrital zircon from different sources indicating a maximum age of the mineralisation of *c*. 2.8 Ga. The original deposition of the various rock types is believed to have taken place in a back-arc setting. Gold is mainly hosted in garnet- and biotite-rich zones in amphibolites often associated with quartz veins. Gold has been found within garnets indicating that the mineralisation is pre-metamorphic, which points to a minimum age of the mineralisation of *c*. 2.6 Ga. The geochemistry of the gold-bearing zones indicates that the initial gold mineralisation is tied to fluid-induced sericitisation of a basic volcanic protolith. The hosting rocks and the mineralisation are affected by several generations of folding.

Regional geology

The Nuuk region is renowned for the presence of rocks representing at least three major episodes of crustal accretion during the first billion years of the Earth's history. Each episode is characterised by early formation of supracrustal rocks followed by intrusion of tonalites now occurring as grey hornblende-biotite gneisses. The rock packages have subsequently been deformed and metamorphosed, resulting in often very complex outcrop patterns. Hollis *et al*. (2006) outlined the following sequence of events. The Eoarchaean Isua supracrustal belt (3.87–3.71 Ga) is cut by 3.85 to 3.65 Ga tonalites deformed and metamorphosed at *c*. 3.65 Ga. The next sequence of supracrustal rocks was formed at *c*. 3.1–3.07 Ga, intruded by tonalites at *c*. 3.07–3.05 Ga, and deformed and metamorphosed at *c*. 2.98 Ga. The supracrustals linked to the third episode were formed at *c*. 2.85 to 2.8 Ga, intruded by tonalites at *c*. 2.83 to 2.75 Ga, and deformed and metamorphosed at 2.7 to 2.6 Ga. The last major event in the region was the intrusion of the Qorqut Granite at *c*. 2.53 Ga. The rocks formed during these episodes crop out in a complex pattern of blocks or terranes often only a few tens of kilometres wide. Attempts have been made to map and name these terranes (e.g. Nutman *et al*. 2004; Friend & Nutman 2005), but as the rock types belonging to the different episodes are very similar, it has proved to be very difficult to distinguish and map the terranes in the field (Hollis *et al*. 2006).

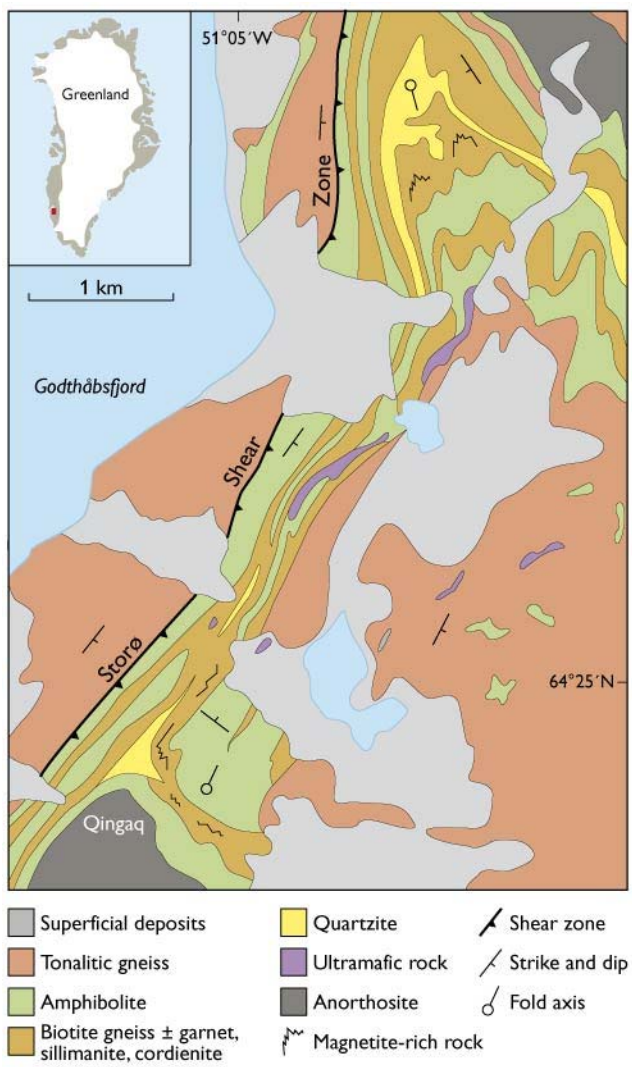

Fig. 1. Map of supracrustal units in the central part of Storø. The supracrustal rocks are cut by numerous pegmatites not shown on this map.

Fig. 2. View of the Storø supracrustal units looking north-east from Qingaq. To the left, the south-west-dipping Storø shear zone is visible. The rusty weathering rocks are supracrustals mainly thought to be of metasedimentary origin. The amphibolites are dark grey and the anorthosite body light grey. Highest summit at left is 1425 m.

The gold-hosting supracrustal sequence overlies the Storø shear zone (Figs 1, 2), an oblique ductile thrust which juxtaposes the supracrustal sequence against the *c.* 3050 Ma tonalitic Nûk gneisses to the west. The gneisses to the south-east are thought to be Palaeoarchaean tonalites. The thrusting along the Storø shear zone occurred syn-to-post the latest folding event and is broadly coeval with a phase of pervasive intrusion by pegmatites at 2630 Ma.

Lithologies

The supracrustal rocks on Storø comprise a range of lithologies including quartzites, quartzo-feldspathic gneisses, aluminous schists and gneisses, amphibolites and ultramafic rocks. The distribution and relative abundance of rocks in the central part of the island is shown in Fig. 1. The rocks are metamorphosed to amphibolite facies, and the dominant lithology is mafic amphibolite.

The amphibolites (mafic, foliated, amphibole-dominated rocks) can be divided into a number of types. They are all highly strained while compositional layering varies from subtle variations on dm- to m-scale in dark amphibolite, to more distinct cm-scale compositional layering in more leucocratic amphibolites. The most common type is homogeneous amphibolite, a medium- to coarse-grained, black to dark grey rock mainly composed of hornblende and plagioclase. The proportion of plagioclase to hornblende varies, and minor amounts of quartz, biotite, sphene, apatite and ilmenite occur. Locally, near some large anorthosite bodies at the structural base of the sequence, the hornblende or the plagioclase in the amphibolite occurs as cm-sized aggregates, suggesting that the amphibolite here may represent metamorphosed gabbroic rock. Varieties of the homogeneous amphibolites include garnet amphibolites and diopside amphibolites.

Several types and generations of quartz veins have been observed in the amphibolites. These include (1) 1–2 cm thick sheeted quartz veins, with sharp contacts to the host rocks, concordant and generally isoclinally folded; (2) thin, spidery quartz veins anastomosing through the rocks; (3) centimetre to decimetre thick agmatitic quartzo-feldspathic veins that anastomose within 0.5–2 m wide zones; and (4) generally concordant quartzo-feldspathic veins, commonly with minor garnet.

A suite of foliated felsic and aluminous gneisses is interleaved with the amphibolites on Storø (Fig. 2). Near the structural base of the supracrustal sequence, grey compositionally layered felsic biotite-hornblende gneisses of intermediate composition are often seen. The layering is expressed by variable proportions of hornblende, biotite, quartz and plagioclase. Sphene, apatite and ilmenite are common accessory minerals while garnet is uncommon. The aluminous gneisses contain high and variable amounts of garnet, biotite, sillimanite and cordierite, and minor amounts of staurolite and tourmaline. These rocks are characterised by strong foliation combined with compositional layering (cm- to dm-scale) to lamination (mm-scale; Fig. 3A). Amongst these rocks, a garnet-biotite gneiss, a sillimanite-garnet-biotite gneiss and a cordierite-garnet-biotite gneiss can be mapped as lithological units. These gneisses are characterised by a rusty brownish weathering colour (Fig. 2) mainly due to the high content of biotite. Within the package of aluminous gneisses, a *c.* 1 m thick characteristic and mappable unit with a very high content of magnetite and garnet occurs (Fig. 1). A magnetite-free quartz-garnetite, consisting of up to 90% garnet is interlayered with the magnetite-bearing rocks. Where the degree of exposure is high and using the garnet-magnetite rock as a marker horizon, a tight to isoclinal fold pattern with repetition of the tectono-stratigraphic units can be identified in the biotite-garnet gneiss.

Within these aluminous gneisses, a unit dominated by quartzite occurs. The composition varies from pure quartzite (>90% quartz) to a rock composed predominantly of quartz with feldspar, sillimanite and light green muscovite, and locally with minor fuchsite, biotite or garnet.

At the other end of the spectrum, ultramafic lenses (boudins) form a characteristic component in the supracrustal sequence. The size of the lenses varies from round pods tens of metres in diameter to elongate lenses hundreds of metres thick and up to 1 km long (Fig. 1). The modal composition of the ultramafic rocks varies substantially. In the cores of the major bodies the rock is mainly composed of olivine, pyroxene (both orthopyroxene and clinopyroxene)

and amphibole (hornblende and tremolite). The margins of these bodies consist commonly of tremolite-phlogopite schist with variable chlorite and actinolite. This rock is locally affected by prograde breakdown of chlorite producing a conspicuous texture where large aggregates of parallel platy olivine crystals are intergrown with large chlorite crystals at high angles to the foliation (Fig. 3B). The ultramafic rocks are locally altered to serpentinite.

Gold mineralisation

Gold occurrences are located in the amphibolite-dominated parts of the supracrustal sequence. They are often found in zones where the amphibolite is enriched in biotite and garnet and often associated with pyrrhotite, arsenopyrite and loellingite ($FeAs_2$). Gold is found both in sericitised plagioclase and within garnet (Juul-Pedersen *et al.* in press), indicating that the gold mineralisation predates the metamorphic event at *c.* 2700–2630 Ma (Hollis 2005). The gold is also often associated with quartz veins, and in these visible gold is locally found.

Geochemistry

The amphibolites have a composition equivalent to tholeitic basalts and are interpreted as metamorphic equivalents of basalts. Based on their geochemistry, Polat (2005) stated that the amphibolites have a subduction zone geochemical signature. The common occurrence of calc-silicates is taken as a sign of hydrothermal alteration in a sea-floor environment (Polat *et al.* 2007). The grey biotite hornblende gneiss of intermediate composition could be the metamorphic equivalent of an intermediate volcanic rock. The ultramafic rocks have MgO in the range of 20 to 40 wt%, high Cr and Ni (1500 to 4000 ppm) and CaO/Al_2O_3 ratios around 1, suggesting a komatiitic protolith. The garnet-biotite gneiss, cordierite-garnet-biotite gneiss and sillimanite-garnet biotite gneiss are generally characterised by high Al contents consistent with a sediment protolith, which is supported by the observation of detrital zircon grains in these rocks (Hollis *et al.* 2006). The gneisses of supposed sedimentary origin have distinctly different Zr/TiO_2 ratios compared to the amphibolites (Fig. 4). There are, however, some extremely aluminous rocks (consisting primarily of garnet and sillimanite together with quartz, feldspar and biotite) in contact with the amphibolite on Qingaq, and these rocks have Zr/TiO_2 ratios similar to the amphibolites (Fig. 4). As neither Zr nor Ti is likely to be mobile in a non-alkaline environment they have probably been derived from basalt by sericitisation caused by hydrothermal alteration (cf. Garde *et al.* 2007 – this volume). This process can lead to volume loss due to loss of elements

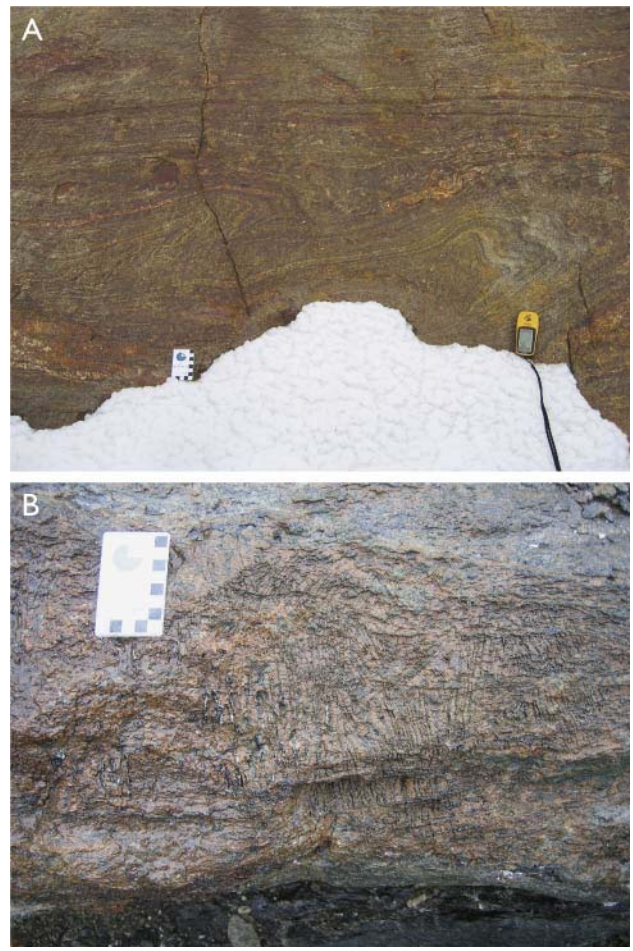

Fig. 3. Appearance of selected lithologies. **A**: Thinly laminated, rusty, garnet-sillimanite-biotite gneiss with tight to isoclinal folds. **B**: Ultramafic rock with a conspicuous texture consisting of sets of parallel oriented, up to 10 cm large, platy, olivine crystals together with large chlorite crystals.

such as Ca, Si, Fe and Mg, and accordingly to increased concentrations of Al, Ti and other immobile elements together with K (stable in the sericite). This rock type contains gold likely to have been introduced during the intense (premetamorphic) hydrothermal alteration. The more common gold-bearing zones within the amphibolites are characterised by elevated contents of biotite and garnet. These rocks have increased concentrations of Al and K likely to have been caused by a similar process.

Ages and structural relations

Detrital zircon from a garnet-biotite-sillimanite-cordierite gneiss and from a quartzite has been analysed (Hollis 2005; Rink-Jørgensen 2006) using laser ablation techniques (cf. Frei *et al.* 2006). The results indicate that there are two distinct sources for these rocks (Fig. 5). The garnet-biotite-sillimanite-cordierite gneiss contains detrital zircon distributed

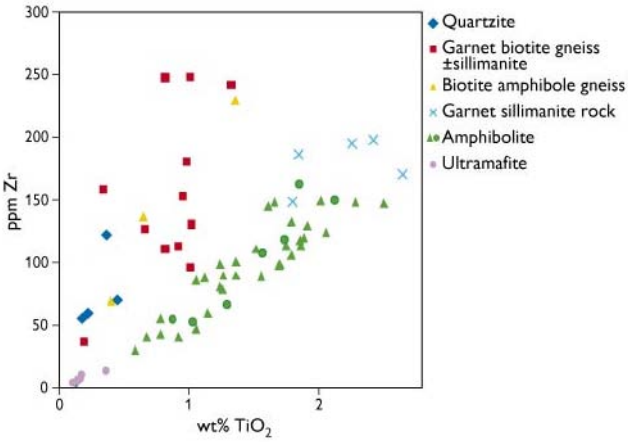

Fig. 4. Plot of Zr ppm vs. TiO_2 wt% in different rock samples from Qingaq on Storø.

Fig. 5. Detrital zircon populations from two rock samples from Storø. Sample 481465 is a garnet-biotite-sillimanite-cordierite gneiss and 481283 is a quartzite.

in two age populations around 2880 and 2830 Ma. We suggest that the rock had an immature sedimentary precursor, possibly derived from erosion of a relatively young volcanic arc formed in two episodes at 2880 and 2830 Ma. The detrital zircon in the quartzite, which is likely to represent a mature sediment, forms populations with main peaks around 2960 and 3010 Ma and a minor peak at 3180 Ma. This rock must have had a distinctly different source and probably represents the erosional products of an older continent (e.g. the Nûk gneisses). This difference in sources is consistent with a model of formation of the supracrustal rocks in a back-arc environment. The immature sediments are likely to have been derived from the relatively young rocks in the arc, whereas the mature quartzites are likely to originate from the older rocks located on the continent side of the back-arc basin. This is supported both by the observation that the amphibolites formed in an arc environment and by the suite of rocks present. This environment is very similar to that envisaged for Canadian Neoarchaean supracrustal belts (Sandeman *et al.* 2006).

References

Frei, D., Hollis, J.A., Gerdes, A., Harlov, D., Karlsson, C., Vasquez, P., Franz, G. & Knudsen, C. 2006: Advanced *in situ* geochronological and trace element microanalysis by laser ablation techniques. Geological Survey of Denmark and Greenland Bulletin **10**, 25–28.

Friend, C.R.L. & Nutman, A.P. 2005: New pieces to the Archaean terrane jigsaw puzzle in the Nuuk region, southern West Greenland: steps in transforming a simple insight into a complex regional tectonothermal model. Journal of the Geological Society (London) **162**, 147–162.

Garde, A.A., Stendal, H. & Stensgaard, B.M. 2007: Pre-metamorphic hydrothermal alteration with gold in a mid-Archaean island arc, Godthåbsfjord, West Greenland. Geological Survey of Denmark and Greenland Bulletin **13**, 37–40.

Hollis, J.A. (ed.) 2005: Greenstone belts in the central Godthåbsfjord region, southern West Greenland: geochemistry, geochronology and petrography arising from 2004 fieldwork, and digital map data. Danmarks og Grønlands Geologiske Undersøgelse Rapport **2005/42**, 215 pp.

Hollis, J.A., Frei, D., van Gool, J.A.M., Garde, A.A. & Persson, M. 2006: Using zircon geochronology to resolve the Archaean geology of southern West Greenland. Geological Survey of Denmark and Greenland Bulletin **10**, 49–52.

Juul-Pedersen, A., Frei, R., Appel, P.W.U., Persson, M. & Konnerup-Madsen, J. 2007: A shear zone related greenstone belt hosted gold mineralisation in the Archean of West Greenland. A petrographic and combined Pb-Pb and Rb-Sr geochronological study. Ore Geology Reviews **32**, 20–36.

Nutman, A.P., Friend, C.R.L., Barker, S.L.L. & McGregor, V.R. 2004: Inventory and assessment of Palaeoarchaean gneiss terranes and detrital zircons in southern West Greenland. Precambrian Research **135**, 281–314.

Polat, A. 2005: Geochemical and petrographic characteristics of the Ivisartoq and Storø greenstone belts, southern West Greenland: progress report. Danmarks og Grønlands Geologiske Undersøgelse Rapport **2005/42**, 80–112.

Polat, A., Appel, P.W.U., Frei, R., Pan, Y., Dilek, Y., Ordónez-Calderon, J.C., Fryer, B., Hollis, J.A. & Raith, J.G. 2007: Field and geochemical characteristics of Mesoarchean (~3075 Ma) Ivisartoq greenstone belt, southern West Greenland: evidence for seafloor hydrothermal alteration in supra-subduction oceanic crust. Gondwana Research **11**, 69–91.

Rink-Jørgensen, M. 2006: *In situ* U-Pb datering af zirkoner i teori og praksis til bestemmelse af alder og populationer af detritale zirkoner, med anvendelse på en prøve fra Nuuk regionen i det sydlige Vestgrønland. Unpublished B.Sc. project, Københavns Universitet, Danmark.

Sandeman, H.A., Hanmer, S., Tella, S., Armitage, A.A., Davis, W.J. & Ryan, J.J. 2006: Petrogenesis of Neoarchaean volcanic rocks of the MacQuoid supracrustal belt: a back-arc setting for the northwestern Hearne subdomain, western Churchill Province, Canada. Precambrian Research **144**, 140–165.

Authors' addresses

C.K. & J.A.M.v.G., *Geological Survey of Denmark and Greenland, Øster Voldgade 10, DK-1350 Copenhagen K, Denmark.* E-mail: *ckn@geus.dk*

C.Ø., *NunaMinerals, Vandsøvej 5, P.O. Box 790, DK-3900 Nuuk, Greenland.*

J.A.H., *Northern Territories Geological Survey, P.O. Box 3000, Darwin NT 0801, Australia.*

M.R.-J., *M.P. & K.S., Institute of Geography and Geology, University of Copenhagen, Øster Voldgade 10, DK-1350 Copenhagen K, Denmark.*

P–T history of kimberlite-hosted garnet lherzolites from South-West Greenland

Mark T. Hutchison, Louise Josefine Nielsen and Stefan Bernstein

Exploration for diamonds in West Greenland has experienced a major boost within the last decade following the establishment of world-class diamond mines within the nearby Slave Province of the Canadian Arctic. Numerous companies have active programmes of diamond exploration and increasingly larger diamonds have been discovered, notably a 2.392 carat dodecahedral stone recovered by the Canadian exploration company Hudson Resources Inc. in January 2007. The Geological Survey of Denmark and Greenland (GEUS) is currently carrying out several studies aimed at understanding the petrogenesis of diamondiferous kimberlites in Greenland and the physical and chemical properties of their associated mantle source regions (e.g. Hutchison 2005; Nielsen & Jensen 2005).

Constraint of the mantle geotherm, i.e. the variation of temperature with depth for a particular mantle volume, is an important initial step in assessing the likelihood of such a volume to grow diamonds and hence the diamond potential of associated deep-sourced magmatic rocks occurring at surface. Cool geotherms are often present within old cratonic blocks such as West Greenland (Garde *et al.* 2000) and provide a good environment for the formation of diamonds (Haggerty 1986). This study aims to constrain the mantle geotherm for the southern extent of the North Atlantic Craton in Greenland by applying three-phase geothermobarometry calculations using chemical compositions of clinopyroxene, orthopyroxene and garnet from four-phase kimberlite-hosted lherzolite xenoliths.

Xenoliths have been sampled from kimberlites from two areas in South-West Greenland: Midternæs and Pyramidefjeld (Fig. 1). Kimberlites in the Pyramidefjeld area principally occur as sheeted sills hosted in the Pyramidefjeld granite complex of Palaeoproterozoic Ketilidian age. In contrast, Midternæs kimberlites occur as outcrops within a single, extensive and undulating sill hosted within pre-Ketilidian granodioritic gneiss and Ketilidian supracrustal rocks.

Pyramidefjeld kimberlites have been shown to be Mesozoic (Andrews & Emeleus 1971), and work is currently being carried out to further constrain the ages of these and the Midternæs kimberlites and also xenoliths using modern methods. No attempt is made herein to provide a correct petrological classification of the rocks hosting the xenoliths; however, the abundance of clinopyroxene reported by Andrews & Emeleus (1971) suggests that further work may more correctly conclude a classification as 'orangeite' after Mitchell (1995). Notwithstanding this, the term 'kimberlite' is employed throughout in order to be consistent with that adopted by previous authors. The Precambrian Pyramidefjeld granite complex and adjacent Archaean granodioritic gneisses are host to several kimberlite sheets located at various levels between 400 and 900 m elevation (Fig. 1A; Andrews & Emeleus 1971, 1975). Kimberlites are mainly found as loose

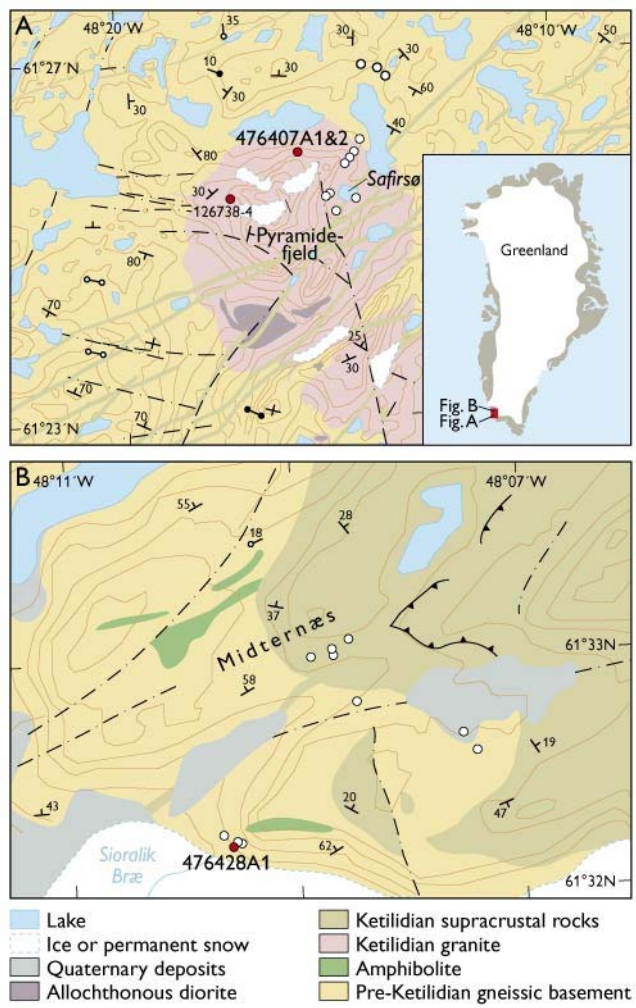

Fig. 1. Location of sample sites with reference to context in South-West Greenland (index map). Red dots indicate location of samples used for pressure and temperature calculation; white dots indicate additional samples. **A**: Sample localities in the Pyramidefjeld region. Geology simplified from Henriksen (1966). **B**: Sample localities in the Midternæs region. Geology simplified from Escher & Jensen (1972).

Fig. 2. Kimberlite sill of approximately 3.5 m thickness intruded within pre-Ketilidian gneiss and cross-cutting a vertical Gardar age (*c.* 1200 Ma) dolerite dyke. Located at Midternæs by the glacier Sioralik Bræ (see Fig. 1B).

blocks in scree; however, these are almost always sourced locally from in situ bodies. Sheets can often be found deep within overhanging clefts, particularly in granitic walls. The kimberlite bodies are gently dipping, typically 20 degrees, and with a range of strikes. The maximum thickness of sills is approximately 2 m but thickness varies significantly over short distances. In many instances, the occurrence of kimberlite is seen to be controlled locally by structures in the country rocks. Field observations of the range of orientations of intrusive bodies do not appear to suggest a particular focal point which could be a likely location for an intrusive centre such as a pipe. This observation is in line with what is seen throughout West Greenland where kimberlite emplacement appears as dykes and sills (Larsen & Rex 1992) rather than the pipes and blows which are common in other world-wide settings. The occurrence of xenoliths amongst Pyramidefjeld kimberlites is highly variable with the most xenolith-rich localities being in the vicinity of Safirsø (Fig. 1A). The majority of xenoliths are dunites with occasional wehrlites and lherzolites (Emeleus & Andrews 1975). Of particular interest from the point of view of thermobarometry is the occurrence of garnet. This is rarely found, even in clinopyroxene-bearing samples, and the two samples chosen for thermobarometry (Fig. 1A) represent the majority of the garnet-bearing xenoliths identified within an estimated total population of 75 xenoliths collected.

The Midternæs kimberlites are hosted in Archaean gneisses and Proterozoic supracrustal rocks (Fig. 1B; Andrews & Emeleus 1971, 1975). The style of kimberlite emplacement and occurrence of garnet-bearing xenoliths are closely similar to those of Pyramidefjeld. Contours of elevation between outcrops suggest that the kimberlites form parts of a largely contiguous single body dipping at approximately 30 degrees to the west-south-west. Individual outcrops as in Pyramidefjeld indicate that the body varies in thickness and undulates in response to local structure. The south-western portion of the body which outcrops near the glacier Sioralik Bræ, is considerably thicker than elsewhere (Fig. 2) and in some places is seen to have a true thickness in excess of 4 m. Xenoliths are less abundant on average than in Pyramidefjeld kimberlites, but a similar variety and proportion of rock types and infrequent occurrence of garnet is observed.

The kimberlites from both areas were intruded along zones of platy jointing which likely were caused by degassing of the magma and formed just prior to the kimberlite intrusion. In contrast to some kimberlites in other cratons, very few xenoliths of local, lower crustal rock types have been recognised in the kimberlites from Pyramidefjeld and Midternæs. The intrusions are therefore believed to have been of a non-explosive nature, perhaps because of host-rock rheology or due to emplacement at relatively deep crustal levels.

Here we report on calculations of equilibrium pressure and temperature using compositions of three-phase assemblages of garnet, orthopyroxene and clinopyroxene from Midternæs and Pyramidefjeld mantle xenoliths.

Measurements

Polished thin sections of garnet-bearing mantle xenoliths were prepared from fresh samples from both localities. Most xenoliths have a coarse granular texture indicative of equilibrium growth amongst clinopyroxene, olivine, orthopyroxene

and garnet. Typically, triple junctions between mineral grains are well defined. Mineral compositions were determined by the JEOL 733 electron microprobe at the Department of Geography and Geology, University of Copenhagen. Analyses were conducted using a 15 kV, 15 nA and 5 µm beam for the elements Si, Ti, Al, Cr, Fe, Mn, Ni, Mg, K and Na. Standardisation was achieved against natural and synthetic standards.

Geothermobarometry

Estimates of the temperatures and pressures within the Earth are essential for the understanding of many geological processes and in particular, in the case of kimberlites, for diamond prospectivity. Geothermobarometry is based on the study of mineral assemblages in chemical and physical equilibrium. As mantle xenoliths often retain information about the physical conditions at the time of formation, they are widely used for such estimates. In this study temperature–pressure calculations are based on the two-pyroxene thermometer and the aluminium-in-orthopyroxene / garnet barometer of Brey & Köhler (1990). Results are presented in the context of standard cratonic mantle geotherm models in Fig. 3. Pressure and temperature estimates from Pyramidefjeld range from 909°C and 3.29 GPa to 975°C and 3.50 GPa. These pressures correspond to a depth range of 106–113 km. Peak assemblages using cores of touching grains for samples from Pyramidefjeld fall on a smooth curve. The Midternæs sample reflects equilibrium conditions of 1087°C and 3.73 GPa corresponding to 120 km depth and therefore deeper than the Pyramidefjeld samples. All values show a similarity with a warm mantle geotherm based on a surface heat flow of 44 mW/m^2 after Pollack & Chapman (1977). However, the location of pressure and temperature points more closely follows the trends in the steady-state geotherm of McKenzie *et al.* (2005) although at an average temperature elevated by approximately 50°C (Fig. 3). Furthermore, the Midternæs sample may reflect the same type of high-T inflection evident under similar conditions from Lesotho kimberlite-hosted xenoliths (Finnerty 1989) although further data are required to confirm this inference.

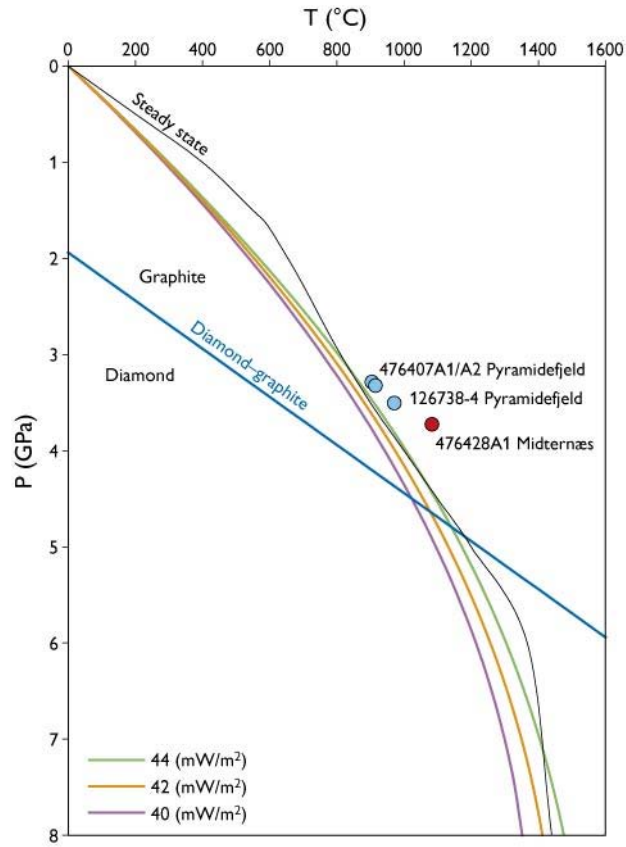

Fig. 3. Temperature–pressure diagram showing positions of equilibrium conditions for garnet lherzolite xenoliths in this study in the context of mantle geotherms. Diamond–graphite phase boundary after Kennedy & Kennedy (1976) and steady-state mantle geotherm after McKenzie *et al.* (2005). Mantle geotherms from Pollack & Chapman (1977) where figures represent surface heat flow for each model in mW/m^2. Calculated pressures and temperatures are for peak conditions (cores of mineral grains).

Discussion and conclusions

The apparent coincidence of pressure and temperature values for xenoliths from Pyramidefjeld and Midternæs along the McKenzie *et al.* (2005) geotherm suggests that the thermal conditions of the mantle sampled from the two localities separated on the ground by 14 km are largely the same. The McKenzie *et al.* (2005) model takes account of lower radiogenic heating in the cratonic crust than previously accepted and shows good correlation with pressure and temperature estimates from kimberlite-hosted mantle xenoliths from northern Canada and central Siberia (McKenzie *et al.* 2005 and references therein). Results from Pyramidefjeld and Midternæs xenoliths are hence also consistent with kimberlite-hosted xenoliths from elsewhere whilst at the same time elevated temperatures observed in this study suggest that the geotherm was slightly warmer in South-West Greenland than in the northern Canada and central Siberian diamond-bearing mantle.

Additional samples are required to more closely constrain the geotherm and also to assess the ranges of depths from which xenoliths were sampled at the two locations; however, the greater depth represented so far at Midternæs may have significance. Midternæs is slightly closer to the central part of the craton, and the greater depths represented in the xenolith suite may thus reflect a thicker cratonic lithospheric root.

Consequently the present data suggest that the Midternæs kimberlite is closer to directly sampling mantle material within the diamond stability field than Pyramidefjeld. Although xenolith suites may be formed under different conditions compared to diamonds found within the same kimberlites (Shee *et al.* 1982), it appears that Midternæs may have a better diamond potential than Pyramidefjeld. Midternæs kimberlites have not so far been tested for the presence of diamonds, and the apparently shallower-sourced kimberlites from Pyramidefjeld have yielded small numbers of diamonds (unpublished company reports collated in Jensen *et al.* 2004). Since Midternæs contains some of the thickest outcropping kimberlite evident in Greenland, the area may merit further attention by diamond prospectors.

Acknowledgements

Graham Pearson, Geoff Nowell and Nadine Wittig (University of Durham) are acknowledged for support. MTH acknowledges the European Community's 6th Framework Program for support under a Marie Curie EIF Fellowship. Disclaimer: This publication reflects the authors' views, and the European Community shall not be held liable for any use of the information contained herein.

References

Andrews, J.R. & Emeleus, C.H. 1971: Preliminary account of kimberlite intrusions from the Frederikshåb district, South-West Greenland. Rapport Grønlands Geologiske Undersøgelse **31**, 26 pp.

Andrews, J.R. & Emeleus, C.H. 1975: Structural aspects of kimberlite dyke and sheet intrusion in South-West Greenland. Physics and Chemistry of the Earth **9**, 43–50.

Brey, G.P. & Köhler, T. 1990: Geothermobarometry in four-phase lherzolites II. New thermobarometers, and practical assessment of existing thermobarometers. Journal of Petrology **31**, 1353–1378.

Emeleus, C.H. & Andrews, J.R. 1975: Mineralogy and petrology of kimberlite dyke sheet intrusions and included peridotite xenoliths from South-West Greenland. Physics and Chemistry of the Earth **9**, 179–197.

Escher, J.C. & Jensen, S.B. 1972: Geological map of Greenland, 1:100 000, Midternæs 61 V.2 Nord. Copenhagen: Geological Survey of Greenland.

Finnerty, A.A. 1989: Xenolith-derived mantle geotherms: whither the inflection? Contributions to Mineralogy and Petrology **102**, 367–375.

Garde, A.A., Friend, C.R.L., Nutman, A.P. & Marker, M. 2000: Rapid maturation and stabilisation of middle Archaean continental crust: the Akia terrane, southern West Greenland. Bulletin of the Geological Society of Denmark **47**, 1–27.

Haggerty, S. 1986: Diamond genesis in a multi-constrained model. Nature **320**, 34–38.

Henriksen, N. 1966: Geological map of Greenland, 1:100 000, Ivigtut 61 V.1 Syd. Copenhagen: Geological Survey of Greenland.

Hutchison, M.T. 2005: Diamondiferous kimberlites from the Garnet Lake area, West Greenland: exploration methodologies and petrochemistry. Danmarks og Grønlands Geologiske Undersøgelse Rapport **2005/68**, 33–42.

Jensen, S.M., Secher, K., Rasmussen, T.M. & Schjøth, F. 2004: Diamond exploration data from West Greenland: 2004 update and revision. Danmarks og Grønlands Geologiske Undersøgelse Rapport **2004/117**, 90 pp.

Kennedy, C. & Kennedy, G. 1976: The equilibrium boundary between graphite and diamond. Journal of Geophysical Research **81**, 2467–2470.

Larsen, L.M. & Rex, D.C. 1992: A review of the 2500 Ma span of alkaline-ultramafic, potassic and carbonatitic magmatism in West Greenland. Lithos **28**, 367–402.

McKenzie, D., Jackson, J. & Priestley, K. 2005: Thermal structure of oceanic and continental lithosphere. Earth and Planetary Science Letters **233**, 337–349.

Mitchell, R.H. 1995: Kimberlites, orangeites and related rocks, 410 pp. New York: Plenum Press.

Nielsen, T.F.D. & Jensen, S.M. 2005: The Majuagaa calcite-kimberlite dyke, Maniitsoq, southern West Greenland. Danmarks og Grønlands Geologiske Undersøgelse Rapport **2005/43**, 59 pp.

Pollack, H.N. & Chapman, D.S. 1977: On the regional variation of heat flow, geotherms and lithospheric thickness. Tectonophysics **38**, 279–296.

Shee, S.R., Gurney, J.J. & Robinson, D.N. 1982: Two diamond-bearing peridotite xenoliths from the Finsch Kimberlite, South Africa. Contributions to Mineralogy and Petrology **81**, 79–87.

Authors' addresses

M.T.H. & S.B., *Geological Survey of Denmark and Greenland, Øster Voldgade 10, DK-1350 Copenhagen K, Denmark.* E-mail: *mhutchis@lpl.arizona.edu*

L.J.N., *Department of Geography and Geology, University of Copenhagen, Øster Voldgade 10, DK-1350 Copenhagen K, Denmark.*

Two tectonically significant enclaves in the Nordre Strømfjord shear zone at Ataneq, central West Greenland

William E. Glassley, John A. Korstgård and Kai Sørensen

The Nordre Strømfjord shear zone is a 1.8 Ga zone of large-scale, transcurrent and sinistral ductile shear (Sørensen *et al.* 2006) within the Nagssugtoqidian Mobile Belt (NMB) of central West Greenland. It has been hypothesised that the NMB is a suture between two Archaean continental masses (Kalsbeek *et al.* 1987). During field work in 2005 along the Nordre Strømfjord shear zone in the fjord Ataneq (Fig. 1), some unusual rock types were discovered that preserve evidence of magmatic and metamorphic processes not previously reported in the area. These observations include the first indication of high-pressure (HP) metamorphism in West Greenland and the first reported occurrence of a cumulate of giant orthopyroxene. The tectonic telescoping of these features together within the Nordre Strømfjord shear zone has important implications for reconstructing the Palaeoproterozoic history of this region, and provides evidence that processes typical of Phanerozoic continent–continent collision zones (e.g. the Caledonian and Alpine systems) operated at least as far back as 1.8 Ga ago.

High-pressure enclave

On the north side of inner Ataneq fjord an approximately 1.2 m wide and 4 m long lens of ultramafic rock occurs within strongly foliated garnet-sillimanite gneisses and schists, and garnet-bearing calc-silicate rock (Fig. 2). The pale yellowish green, ultramafic rock is moderately foliated with its long axis parallel to the fabric in the enclosing gneisses. This core of the

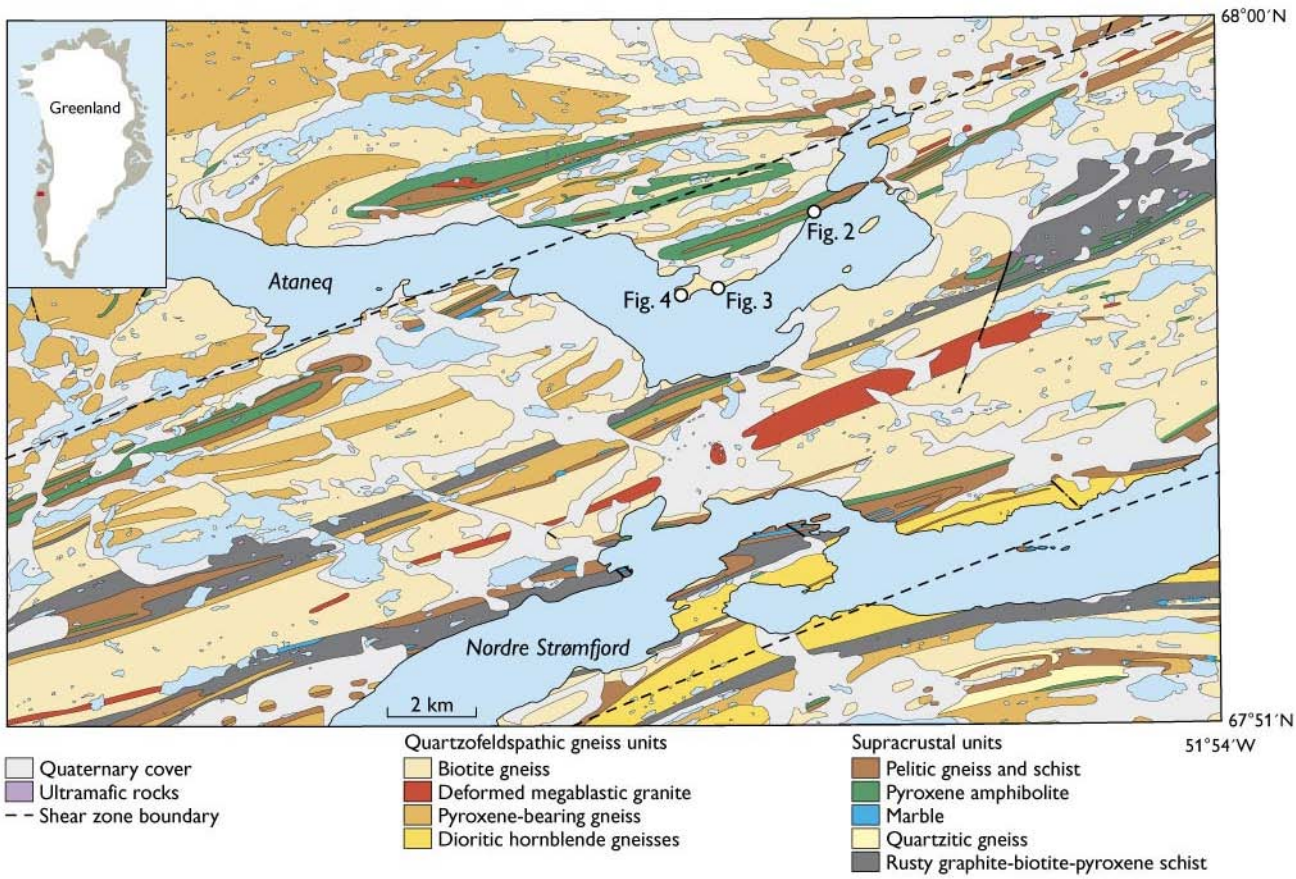

Fig. 1. North-eastern part of the Agto map sheet (Olesen 1984), with the localities of Figs 2, 3 and 4 marked. The Nordre Strømfjord shear zone of the map area is characterised by vertically oriented supracrustal units alternating with quartzofeldspathic units, as also described by Sørensen et al. (2006) from the area to the east. The regional amphibolite to granulite facies transition occurs over the eastern part of the map.

Fig. 2. Lens (boudin?) of yellowish green, ultramafic rock within garnet-biotite-sillimanite gneiss and calc-silicate rock. The hammer (1 m) rests on the ultramafic rock and is just to the right of a dark, 30 cm thick rim (indicated by arrow) that completely encloses the ultramafic lens. The dark rim is the source of the garnet-spinel-olivine-orthopyroxene-clinopyroxene sample. For location see Fig. 1.

enclave consists of anthophyllite with a few minor additional phases. It is surrounded by a dark rim of dense, fine-grained rock approximately 30 cm thick (Fig. 2) that is conformable to the shape of the ultramafic lens. The rim appears to be the result of a reaction between the silica-poor ultramafic rocks and the enclosing aluminium- and silica-rich metasediments, and it consists of olivine-orthopyroxene-clinopyroxene-spinel-garnet-amphibole. The fine-grained nature of the rim rock and its complex textural characteristics make it difficult to unambiguously decipher all aspects of its petrogenetic history. However, certain key observations show that the rim rock records an unusual history involving high-pressure metamorphism. The olivine occurs as remnant crystals that are occasionally seen to be in optical continuity but separated by pyroxene and spinel. Garnets occur as isotropic areas that are nearly completely overgrown by spinel and pyroxene. Garnet also occurs as inclusions in spinel. All combinations of grain-to-grain contacts have been observed, with the exception of garnet-olivine. There are also textural features suggesting that two generations of orthopyroxene and clinopyroxene may be present.

These mineralogical features document a petrogenetic history in which the oldest mineral assemblage preserved in the rim of the enclave is garnet-olivine-orthopyroxene-clinopyroxene (i.e. garnet peridotite). The occurrence of garnet + olivine in ultramafic rocks and the occurrence of eclogite minerals in mafic compositions are the diagnostic mineral assemblages for HP metamorphism. Defined in this way HP metamorphism is intermediate between granulite facies metamorphism and ultra high-pressure metamorphism (UHP) in which diamond and coesite are stable phases. In the HP enclave, the olivine + garnet-bearing assemblage is replaced, via reaction between olivine and garnet, by the assemblage spinel-orthopyroxene-clinopyroxene (i.e. spinel peridotite). Olivine and garnet are preserved because the reaction was arrested before it went to completion. This metamorphism took place at a very low thermodynamic activity of water. Replacement of a garnet peridotite mineral assemblage by that of spinel peridotite is the hallmark of recrystallisation during decompression from minimum pressures of about 18–20 kilobars (>60 km) and temperatures >750°C (Schmädicke & Evans 1997; Fumagalli & Poli 2005).

Preliminary electron microprobe analyses of all of the mineral phases have been conducted. Clinopyroxene-orthopyroxene geothermometry and orthopyroxene-garnet geobarometry (Brey & Köhler 1990) intersect at 785°C and 21 kb. However, uncertainty in identifying cogenetic minerals, as well as the fact that these rocks have experienced extensive recrystallisation during decompression and cooling make it likely that these *P–T* conditions are a minimum; modifications are to be expected as further analyses are conducted.

The electron microprobe data provide support for the argument that the high density rim around the ultramafic rock is, in fact, a metasomatic feature reflecting steep chemical potential gradients between the metasediments and the ultramafic rock. In particular, the very high modal abundance of the spinel (>20%) and the absence of detectable Cr in any of the minerals are inconsistent with primary crystallisation from an ultramafic composition. Rather, these characteristics suggest limited metasomatic reaction between the enclave and the surrounding metasediments into which we envisage the enclave to have been tectonically emplaced.

Giant orthopyroxene cumulate with interstitial anorthosite and associated rocks

Approximately 3 km west of the HP site a series of gabbroic anorthosite and coarse-grained orthopyroxenite lenses occur that are metres to tens of metres in size (Fig. 3). This series of lenses is traceable along the coast over a distance of 1 km. The

Fig. 3. Two 3 m long lenses of gabbro anorthosite approximately 2 km west of the ultramafic lens shown in Fig. 2. Note the duplex structure within the lens. For location see Fig. 1.

margins of these lenses are tectonised at their contact with the enclosing quartzofeldspathic gneisses.

The orthopyroxenites were observed in two distinct forms. One of these is a monomineralic lens of thumb-sized, equant, euhedral to subhedral orthopyroxene crystals. The lens is approximately two metres by four metres in size and exhibits no internal fabric. The other form is a spectacular giant orthopyroxene cumulate containing crystals more than 30 cm long and 15 cm wide that have a strong preferred orientation, with long axes parallel to each other in a classic cumulate texture. The crystals exhibit striking macroscopic kink banding (Fig. 4). Anorthosite is found as discontinuous films along the edges of the orthopyroxene crystals and as cuspate pockets where triple junctions of orthopyroxene crystals occur.

In thin section the orthopyroxenites are seen to have preserved detailed evidence of a complex magmatic history and metamorphic recrystallisation, even though field evidence unequivocally shows these rocks to have been tectonically emplaced into their present setting. The primary magmatic mineral assemblage consists of remnant forsteritic olivine incompletely resorbed by orthopyroxene, green spinel and plagioclase with chromite, rutile, phlogopite, apatite and zircon as additional phases, either primary or a result of exsolution. All of these minerals are observed as inclusions within the orthopyroxene, as well as phases interstitial to orthopyroxene in pockets of anorthosite. Secondary minerals associated with metamorphic recrystallisation are amphibole (as trains of small grains within orthopyroxene, occurring along crystallographically controlled planes) and quartz.

Reconnaissance electron microprobe analyses of the plagioclase show that its composition is affected by its environment: plagioclase grains within the anorthositic pockets are close to An_{60}, while those contained within the orthopyroxene, which generally are associated with amphibole, are approximately An_{40}. The amphibole is nearly pure cummingtonite. Other observations made with the electron microprobe showed the presence of Fe-Ni sulphides and pure Cu spherules. In addition, the spinels and phlogopites are Ti- and Cr-rich.

These characteristics of the orthopyroxenites suggest that the cumulates formed by gravitational settling of giant orthopyroxenes in a magma chamber. The presence of plagioclase, clinopyroxene and rutile exsolution lamellae suggests that the orthopyroxenes crystallised at high pressure (>10 kb), which is consistent with the co-existence of orthopyroxene-olivine-plagioclase-spinel.

It has been postulated that anorthositic massifs form via fractionation of orthopyroxene from magmas of appropriate compositions at or near the base of the continental crust (Emslie 1985). However, such cumulates have never been observed before, and the slivers of cumulate orthopyroxenite observed in Ataneq may be the remnants of such a system that has been tectonically dismembered

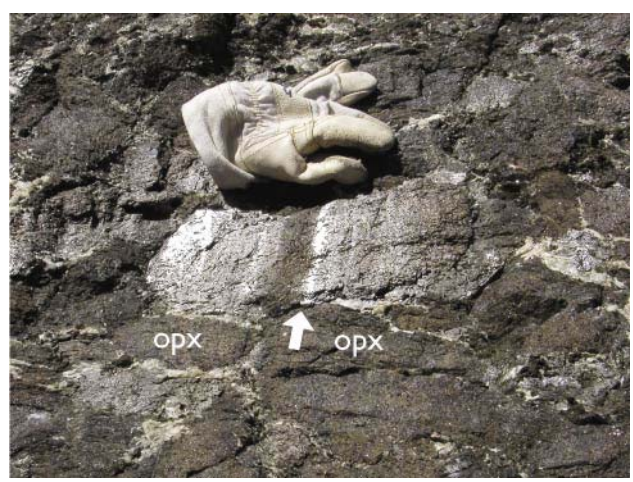

Fig. 4. Giant orthopyroxene crystals (dark olive green except where reflecting) separated by grey and white intercumulus anorthosite. Glove above the large single crystal in the centre of the photograph is approximately 20 cm long. Note kink banding in the central crystal (arrow points towards the kink band). **opx**, orthopyroxene. For location see Fig. 1.

Conclusions

The high-pressure rocks and orthopyroxenite cumulates observed in Ataneq attest to tectonic telescoping of rocks that originated from profoundly different geological environments. They provide evidence that within the Nordre Strømfjord shear zone, samples of the deepest levels of continental crust and the upper mantle are present. These rocks occur within contrasting lithologies of the Nordre Strømfjord shear zone: the HP lens within a supracrustal unit (*sensu* Sørensen *et al.* 2006) and the pyroxenite-anorthosite assemblage within a quartzofeldspathic gneiss unit. Further to the east, a complex of lenses of ultramafic rocks, pillow lavas and unusual tourmaline-phlogopite rocks (interpreted to be the metamorphosed remnant of submarine hot-spring exhalations; Sørensen *et al.* 2006) have been observed enclosed in supracrustal units. These rock types provide compelling evidence that upper mantle, deep continental crust and oceanic crust were tectonically juxtaposed, probably during continent–continent collision, later to be deformed within the Nordre Strømfjord shear zone. The tectonism responsible for the emplacement of these rocks within continental rocks may be thrust stacking as described by van Gool *et al.* (1999) and Sørensen *et al.* (2006) south of the shear zone near the Inland Ice.

Acknowledgement

The work of W.E.G. was funded by the University of Aarhus.

References

Brey, G.P. & Köhler, T. 1990: Geothermobarometry in four-phase lherzolites. II. New thermobarometers and practical assessment of existing thermobarometers. Journal of Petrology **31**, 1353–1378.

Emslie, R.F. 1985: Proterozoic anorthosite massifs. In: Tobi, A.C. & Touret, J.L.R. (eds): The deep proterozoic crust in the North Atlantic Provinces. NATO ASI Series **158**, 39–60.

Fumagalli, P. & Poli, S. 2005: Experimentally determined phase relations in hydrous peridotites to 6.5 Gpa and their consequences on the dynamics of subduction zones. Journal of Petrology **46**, 555–578.

Kalsbeek, F., Pidgeon, R.T. & Taylor, P.N. 1987: Nagssugtoqidian mobile belt of West Greenland: a cryptic 1850 Ma suture between two Archaean continents – chemical and isotopic evidence. Earth and Planetary Science Letters **85**, 365–385.

Olesen, N.Ø. 1984: Geological map of Greenland, 1:100 000, Agto, 67 V.1 Nord. Copenhagen: Geological Survey of Greenland.

Schmädicke, E. & Evans, B.W. 1997: Garnet-bearing ultramafic rocks from the Erzgebirge, and their relation to other settings in the Bohemian Massif. Contributions to Mineralogy and Petrology **127**, 57–74.

Sørensen, K., Korstgård, J.A., Glassley, W.E. & Stensgaard, B.M. 2006: The Nordre Strømfjord shear zone and the Arfersiorfik quartz diorite in Arfersiorfik, the Nagssugtoqidian orogen, West Greenland. Geological Survey of Denmark and Greenland Bulletin **11**, 145–161.

van Gool, J.A.M., Kriegsman, L.M., Marker, M. & Nichols, G.T. 1999: Thrust stacking in inner Nordre Strømfjord area, West Greenland: significance for the tectonic evolution of the Palaeoproterozoic Nagssugtoqidian orogen. Precambrian Research **93**, 71–86.

Authors' addresses

W.E.G. & J.A.K., *Geological Institute, University of Aarhus, Høegh-Guldbergsgade 2, DK-8000 Århus C, Denmark.* E-mail: *geobg@nf.au.dk*

K.S., *Geological Survey of Denmark and Greenland, Øster Voldgade 10, DK-1350 Copenhagen K, Denmark.*

A well-preserved bimodal Archaean volcanic succession in the Tasiusarsuaq terrane, South-West Greenland

Henrik Stendal and Anders Scherstén

During the field campaign in the Nuuk region, one of the objectives was to describe Archaean primary geological environments (Hollis *et al.* 2006). On Nunatak 1390, which is part of the Tasiusarsuaq terrane (Figs 1, 2), a bimodal volcanic succession is preserved and interpreted as former ocean floor. The field investigation included geological mapping and sampling of the volcanic sequence comprising mafic to ultramafic rocks, and associated acid volcanic rocks and granite intrusions.

The Tasiusarsuaq terrane

The Tasiusarsuaq terrane is dominated by mafic rocks (amphibolite), tonalitic gneiss and granodiorite yielding ages of 2.92–2.86 Ga (Fig. 1; Schiøtte *et al.* 1989; Friend & Nutman 2001; Crowley 2002). Metamorphic grade ranges from greenschist to granulite facies conditions, with peak metamorphism dated at ~2.79 Ga (Pidgeon & Kalsbeek 1978). The mafic rocks comprise greenschist facies mafic rocks with pillow structures, metagabbroic and ultramafic pods, and dykes. The thicknesses of the mafic to ultramafic sequences vary from 50 m up to more than 1000 m. The Tasiusarsuaq terrane rocks are cross-cut by brown-weathering E–W-trending dolerite dykes (up to 30 m wide) with well-developed chilled margins. Alterations such as calc-silicate formation are common within the mafic-ultramafic rocks. The pillowed mafic sequences contain intercalations of 1–2 m wide, rusty, sulphide-bearing layers and tourmalinites (exhalites). The sulphides recorded include pyrite, pyrrhotite, chalcopyrite and arsenopyrite.

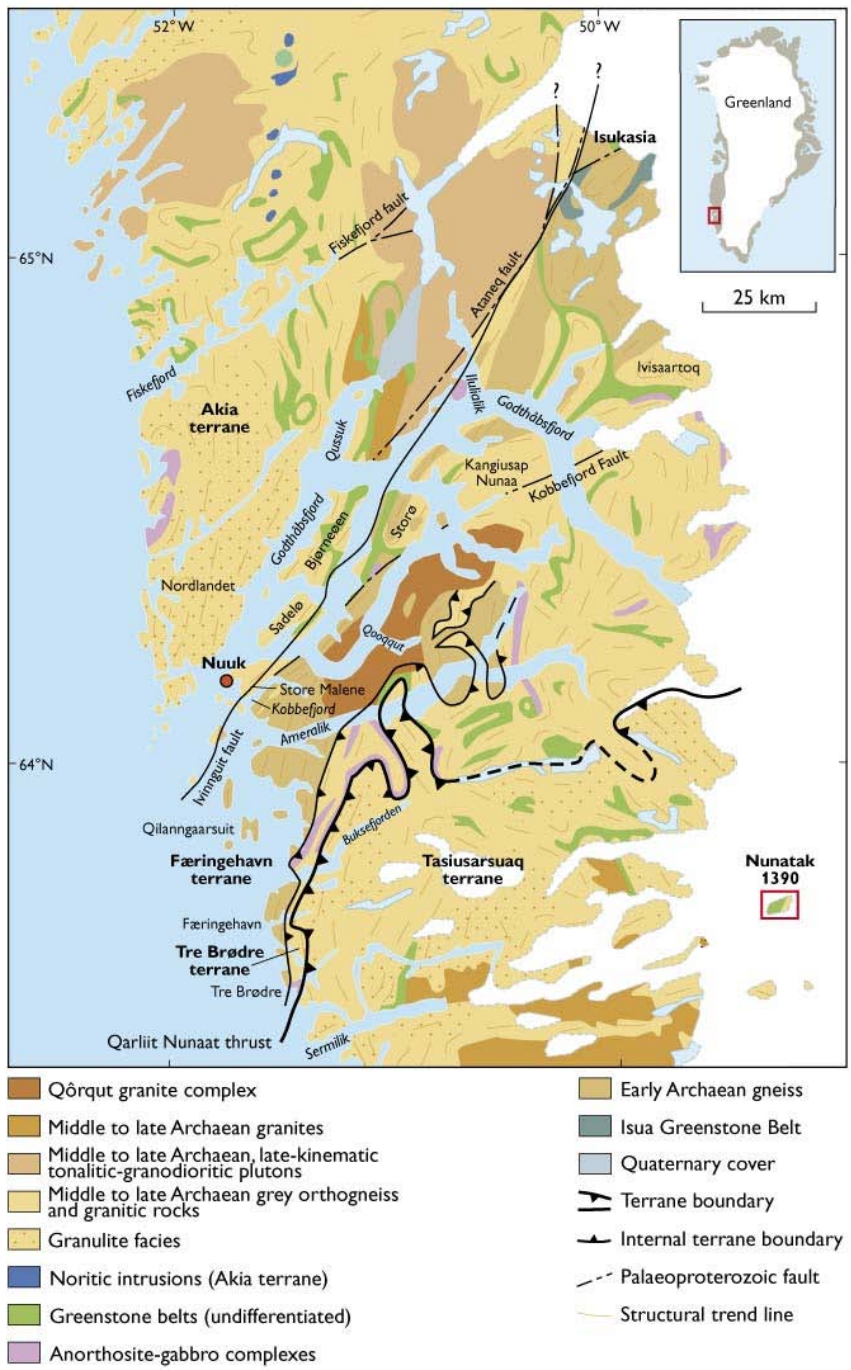

Fig. 1. Geological map of the Nuuk region and location of the Nunatak 1390 study area (modified from Escher & Pulvertaft 1995).

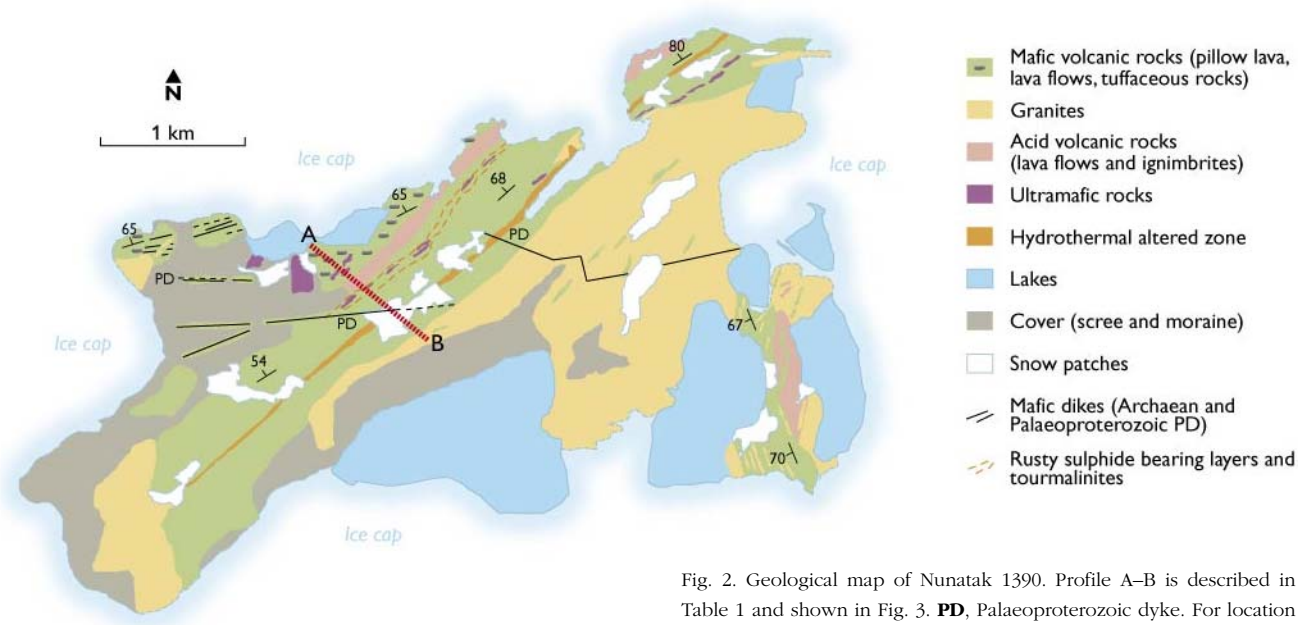

Fig. 2. Geological map of Nunatak 1390. Profile A–B is described in Table 1 and shown in Fig. 3. **PD**, Palaeoproterozoic dyke. For location see Fig. 1.

Nunatak 1390

Nunatak 1390 is located within the Inland Ice east of Alangorlia and was first described by Escher & Pidgeon (1976; Figs 1, 2). The entire volcanic package (Fig. 3; Table 1) is north-east-striking and dips steeply to the north-west. Although slightly to moderately deformed with lineations, folding, faulting and shearing, the rocks show well-preserved primary textures.

Stratigraphy

The lower mafic pillow sequence shows large deformed pillow structures (50–100 cm across) and pillow breccias with calc-silicate alteration in the matrix between the pillows and in the centre of some pillows. The calc-silicate minerals include epidote, diopside and carbonates and make up to 20 vol.% of the rock. The pillowed sequence is cut by a slightly deformed E–W-trending swarm of mafic dykes (1–5 m thick). The dykes are fine- to medium-grained gabbroic or noritic rocks.

Ultramafic greenstones and soapstones occur between the upper and lower pillow lava sequences. These magnetite-bearing rocks were probably originally sills. The upper pillow sequence contains very well-preserved primary structures in pillows, lava flows and ash layers (Fig. 4). The least deformed pillow lavas and flows contain relic vesicles. Way-up can readily be determined from the pillow structures and consistently youngs to the south. The upper mafic pillow sequence is overlain by a unit of acid volcanic and pyroclastic rocks, including ignimbrites, 80 m in thickness (Fig. 5). Fine-grained, grey to light-coloured porphyritic dykes (0.3–0.8 m wide) cut the volcanic rocks and are interpreted as feeder dykes to the acid rocks. Mafic flows and ash layers are intercalated with ultramafic sills, and mafic rusty layers contain sulphides and tourmalinites. The tourmalinite forms an up to one metre thick layer.

A prominent hydrothermal zone, strongly silicified and epidotised, strikes parallel with the mafic ash layers. It follows

Table 1. Stratigraphy of the volcanic sequence on Nunatak 1390

Rock type	Thickness (m)	Description
Mafic dyke	1–20	Undeformed Palaeoproterozoic brown dykes
Granite(s)	?	Porphyritic granite, altered granite and pegmatite
Tuff	700–800	Finely laminated tuff layers intruded by granitoids
Hydrothermally altered zone	50	Altered mafic tuff, and silicified and epidotised rocks
Mafic volcanic flows/tuff	120	Basaltic–komatiitic/mafic–ultramafic flows and tuff, intercalated with ultramafic sills, mafic rusty layers, sulphides (exhalites) and tourmalinites
Acid flows and pyroclastites	80	Acid lava flows and ignimbrites
Upper mafic volcanic pillows	~200	25–100 cm large pillows, pillow breccias and calc-silicate alterations
Ultramafic greenstone/sill	10–50	Ultramafic greenstone/sill between lower and upper pillow sequence
Lower mafic pillow sequence	>500	Deformed pillow lavas with extensive calc-silicate alterations that are cut by mafic dykes

Fig. 3. Central part of the stratigraphy of profile A–B on Nunatak 1390 (see Table 1).

Fig. 4. Pillow lava structures in the upper pillow lava sequence. Hammer (50 cm) for scale.

a fault lineament, is up to 50 m wide and can be recognised from the light brownish surface colour of the altered rocks. The hydrothermal zone is overlain by a thick sequence (700–800 m) of finely laminated tuff layers. Granite intrusions in the tuffs increase in abundance upwards and pass upwards into porphyritic granite with tuff xenoliths.

Two phases of granite occur: one is porphyritic with K-feldspar phenocrysts up to several centimetres in length; the other is more homogeneous, medium-grained, slightly foliated and muscovite-bearing. Parts of the granites, especially in the western part of the exposure, are altered and have a distinct pink coloration due to hematite formation.

On a regional scale, it should be noted that western and southern parts of the Tasiusarsuaq terrane preserve remnants of volcanic rocks at several localities, probably of similar age to that on Nunatak 1390 (Escher & Myers 1975).

Geochemistry

Twenty samples representing most rock types found on Nunatak 1390 were analysed by Actlabs, Canada (Research Package 4E). Altered samples were screened using e.g. K2O/P2O5, and those with anomalous ratios are not considered any further. Melanocratic–ultramafic pillow lavas, flows and ash have komatiitic and Mg- and Fe-rich basalt compositions and plot along a well-defined tholeiitic trend (Fig. 6A). The acid rock, which intercalates with the tholeiites, forms a loosely defined calc-alkaline group of andesitic to dacitic composition (Fig. 6A).

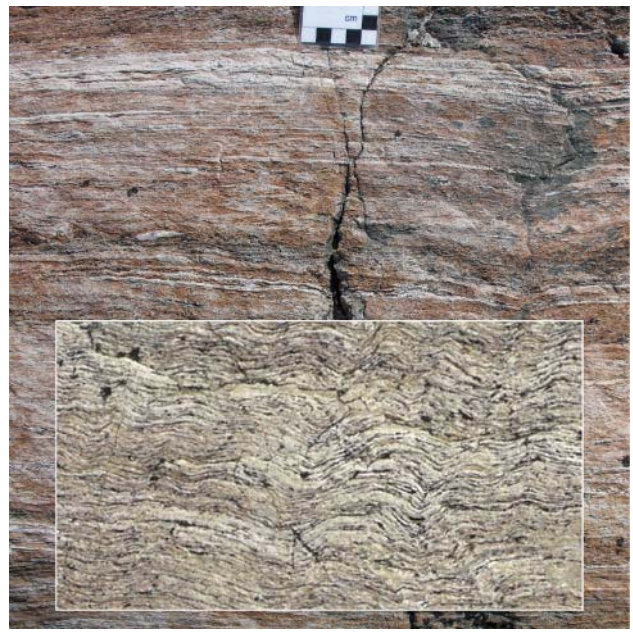

Fig. 5. Laminated acid volcanic rock (ignimbrite). Inset is an enlargement (inset is about 5 cm wide).

The tholeiites are characterised by near chondritic relative REE abundances (mean La/SmN = 1.2 ± 0.4 1σ; La/YbN = 1.3 ± 0.3 1σ, n = 9), while the acid rocks are more enriched and varied in their LREE (mean La/SmN = 5 ± 1 1σ; La/YbN = 24 ± 17 1σ, n = 5; Fig. 6B). The different incompatible trace element abundances in the tholeiites and acid rocks persist through all the elements, albeit with more scatter in the mobile elements. Important immobile, incompatible element ratios are indicative of potentially different tectonic settings for the tholeiites and the acid rocks. Nb/La ratios do not vary with Nb or other incompatible elements, which implies insignificant effects of fractional crystallisation and insignificant amounts of crustal contamination (Fig. 6C). The tholeiite mean Nb/La ratio is 0.6 ± 0.1 (1σ; n = 9), while the acid rocks have a substantially lower ratio of 0.14 ± 0.03 (1σ; n = 5). The ratios of the tholeiites are reminiscent of lower crust, while the low ratios of the acid rocks are typical of volcanic arc related rocks (Hawkesworth & Kemp 2006). Even though metamorphic element mobility may disturb e.g. Ce/Pb ratios, the consistent and low ratios of the acid rocks corroborate an arc origin (Fig. 6D), which we postulate for these rocks. The tholeiites are more ambiguous and are akin to MORB or island arc tholeiites. The spatial relationship

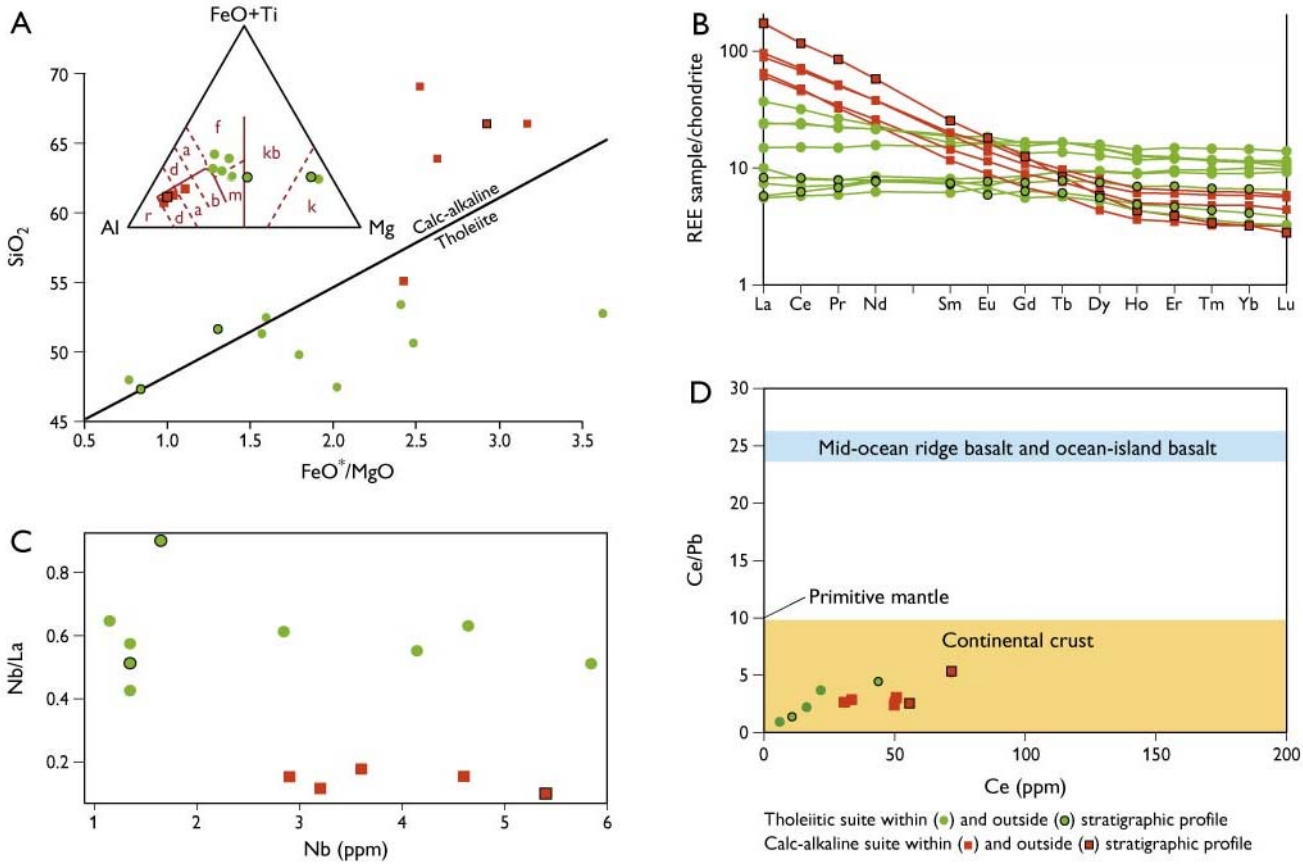

Fig. 6. **A**: FeO_t/MgO versus SiO_2 variation diagram, and Jensen cation plot; rhyolite (**r**), dacite (**d**), andesite (**a**), basalt (**b**), Mg tholeiite basalt (**m**), Fe tholeiite basalt (**f**), komatiitic basalt (**kb**) and komatiite (**k**). **B**: REE distribution of the tholeiitic suite (**green**) and calc-alkaline suite (**red**). **C**: Nb versus Nb/La of the tholeiitic suite (**green**) and calc-alkaline suite (**red**). **D**: Ce/Pb ratios variation versus Ce of the tholeiitic suite (**green**) and calc-alkaline suite (**red**).

between the acid rocks and the tholeiites seems to support a common origin, in which case an arc setting seems most plausible. By analogy with modern arc systems, the two components may reflect input from trench-side (tholeiites) and back arc-side (calc-alkaline) volcanoes respectively, or temporal shifts in the petrogenetic processes.

References

Crowley, J.L. 2002: Testing the model of late Archean terrane accretion in southern West Greenland: a comparison of the timing of geological events across the Qarliit nunaat fault, Buksefjorden region. Precambrian Research **116**, 57–79.

Escher, J.C. & Myers, J.S. 1975: New evidence concerning the original relationships of early Precambrian volcanics and anorthosites in the Fiskenæsset region, southern West Greenland. Rapport Grønlands Geologiske Undersøgelse **75**, 72–76.

Escher, J.C. & Pidgeon, R.T. 1976: Field mapping of nunatak 1390 m, east of Alángordlia, southern West Greenland. Rapport Grønlands Geologiske Undersøgelse **80**, 84–87.

Escher, J.C. & Pulvertaft, T.C.R. 1995: Geological map of Greenland, 1:2 500 000. Copenhagen: Geological Survey of Greenland.

Friend, C.R.L. & Nutman, A.P. 2001: U-Pb zircon study of tectonically bounded blocks of 2940–2840 Ma crust with different metamorphic histories, Paamiut region, South-West Greenland: implications for the tectonic assembly of the North Atlantic craton. Precambrian Research **105**, 143–164.

Hawkesworth, C.J. & Kemp, A.I.S. 2006: Evolution of the continental crust. Nature **443**, 811–817.

Hollis, J.A., Schmid, S., Stendal, H., van Gool, J.A.M. & Weng, W.L. 2006: Supracrustal belts in Godthåbsfjord region, southern West Greenland. Progress report on 2005 field work: geological mapping, regional hydrothermal alteration and tectonic sections. Danmarks og Grønlands Geologiske Undersøgelse Rapport **2006/7**, 171 pp.

Pidgeon, R.T. & Kalsbeek, F. 1978: Dating of igneous and metamorphic events in the Fiskenaesset region of southern West Greenland. Canadian Journal of Earth Sciences **15**, 2021–2025.

Schiøtte, L., Compston, W. & Bridgwater, D. 1989: U-Pb single-zircon age for the Tinissaq gneiss of southern West Greenland: a controversy resolved. Chemical Geology (Isotope Geoscience Section) **79**, 21–30.

Authors' address

Geological Survey of Denmark and Greenland, Øster Voldgade 10, DK-1350 Copenhagen K, Denmark. E-mail: *hst@geus.dk*

Seismic hazard assessment of Greenland

Peter Voss, Stine Kildegaard Poulsen, Sebastian Bjerregaard Simonsen and Søren Gregersen

Earthquake activity in Greenland has been registered and mapped since 1907 (Larsen *et al.* 2006) and thus a long (albeit relatively sparse) record of seismic activity is available for evaluation of seismic hazard and risk. Seismic hazard assessment is carried out by judging the probability of future earthquakes in a given region and is based on statistic treatment of earthquake data. The determination of the seismic hazard is the first step in an evaluation of seismic risk, i.e. the possible economic costs and loss of human life after an earthquake. The motivation for this seismic hazard study is the registration of four significant earthquakes in Greenland in 2005. The Geological Survey of Denmark and Greenland (GEUS) received reports of all four earthquakes from residents who had felt the shaking. The 2005 earthquakes were located at or near Qeqertarsuaq on 30 March, Sisimiut on 23 July, Station Nord on 30 August and Attu on 23 October (Fig. 1), with magnitudes on the Richter scale of 4.3, 4.1, 5.1 and 2.5, respectively. The earthquake in Attu led to the inhabitants fleeing in their boats.

Earthquake activity

Seismic hazard is just one of many natural hazards in Greenland. Other natural hazards include: continuous permafrost that constitutes a serious obstacle to development over the northern two-thirds of Greenland; strong katabatic winds that occur along the edge of the ice cap; very low wind chill and cold sea water, and; landslides and landslide-generated tsunamis (e.g. Dahl-Jensen *et al.* 2004). Offshore geohazards have been studied by GEUS for the 2002 licensing round off the Greenland west coast (Christiansen *et al.* 2002).

A first estimate of the seismic hazard of Greenland was presented during the Global Seismic Hazard Assessment Program (GSHAP; Giardini *et al.* 1999). For Greenland GSHAP used the very sparse data set that was collected prior to the mid-1990s. Since that time the data set has been much improved. The earthquake information used in this seismic hazard study has been extracted from the GEUS earthquake database and constitutes 227 events that occurred from November 1971 to February 2006 (Figs 1, 2). The majority of these events had a magnitude between 3.0 and 5.0, but since 2005 improved analytical methods have lowered the detection threshold from 3.0 to 1.0 in some areas. The earthquakes were primarily shallow; 93% have been located between 0 and 40 km depth.

The location of the earthquakes in the GEUS earthquake database is determined primarily by using measurements from the network of permanent and temporary seismic sta-

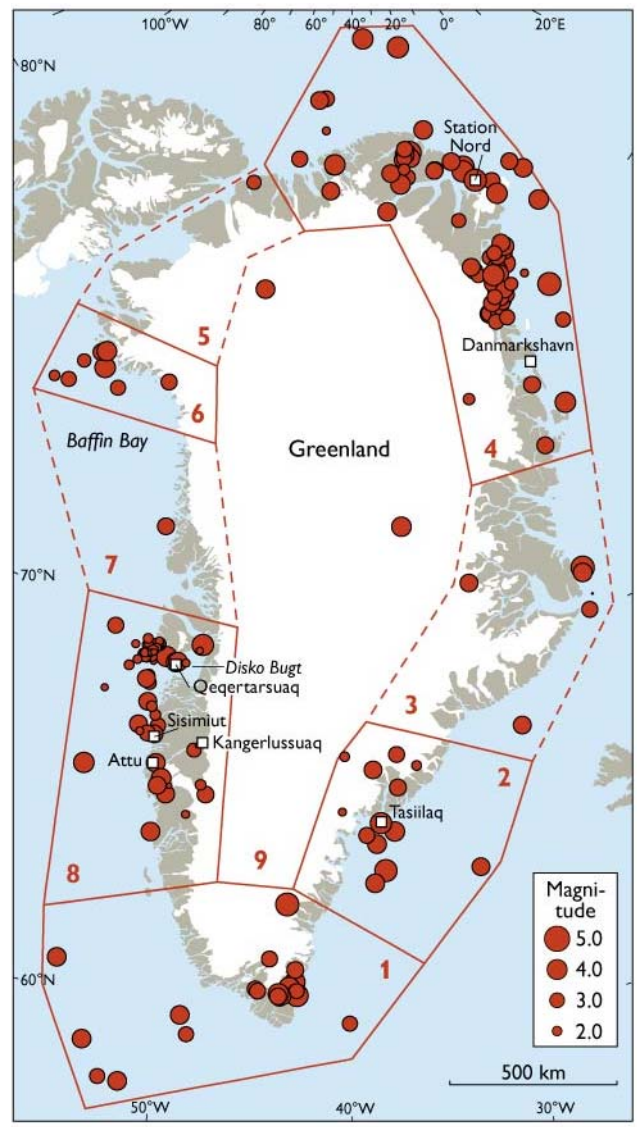

Fig. 1. Map showing the nine seismic source zones chosen for seismic hazard assessment of Greenland and the location and magnitude of earthquakes registered in the period November 1971 to February 2006 used in this study. In zones bordered by dashed lines the number of earthquakes is too low to provide input values to hazard assessment (see Table 1).

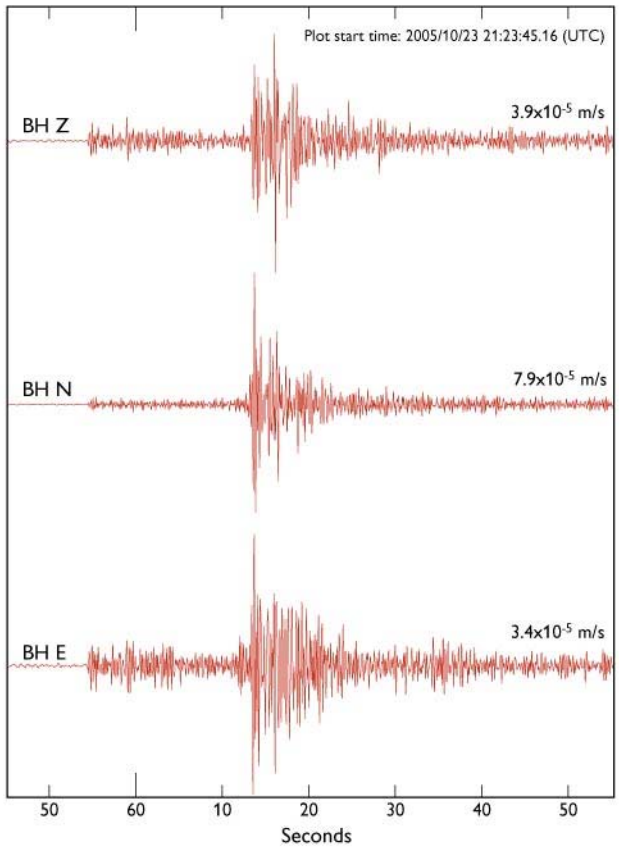

Fig. 2. Seismogram for the Richter scale 2.5 Attu earthquake on 23 October, 2005 recorded at the seismic station in Kangerlussuaq. Each trace shows the ground velocity in the direction indicated. The seismogram is band-pass filtered between 1 and 5 Hz, and the scale of the maximum amplitude is given at the end of each trace.

tions. By the end of 2006, the network of broadband, seismic stations in Greenland included four permanent and 14 temporary stations (Larsen *et al.* 2006). If an earthquake in Greenland has been recorded by a seismic network in a neighbouring country, these recordings are included in the database. The neighbouring networks that have provided most data are operated by the Geological Survey of Canada, the Norwegian Seismic Array (NORSAR) and the University of Bergen, Norway.

Table 1. Input parameters used in seismic hazard computation

Zone	Number of earthquakes	Activity [year^{-1}]	b-value [log]	Max. expected magnitude	Max. observed magnitude	Magnitude threshold
1	20	1.062	2.556	5.5	5.0	3.7
2	13	0.371	2.072	5.7	5.2	3.8
3	6	-	-	-	-	-
4	77	2.166	2.072	5.9	5.4	3.8
5	1	-	-	-	-	-
6	8	0.213	1.105	5.4	4.9	3.5
7	1	-	-	-	-	-
8	70	1.012	2.717	5.6	5.1	3.8
9	2	-	-	-	-	-

Note: Number of earthquakes in zones 3, 5, 7 and 9 is insufficient to provide input values to hazard assessment

Data analysis

The input for this seismic hazard study is the location, time and magnitude of the observed earthquakes. The location and time are determined using a 1D Earth model and an iterative linear inversion scheme (Lienert & Havskov 1995; Havskov & Ottemöller 2003). The magnitude used is the body wave magnitude m_b, and if that is not available, the local magnitude M_L (Gregersen 1982). The attenuation of seismic L_g waves is known at a few seismic stations as described by Gregersen (1982), but a full attenuation model for Greenland is at present not available. We have therefore applied the global reference model SEA96 by Spudich *et al.* (1997) that describes attenuation from normal faults in hard-rock conditions. Focal plane solutions have been estimated for only five earthquakes in Greenland (e.g. Gregersen 2006), and have thus not been included in this study. Palaeoseismic information could be of interest if available, but has not been included since palaeoseismic data are of little influence for return periods less than 1000 years in intraplate settings (Atakan *et al.* 2001). Offshore reflection seismic profiles along the west coast of Greenland (Chalmers & Pulvertaft 2001) show the presence of major fault systems that should be taken into account for return periods longer than 1000 years.

The coastal area of Greenland has been divided into eight seismic source zones that were chosen according to geological structures and the seismicity of the area (Fig. 1). The central part of the ice cap is represented by a single zone. Input values for the hazard assessment for each seismic source zone were determined from b-value and magnitude estimates (see Table 1 and Fig. 3). As an example, the computation of the b-value for seismic source zone 4 is shown in Fig. 3. The hazard computation is in the form of estimated maximum acceleration for a return period of 475 years, and is described in detail by Poulsen & Simonsen (2006).

Ice cap seismic hazards

Earthquake measurements on the Greenland ice cap have shown that the seismic energy is transmitted through the ice for both local and teleseismic earthquakes. The attenuation model we have applied to estimate the seismic hazard in Greenland is based on hard-rock conditions; thus, the approach used in this study and the results obtained do not apply for conditions on the ice cap. Ground shaking from the newly discovered glacial earthquakes, or icequakes, (Ekström *et al.* 2003, Larsen *et al.* 2006) has not been taken into account either. Only a very few earthquakes have been located below the ice cap (see Fig. 1), and seismic hazard in the interior of Greenland is therefore considered to be even lower than the lowest hazard in any coastal area.

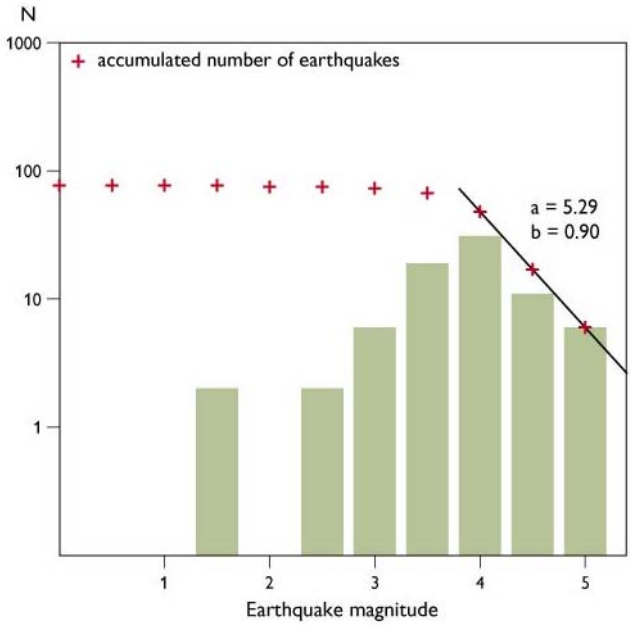

Fig. 3. Histogram showing the number and magnitude of earthquakes determined in seismic source zone 4. It is a global experience in seismology that the number of earthquakes (N) of various magnitudes (M) can be expressed in a logarithmic relation: $\log N = a - b \times M$ (black line). The a-value is a measure of regional seismicity, whereas the b-value may be viewed as a regional physical constant.

Seismic hazard

The seismic hazard assessment of Greenland is computed for a return period of 475 years as shown in Fig. 4. The maximum hazard is found in seismic source zone 4 at a value of 0.051 g (50.37 cm/s^2). From this result we assess the general seismic hazard in Greenland to be low, following the classification of Jiménez *et al.* (2003) in which low, moderate and high hazards correspond to peak ground accelerations of 0.0–0.08 g, 0.08–0.24 g and above 0.24 g, respectively, for a 475-year return period.

Seismic source zone 4 covering the northern and north-eastern parts of Greenland is the area with the highest seismic hazard; the seismic hazard is below 0.05 g in the other seismic source zones where the highest hazards are encountered in the Disko Bugt – Sisimiut area (seismic source zone 8) followed by southern Greenland (seismic source zone 1). These results differ considerably from the GSHAP estimates that are below 0.02 g for the northern and the north-eastern parts of Greenland. Along the east coast of the Baffin Bay we find the seismic hazard to be below 0.024 g, where GSHAP reported a hazard of up to 0.08 g.

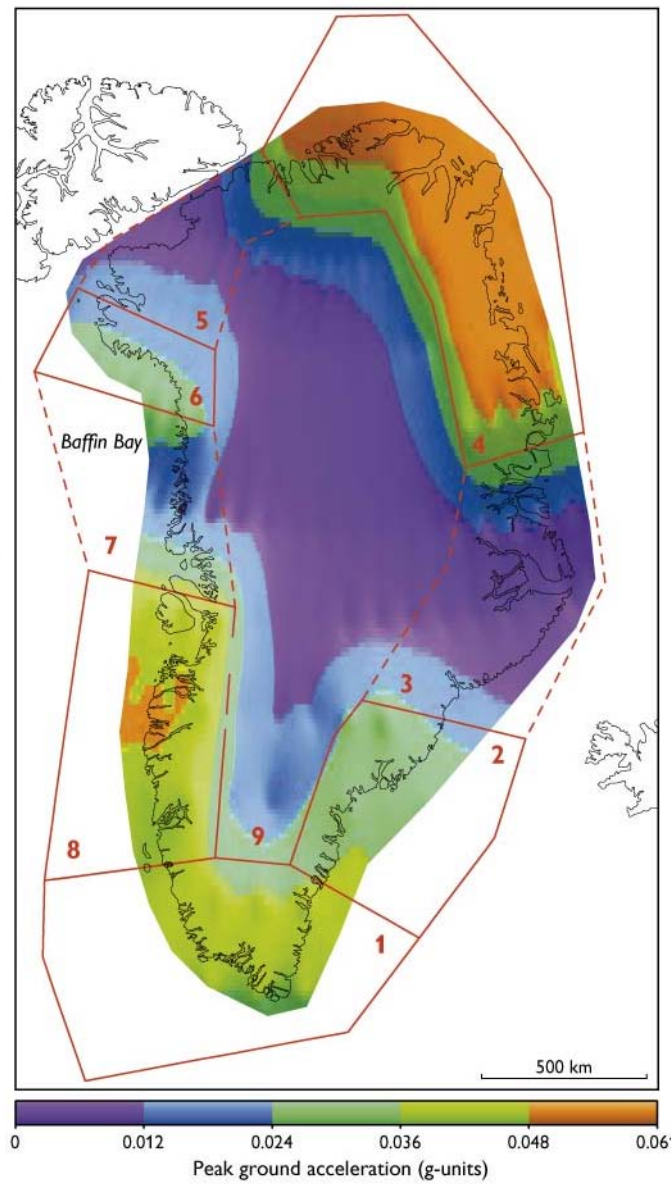

Fig. 4. Map showing seismic hazard in Greenland for a 475-year return period, corresponding to the 10% probability of exceeding a given g-value in a 50-year period (hard-rock conditions). Seismic source zones from Fig. 1 indicated.

Seismic risk

A full evaluation of seismic risk would include collecting in-depth knowledge of factors such as infrastructure, building standards and population density distribution, work that is beyond the scope of this study. Here we outline only the expected, relative seismic risk for the four areas of highest seismic hazard. Though the highest seismic hazard is found in the northern and north-eastern parts of Greenland (seismic zone 4), the seismic risk is very low, since the only permanent residents are the five Danish Air Force personnel at Station

Nord and the staff at the Danmarkshavn weather station, where the buildings are designed to withstand the Arctic climate. The next two zones in order of decreasing seismic hazard are the Disko Bugt – Sisimiut area (seismic zone 8) and southern Greenland (seismic zone 1). Larger infrastructure and denser population in seismic zones 1 and 8 indicate that these are judged to be at the highest seismic risk in the whole of Greenland.

Concluding remarks

The results presented in this study have completely changed the seismic hazard assessment of Greenland compared to the seismic hazard map compiled by GSHAP (Giardini *et al.* 1999). GSHAP overestimated the seismic hazard of the area north of Disko Bugt and underestimated the seismic hazard for the southern, the northern and the north-eastern parts of Greenland.

During recent years, the majority of reports received by GEUS of earthquakes felt by the resident population are from Tasiilaq (seismic zone 2), but our results show that the seismic hazard in this area is low because these earthquakes are small.

The overall seismic hazard in Greenland is low compared to the many other natural hazards. However, large destructive earthquakes can occur unexpectedly even in areas with low seismicity, as illustrated by the magnitude 6.3 Latur earthquake in central India on 30 September, 1993 (Gupta 1993).

Acknowledgements

GeoForschungsZentrum (GFZ) Potsdam, Germany, provides instrumentation and technical support to the seismograph in Danmarkshavn and, together with the Incorporated Research Institutions for Seismology (IRIS), USA, to the seismograph in Kangerlussuaq. GFZ has also contributed to the installation and operation of several temporary seismic stations. The Bureau of Minerals and Petroleum, Government of Greenland, provided financial support for several temporary installations.

References

Atakan, K., Ojeda, A., Camelbeeck, T., & Meghraoui, M. 2001: Seismic hazard analysis results for the Lower Rhine Graben and the importance of paleoseismic data. Netherlands Journal of Geosciences **80**, 305–314.

Chalmers, J.A. & Pulvertaft, T.C.R. 2001: Development of the continental margins of the Labrador Sea: a review. Geological Society (London) Special Publications **187**, 77–105.

Christiansen, F.G., Bojesen-Koefoed, J.A., Chalmers, J.A., Dalhoff, F., Marcussen, C., Nielsen, T., Nøhr-Hansen, H. & Sønderholm, M. 2002: Petroleum geological activities in West Greenland in 2001. Geology of Greenland Survey Bulletin **191**, 57–60.

Dahl-Jensen, T., Larsen, L.M., Pedersen, S.A.S., Pedersen, J., Jepsen, H.F., Pedersen, G., Nielsen, T., Pedersen, A.K., von Platen-Hallermund, F. & Weng, W. 2004: Landslide and tsunami 21 November 2000 in Paatuut, West Greenland. Natural Hazards **31**, 277–287.

Ekström, G., Nettles, M., & Abers, G.A. 2003: Glacial earthquakes. Science **302**, 622–624.

Giardini, D., Grünthal, G., Shedlock, K.M., & Zhang, P. 1999: The GSHAP global seismic hazard map. Annali di Geofisica **42**, 1225–1230.

Gregersen, S. 1982: Seismicity and observations of Lg wave attenuation in Greenland. Tectonophysics **89**, 77–93.

Gregersen, S. 2006: Intraplate earthquakes in Scandinavia and Greenland. Neotectonics or postglacial uplift. Journal of Indian Geophysical Union **10**, 25–30.

Gupta, H.K. 1993. The deadly Latur earthquake. Science **10**, 1666–1667.

Havskov, J., & Ottemöller, L. 2003: SEISAN: the earthquake analysis software for Windows, Solaris and Linux, version 8.0, 244 pp. Bergen: Institute of Solid Earth Physics, University of Bergen, Norway.

Jiménez, M.-J., Giardini, D. & Grünthal, G. 2003: The ESC-SESAME unified hazard model for the European-Mediterranean region, EMSC/CSEM Newsletter **19**, 2–4.

Larsen, T.B., Dahl-Jensen, T., Voss, P., Jørgensen, T.M., Gregersen, S. & Rasmussen, H.P. 2006: Earthquake seismology in Greenland – improved data with multiple applications. Geological Survey of Denmark and Greenland Bulletin **10**, 57–60.

Lienert, B.R.E. & Havskov, J. 1995: A computer program for locating earthquakes both locally and globally. Seismological Research Letters **66**, 26–36.

Poulsen, S.K. & Simonsen, S.B. 2006: Seismic hazard analysis of Greenland and a distribution of earthquakes, 68 pp. Unpublished B.Sc. thesis, University of Copenhagen, Denmark.

Spudich, P. *et al.* 1997: SEA96 – a new predictive relation for earthquake ground motions in extensional tectonic regimes. Seismological Research Letters **68**, 71–79.

Authors' addresses

P.V & S.G., *Geological Survey of Denmark and Greenland, Øster Voldgade 10, DK-1350 Copenhagen K, Denmark.* E-mail: *pv@geus.dk*

S.K.P. & S.B.S., *Niels Bohr Institute, University of Copenhagen, Juliane Maries Vej 30, DK-2100 Copenhagen Ø, Denmark.*

Development of marine landscape maps for the Baltic Sea and the Kattegat using geophysical and hydrographical parameters

Zyad K. Al-Hamdani, Johnny Reker, Jørgen O. Leth, Anu Reijonen, Aarno T. Kotilainen and Grete E. Dinesen

The Baltic Sea is one of the largest brackish water bodies in the world (Segerstråle 1957) with a number of basins varying from almost fresh water in the northern part of the Bothnian Bay via the more brackish conditions in the southern part to the saline waters of the Kattegat. The Baltic Sea is subject to severe environmental degradation caused by commercial and leisure activities, including fisheries, dredging, tourism, coastal development and land-based pollution sources. This causes severe pressures on vulnerable marine habitats and natural resources, and a tool for aiding marine management is therefore strongly needed.

The marine landscape concept presented by Roff &Taylor (2000) is based on the use of available broad-scale geological, physical and hydrographical data to prepare ecologically meaningful maps for areas with little or no biological information. The concept, which was elaborated by Day & Roff (2000) was applied in UK waters (Connor *et al*. 2006) before it was adopted by the BALANCE project described here. The aim of developing marine landscape maps is to characterise the marine environment of the Baltic Sea region (the Baltic Sea together with the Kattegat) using geophysical and hydrographical parameters. Such maps can be applied, for example, to an assessment of the Baltic-wide network of marine protected areas, and thus provide a sustainable ecosystem-based approach to the protection of the marine environment from human activities, and contribute to the conservation of marine biodiversity.

The BALANCE project is based on transnational and cross-sectoral co-operation with participants from nine countries surrounding the Baltic Sea as well as Norway (Fig. 1), and is partially financed by the European Union through the BSR INTERREG IIIB programme.

Data collation and harmonisation

One of the most challenging aspects of marine landscape map production is collating and harmonising data sets from different sources and with different formats. The data sets include: bathymetry, seabed sediment types, the photic zone, ice cover, halocline depth, temperature, current velocity and bottom salinity. The data sets provided by the individual partners in the BALANCE project were analysed in detail before merging in a GIS platform to produce the final benthic marine landscape map (Al-Hamdani & Reker in press).

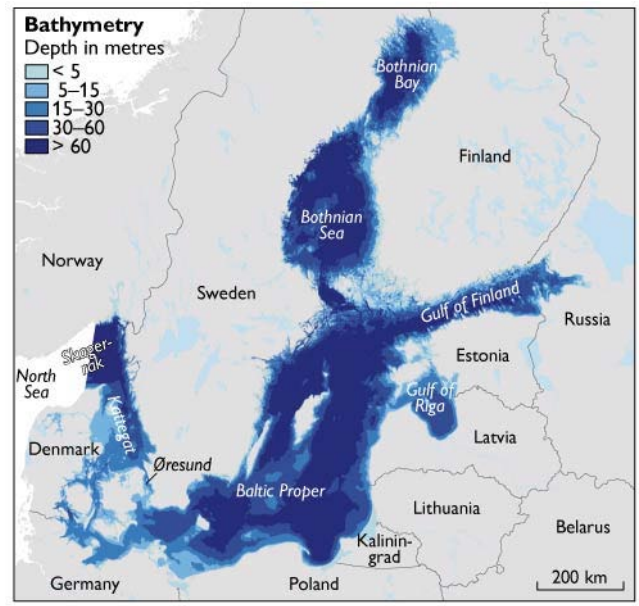

Fig. 1. Bathymetry of the Baltic Sea, the Kattegat and the Skagerrak, the working area of the BALANCE project. Data source: Geological Survey of Denmark and Greenland, Geological Survey of Sweden and Geological Survey of Finland

The data sets were obtained through a combination of field measurements and modelling. Other data were considered, but not acquired for the entire area; these include oxygen depletion, stratification, wave exposure and pycnocline depth.

Development of marine landscape maps

The uniqueness of the Baltic Sea region originates in part from its salinity distribution. A stable salinity gradient and stratification is observed in both vertical and horizontal dimensions. This results in wide biogeographic variation as the water salinity changes from marine in Skagerrak to nearly fresh waters in the Bothnian Bay. Thus a wide variety of complex marine landscapes reflecting the complexity of the *in situ* regimes of physical factors is expected. The physical factors chosen for defining the marine landscapes in the Baltic Sea

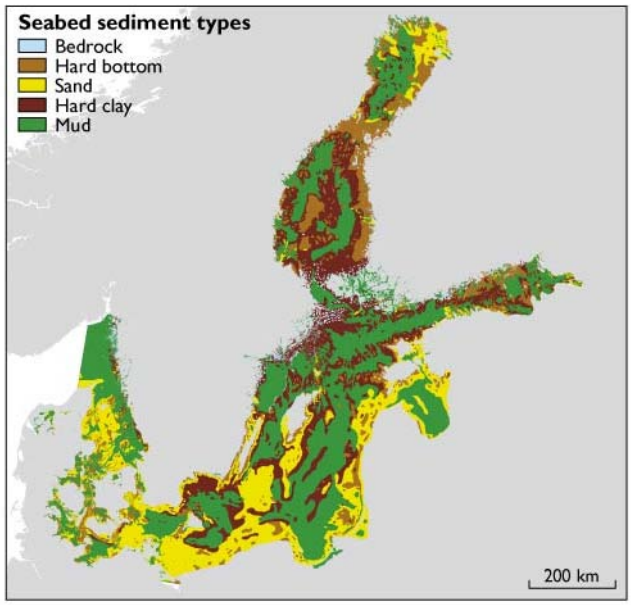

Fig. 2. Map of the seabed sediments. Data source: Geological Survey of Denmark and Greenland, Geological Survey of Sweden and Geological Survey of Finland.

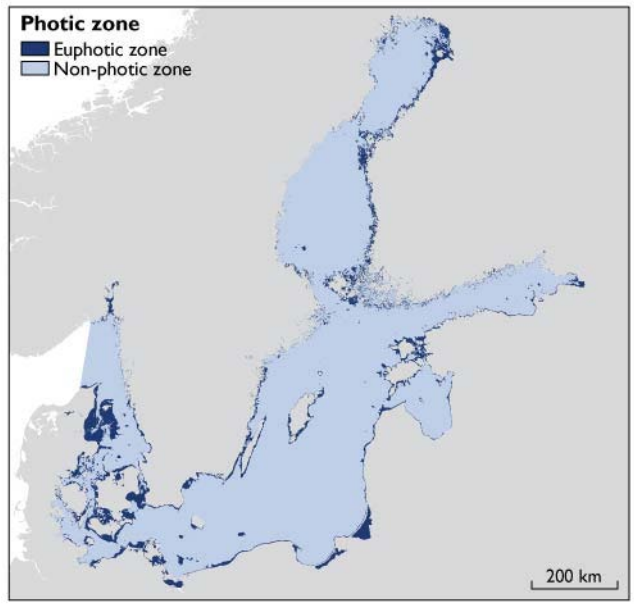

Fig. 3. Map of the photic zones. The original modelled data set is a 620 m grid of the average Secchi depth measured from March to the end of November for the period from 1980 to 1998. Data source: Danish Hydraulic Institute.

region are considered important for structuring the distribution of major biological assemblages in the region. Three physical parameters were adopted in this work to produce the benthic marine landscape map: sediment type, the photic zone, and bottom salinity. The best way to produce a benthic marine landscape map from a number of different sources is by using raster map algebra in a GIS platform. This method allows the combining of several different parameters stored in separate layers into a single map layer.

One of the major tasks in the production of marine landscape maps for the Baltic Sea region was to split the chosen environmental data sets in such a way as to produce ecologically relevant classes. The justification for the classification of each data layer is explained separately below, bearing in mind that this is the first attempt to classify such features in the Baltic Sea; future amendments are thus to be expected.

Seabed sediment types

The data sets for this layer were gathered from different governmental and research institutes of the Baltic Sea countries and Norway. The existing data are abundant and very diverse and have been acquired using different field techniques during the past several decades. Seabed sediment maps from offshore and coastal areas exist at a wide range of scales from local (1:20 000) to regional (up to 1:1 000 000). Terminology and classifications vary as well, since the nine circum-Baltic nations together with Norway have interpreted their own data according to different national classification schemes.

National seabed sediment classification categories needed to be harmonised in order to produce the regional map for seabed sediment types (Fig. 2). The resulting classification scheme consists of five sediment classes, which can be extracted from existing data. These sediment classes are:

1. Hard bottom, including bedrock (crystalline and sedimentary) and bedrock covered with boulders.
2. Hard bottom composite, including complex, patchy hard surface and coarse sand (sometimes also clay to boulders).
3. Sand, including fine to coarse sand (with gravel exposures).
4. Hard clay, sometimes/often/possibly exposed or covered with a thin layer of sand/gravel.
5. Mud, including gyttja-clay to gyttja-silt.

The photic zone

From an ecological point of view, available light is one of the primary physical factors influencing and structuring the biological communities in the marine environment, as it is the driving force behind primary production by providing energy for photosynthesis. The depth of the euphotic zone is traditionally defined as the depth where 1% of the surface irradiance (as measured just below the water surface) is available for photosynthesis. This value was calculated by multiplying the actual measured Secchi depths by a factor of 1.9 (A. Erichsen, personal communication 2006). Based on the irradiation depth, the photic zone was split into two intervals: the euphotic zone and the non-photic zone. These two zones

reflect the significant ecological difference between the shallow-water environment where primary production takes place, and the deeper waters where species and biomass are dominated by fauna and bacteria (Fig. 3).

Bottom salinity

Salinity is one of the primary physical factors structuring the distribution of species within the Kattegat and the Baltic Sea, varying from almost fresh water in the Bothnian Bay to normal marine waters in Skagerrak (Fig. 4). The classification of the salinity data set and justification of the classification are presented in Table 1.

The three layers, sediment, photic zone, and bottom salinity were combined using the Spatial Analysis tool in the GIS program resulting in the benthic marine landscape map of the Baltic Sea region shown in Fig. 5. This map shows the distribution of 60 marine landscape types each representing different physical conditions at the seabed. The marine landscape map was further analysed with a statistical tool in GIS program to extract the diversity in marine landscape distribution (Fig. 6).

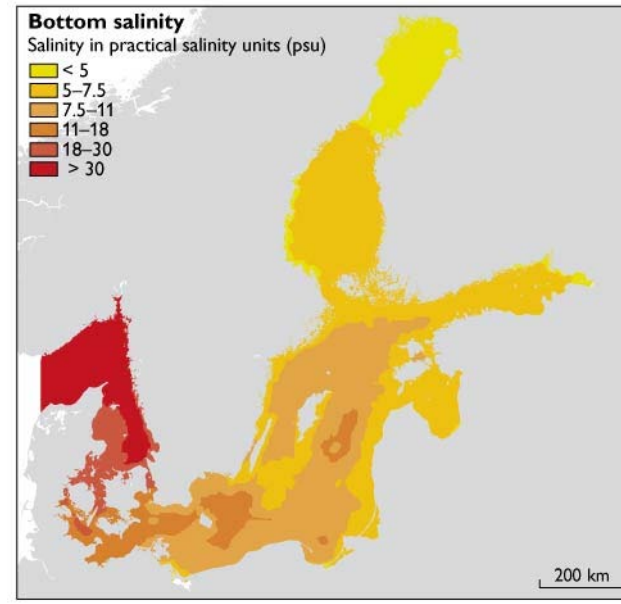

Fig. 4. Map of the bottom salinity. The original modelled data set is a 7.5 km grid horizontal resolution and 20 vertical layers. The model is based on monthly, averaged values from August 2003 over a period of one year. Data source: National Environmental Research Institute, Denmark.

Application of marine landscape maps

The marine landscape maps developed for the Baltic Sea region are a first approach to a broad-scale, physical characterisation of the marine environment of the Baltic Sea and the Kattegat. It will be used throughout the BALANCE project to assess the representativity of the network of marine protected areas (MPAs) within the Baltic Sea region. This assessment will identify whether some marine landscape types are missing or over-represented within the existing MPA network and thus help inform environmental managers whether the existing network is protecting and representing the marine diversity of the Baltic region. The landscape map can also be used to show the complexity of the marine environment within a certain area (Fig. 5) to enhance future management and protection of the marine ecosystem.

In addition to a continuous validation process and confidence rating of the data layers and maps there are many

Table 1. Baltic Sea salinity classification and justification

Interval	Salinity range*	Justification
Oligohaline I	< 5 psu	This picks up the biogeographic boundary in the Bothnian Bay area. Many freshwater species are able to survive in salinities below 5 psu including invertebrates, fish and plants.
Oligohaline II	5–7.5 psu	7.5 psu equals roughly to the area where *Fucus serratus* has its distributional boundary (Baltic Proper) making *Fucus vesiculosus* the dominating sublittoral brown algae. It is the interval with the lowest number of species and thus the most vulnerable part of the Baltic Sea.
Mesohaline I	7.5–11 psu	11 psu is the minimum requirement enabling cod (*Gadus morhua*) eggs to float. As cod is an important commercial species for the Baltic Sea region this interval is chosen in order to increase applicability of the marine landscapes map for environmental management. It also helps to separate offshore environment from coastal areas in large parts of the Baltic Proper.
Mesohaline II	11–18 psu	18 psu is the minimum requirement (roughly) for sexual reproduction or limiting distribution of many marine macroalgae, e.g. *Laminaria digitata* and *Ascophyllum nodosum*, and of e.g. echinoderms. The interval picks up the biogeographic boundary in Øresund. 18 psu is also the figure mentioned in the EU Water Framework Directive further increasing the applicability of the marine landscape maps.
Polyhaline	18–30 psu	Most marine species are able to survive within this interval. It is also an interval mentioned in the EU Water Framework Directive.
Euhaline	> 30 psu	Requirement of truly stenohaline species separating the marine parts of the Skagerrak and the North Sea from the freshwater influenced water masses of the Kattegat and the Baltic Sea region. The interval is also mentioned in the EU Water Framework Directive.

* psu: practical salinity units.

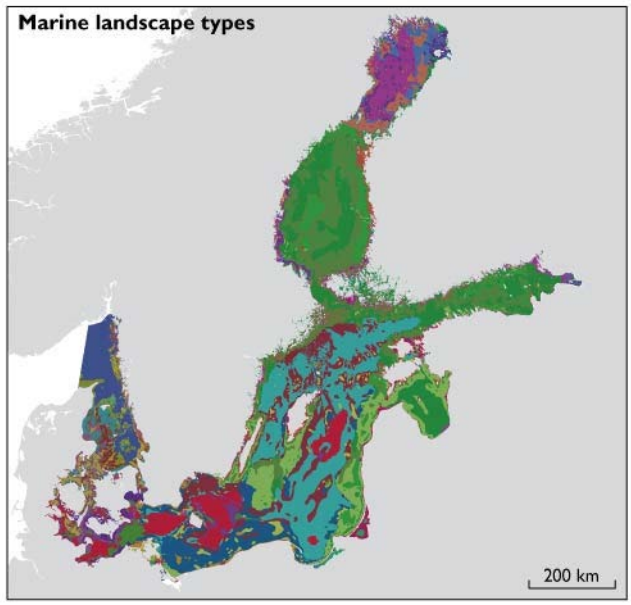

Fig. 5. Map showing the 60 marine landscape types recognised in the Baltic Sea, the Kattegat and the Skagerrak. For further details see Al-Hamdani & Reker (in press).

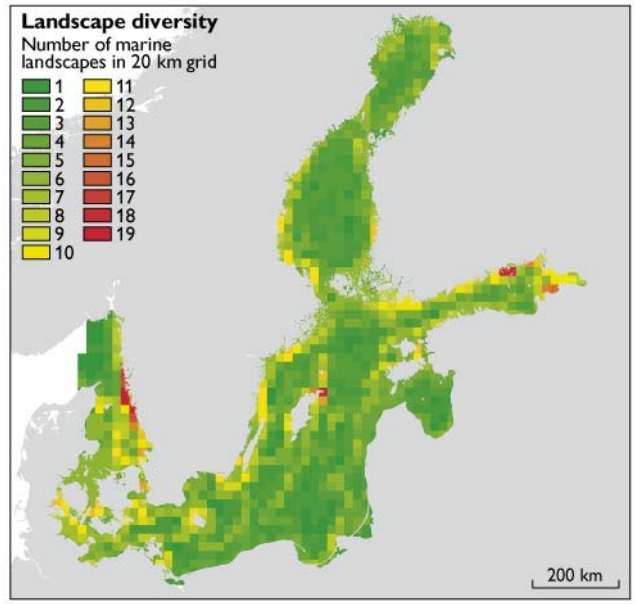

Fig. 6. Map showing diversity of marine landscape types.

future challenges for the marine landscape maps. These will include adapting them as a tool for various EU directives implementation, using the maps as (1) a strategic tool for planning future field surveys for mapping (e.g. Natura 2000 habitats in the EU Habitats Directive, (2) a physical characterisation of the marine environment in the proposed Marine Strategy Directive, or (3) part of the typologies in the EU Water Framework Directive. The approach described here should, of course, be improved and adapted to this legislative framework, including more physical layers depending on end-user requirements. Similarly, development of pelagic marine landscape maps could be combined with data on e.g. commercial fish species or marine mammals, to provide valuable information to improve management of the marine environment.

In conclusion, marine landscape mapping in the Baltic Sea region is just beginning and although much work has been put into this first step, there are still many challenges ahead. These include access to existing data from the entire Baltic region, assigning confidence ratings to the map, improving data layers classification and most importantly, providing good practice examples on how this characterisation can be applied in implementing EU legislation and planning.

Acknowledgements

Data, analysis and stimulating discussions for the production of the marine landscape maps were provided by David Connors (Joint Nature Conservation Committee UK), Karsten Dahl, Johan Söderkvist and Jørgen Bendtsen (National Environmental Research Institute, Denmark), Jesper H. Andersen and Anders Erichsen, (Danish Hydraulic Institute, Water Environment & Health), Lisbeth Tougaard (Geological Survey of Denmark and Greenland) and Daria Ryabchuk (All-Russian Geological Institute, St. Petersburg).

References

Al-Hamdani, Z.K. & Reker, J. (eds) in press: Towards marine landscapes in the Baltic Sea. Copenhagen: Geological Survey of Denmark and Greenland.

Connor, D.W., Golding, N., Robinson, P., Todd, D. & Verling, E. 2006: UKSeaMap: The mapping of marine seabed and water column features of UK seas, 104 pp. Peterborough: Joint Nature Conservation Committee.

Day, J.C. & Roff, J.C. 2000: Planning for representative marine protected areas: a framework for Canada's oceans, 147 pp. Toronto: World Wildlife Fund Canada.

Roff, J.C. &. Taylor, M.E. 2000: Viewpoint. National frameworks for marine conservation – hierarchical geophysical approach. Aquatic Conservation. Marine and Freshwater Ecosystems **10**, 209–223.

Segerstråle, S.G. 1957: The Baltic Sea. In: Hedgpeth, J.H. (ed.): Treatise on marine ecology and paleocology, **1**. Ecology. Geological Society of America Memoir **67**, 751–800.

Authors' addresses

Z.K.A. & J.O.L., *Geological Survey of Denmark and Greenland, Øster Voldgade 10, DK-1350 Copenhagen K, Denmark.* E-mail: *azk@geus.dk*

A.T.K. & A.R., *Geological Survey of Finland, P.O. Box 96, FIN-02151 Espoo, Finland.*

J.R. & G.E.D., *Danish Forest and Nature Agency, Haraldsgade 53, DK-2100 Copenhagen Ø, Denmark.*

Shallow groundwater quality in Latvia and Denmark

Edmund Gosk, Igors Levins and Lisbeth Flindt Jørgensen

Experience and results from the Danish groundwater monitoring programme that has been carried out systematically since 1990, have been used in a co-operative project between Latvia and Denmark. The main objective of the project was to obtain more detailed knowledge of the shallow Latvian groundwater, to optimise the Latvian groundwater monitoring programme and to support the implementation of European legislation such as the Water Framework Directive, the Nitrate Directive and the Groundwater Directive in Latvia.

Comprehensive summaries describing the methodology of groundwater quality monitoring as well as the major results from the Danish groundwater monitoring network can be found in GEUS (2005) and Stockmarr (2005). Until recently only few data on Latvian groundwater quality were available, but in a project running from 2003 to 2006, 800 samples from groundwater, springs and drains have been analysed for a large number of components resulting in a comprehensive overview of the status of Latvian groundwater (Fig. 1; Gosk *et al*. 2006).

The project *Agricultural influence on groundwater in Latvia* was carried out by the State Geological Survey of Latvia and the Geological Survey of Denmark and Greenland (GEUS) and was supported by the Danish Environmental Protection Agency within the framework of the DANCEE programme (Danish Co-operation for Environment in Eastern Europe). As a spin-off of the project this paper compares groundwater quality in the two countries.

Groundwater use and agricultural load

Drinking-water production in Denmark is almost entirely based on groundwater abstracted from both shallow and moderately deep Quaternary and pre-Quaternary aquifers covered by more or less protective layers of till of variable thickness.

The annual groundwater recharge is relatively large in Denmark and is on an average, national scale sufficient to cover needs (Henriksen & Sonnenborg 2003). However,

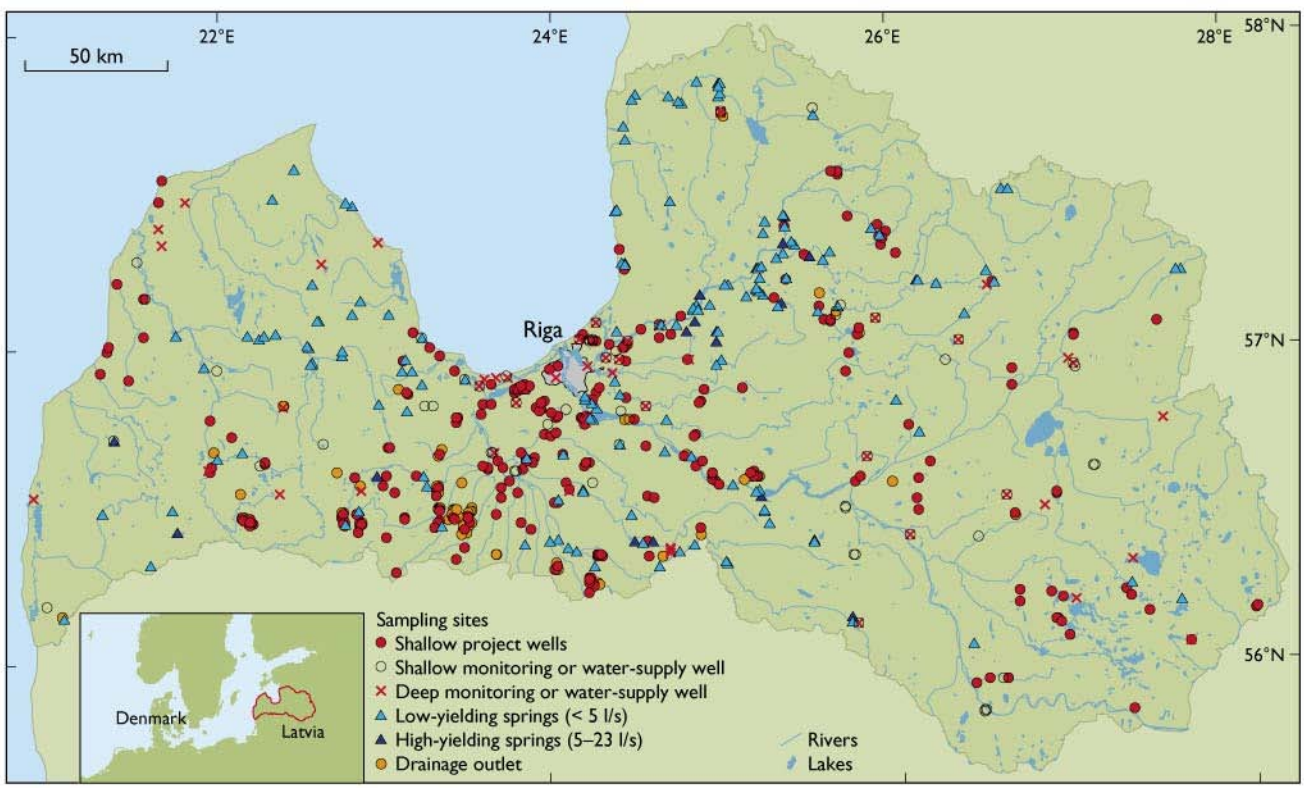

Fig. 1. Sampling sites of Latvian groundwater.

abstraction exceeds recharge in some areas, especially around the largest cities. Furthermore, diffuse groundwater contamination by pesticides and nitrate has become an increasing problem since the middle of the last century, and a number of water-supply wells have been closed. Up to now it has been possible to find new, clean groundwater resources, either by drilling deeper wells or by moving wells to less impacted areas.

More than 60% of the Danish territory is defined as arable land. The impact of agriculture on water quality has been known for many years, and measures aiming at a reduction of nutrient load started in the 1980s with the adoption of the first Action Plan on the Aquatic Environment. At that time the average nitrogen load had reached 130 kg N/ha, which resulted in a high risk of groundwater contamination and in actual quality problems in some areas of the country.

Drinking-water production in Latvia is also primarily based on groundwater. Only Riga Water Supply uses a substantial amount of surface water to produce about half of the drinking water consumed in the Latvian capital.

The thick till layer that covers most of Latvia is characterised by poor aquifer conditions where only little groundwater abstraction is possible from small, local water-bearing lenses. The centralised drinking-water supply in Latvia is therefore typically based on confined aquifers screened at depths greater than 50 m. In areas with intensive agriculture (the southern and central parts of the country) the average depth of wells exceeds 100 m.

Due to the dramatic political and economical changes in Latvia at the beginning of the 1990s groundwater abstraction decreased by a factor of 2–3 resulting in a significant, still progressing recovery of groundwater levels in the central and south-western parts of the country. In the remaining parts of the country groundwater levels have never been affected by abstraction.

During the same period, the acreage of arable crops, the use of mineral fertilisers, the number of livestock and other parameters related to agricultural load, decreased by a factor of 3–10 (Stålnacke *et al*. 2003). At present only 13% of the Latvian area is under cultivation, and the average crop yield is about half of the Danish figures.

Groundwater monitoring and knowledge of diffuse contamination

Due to the pressure from diffuse sources, groundwater monitoring plays an important role in water management and protection of groundwater resources in Denmark. More than 6000 drinking-water supply wells, a network of more than 1400 specially selected screens in 70 groundwater monitoring areas, as well as five agricultural watershed monitoring areas equipped with a total of about 100 shallow screens (Stockmarr 2005), together form the basis of the Danish groundwater monitoring system. The detailed groundwater quality monitoring includes analyses of 97 elements, comprising 14 heavy metals and 34 pesticides and their metabolites (NERI 2005).

The regional groundwater quality monitoring network in Latvia, established in the 1970s and 1980s, is based on 150 wells located within 45 monitoring stations. This network was designed to control depression cones (quantitative monitoring) rather than to monitor the various forms of diffuse pollution (qualitative monitoring). Monitoring wells are typically screened in deep aquifers used for abstraction. Until recently, the parameters analysed comprised major ions and nitrogen compounds, but no analyses of heavy metals and pesticides were made. Groundwater quality data from abstraction wells consisted mainly of information collected during drilling.

Monitoring of drinking-water quality in Latvia is almost entirely limited to sampling of tap water. Although some of the larger water-supply companies collect samples from abstraction wells, the centralised data processing system for this type of analysis is not yet established.

The amount of groundwater data recently collected in Latvia is much smaller than comparable data collected in Denmark. However, a large amount of information on the youngest groundwater in shallow aquifers has been collected in the period 2003–2005 as part of the present project. About 800 groundwater samples were analysed for a wide spectrum of elements, including heavy metals and pesticides (Gosk *et al*. 2006).

The determination of background concentration of various elements was based on data from shallow wells located outside local point-pollution plumes and urbanised and industrial areas.

Nitrates and pesticides

As expected, the distribution of nitrates in Danish and Latvian groundwater differs considerably (Fig. 2A). In the shallowest groundwater, the concentration of nitrates exceeds the quality standards of drinking water (50 mg/l NO_3) in 15% and 3.5% of the monitoring screens in Danish and Latvian wells, respectively. Furthermore, the decrease of nitrate concentration with depth is much faster in the Latvian than in the Danish groundwater.

The differences observed are caused by a lower agricultural load in Latvia as well as by a higher denitrification potential and confinement degree of Latvian aquifers and aquitards (Fig. 2B). A statistical comparison of the groundwater residence times is impossible due to the very limited number of

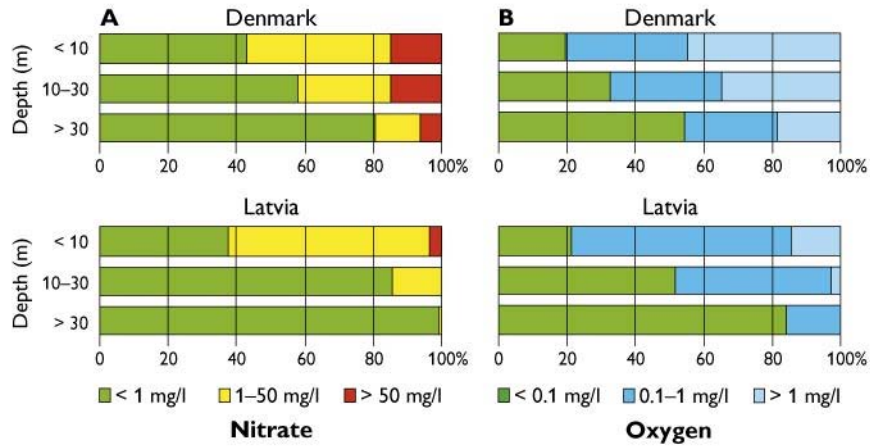

Fig. 2. **A**: Distribution of nitrate in Danish and Latvian wells compared to screen depth. Danish data from 719 monitoring screens averaged for the period 1998–2003. Latvian data from 717 monitoring and water-supply wells averaged for the period 2000–2005. **B**: Distribution of dissolved oxygen in Danish and Latvian wells as a function of screen depth. Danish data from 706 monitoring screens are averaged for the period 1998–2003. Latvian data from 160 monitoring and investigative screens are averaged for the period 2003–2005.

age determinations of Latvian groundwater (27 water samples were analysed by the CFC method). However, it seems that Latvian groundwater is about twice as old as Danish groundwater from the same depth.

The recent investigations in Latvia revealed some unexpected results with respect to nitrate in shallow aquifers. Latvian springs capturing the youngest and the most mobile part of groundwater flow seem to be characterised by higher average nitrate concentrations compared to shallow wells drilled to the same aquifers (Fig. 3). Even springs located within areas without obvious nitrate load show persistently higher nitrate concentrations than neighbouring wells. After recognition of this phenomenon several high-yielding springs have been included in the groundwater monitoring network to better understand flow patterns and problems of diffuse nitrate pollution.

Investigations of contamination of Latvian groundwater by pesticides have only just started, and the extent of this problem is not fully clear. Vulnerable areas were identified in the project, and 111 groundwater samples from wells in these areas were analysed for a number of expected pesticides. In 30% of the samples, concentrations of pesticides exceeded the quality standards of drinking water (0.1 µg/l). This figure

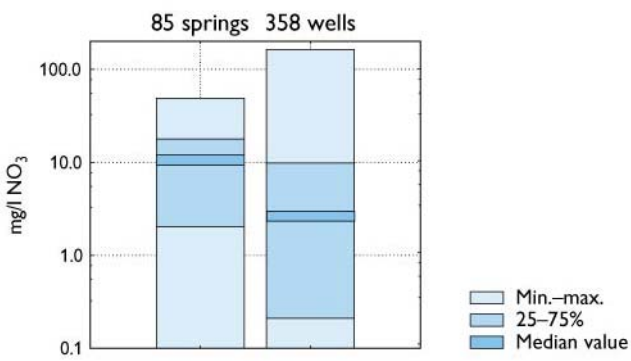

Fig. 3. Distribution of nitrate in 85 springs and 358 shallow wells within Latvian agricultural areas.

is identical to the frequency in shallow Danish monitoring screens (Stockmarr 2005). In Denmark the most often found pesticide is BAM (2,6-dichlorobenzamide), a metabolite from dichlobenil and chlorothiamide that prior to 1997 was commonly used as a total herbicide in urban areas, along roads, railways and at farm yards. The triazine group is the second most found pesticide group, but in Latvia this group comes in third place, after the chlorophenoxy acids and trichloroacetic acid (TCA); the latter was the most widely utilised herbicide during the Soviet time and a by-product from the chemical industry.

As the investigation was focused on potentially vulnerable areas and in the uppermost aquifers, an estimate of 30% occurrence of pesticides is highly pessimistic if the entire Latvian groundwater is considered. Taking into account the smaller acreage of treated areas and a higher confinement degree of main aquifers, the risk of contamination of water-supply wells by pesticides in Latvia should be significantly lower than in Denmark. However, as the pesticides were mainly used in the 1980s they may not yet have reached the main Latvian aquifers containing groundwater older than 50 years.

Minor elements

In order to compare Danish and Latvian shallow groundwater chemistry, distribution curves of twelve selected minor elements are presented in Fig. 4.

Shallow Latvian groundwater is characterised by higher background concentrations of aluminium and fluoride and lower concentrations of bromide, lithium, manganese, phosphorus and strontium when compared to the Danish data. A majority of the observed differences reflect the difference in basic groundwater chemistry: the median values of the chloride, sulphate and permanganate indices in the Danish data set (30, 45 and 3.1 mg/l, respectively) are significantly higher than the corresponding values for the Latvian data set (10, 20 and 1.4 mg/l, respectively).

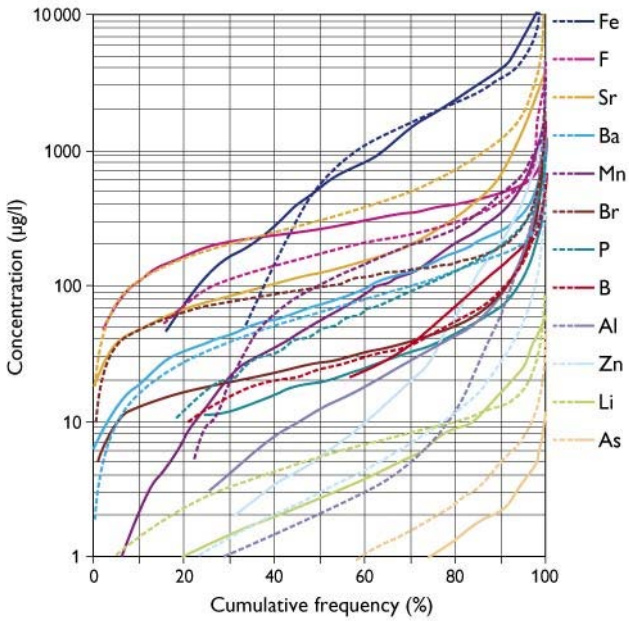

Fig. 4. Distribution of selected minor elements in shallow Latvian groundwater (full lines indicate data from 477 wells and springs for the period 2003–2005) and in shallow Danish groundwater (dotted lines indicate data from 723 monitoring screens for the period 1998–2003).

The anoxic and neutral conditions in the majority of Latvian aquifers are unfavourable for migration of most heavy metals, whose concentrations are well below the quality standards of drinking water. Exceptions are manganese and arsenic that migrate in reducing environments. The concentrations of these elements exceed the quality standards (50 and 10 µg/l, respectively) in 22% and 1% of the samples. Boron and selenium exceed the quality standards (300 and 10 µg/l, respectively) only in saline groundwater, where the concentrations of sulphate or chloride are significantly higher than quality standards for drinking water. In general, heavy metals in Latvian groundwater are a smaller problem than in Denmark where manganese and arsenic exceed quality standards of drinking water in 63% and 9% of the monitoring screens, respectively. However, these compounds do not pose a problem for the drinking-water supply in general in Denmark due to sorption in natural sand filters at the water-treatment plants.

In Latvia, nickel concentrations higher than the quality standard of drinking water (20 µg/l) were not observed in groundwater below 10 m. In Denmark, high nickel concentrations locally create problems where large-scale depression cones in the groundwater table result in oxidation of sulphide minerals. Lowering of the groundwater table in Latvian aquifers occurs only in deep, confined aquifers rather than in the vicinity of the groundwater table.

Conclusions

The distribution patterns of minor elements in Latvian and Danish groundwater are somewhat similar and are governed by the basic groundwater chemistry. In general, the background concentrations of aluminium and fluoride are higher, and the concentrations of bromide, lithium, manganese, phosphorus and strontium are lower in shallow groundwater in Latvia compared to the Danish aquifers.

The lower anthropogenic pressure combined with a higher confinement degree of major water-supply aquifers explains why diffuse contamination of Latvian groundwater is lower than in Denmark. At present, the limited data on pesticides and on the age of groundwater do not allow an assessment of the extent of the pesticide problem in Latvian groundwater with sufficient accuracy.

Acknowledgements

Our much appreciated friend and colleague, Edmund Gosk, passed away on 24 November 2006 after a long struggle against cancer. We wish to acknowledge his engaged involvement in this project in Latvia, as well as in his many other tasks.

References

GEUS 2005: Grundvand 2004. Status og udvikling 1989–2004. København: Danmarks og Grønlands Geologiske Undersøgelse (in Danish with English summary). Available on: www.geus.dk/publications/grundvandsovervaagning/1989_2004/index.html

Gosk, E., Levins, I. & Jørgensen, L.F. 2006: Agricultural influence on groundwater in Latvia. Danmarks og Grønlands Geologiske Undersøgelse Rapport **2006/85**, 98 pp.

Henriksen, H.J. & Sonnenborg, A. (eds) 2003: Ferskvandets kredsløb. NOVA 2003 temarapport, 230 pp. København: Danmarks og Grønlands Geologiske Undersøgelse, Danmarks Miljøundersøgelser, Danmarks Jordbrugsforskning and Danmarks Meteorologiske Institut (in Danish with English summary).
Also available on: http://vandmodel.dk/ferskvands_2003_final.htm

NERI 2005: NOVANA – National monitoring and assessment programme for the aquatic and terrestrial environment. Programme description, part 2. NERI Technical Report **537/2005**, 137 pp.

Stålnacke, P., Grimvall, A., Libiseller, C., Laznik, M. & Kokoite, I. 2003: Trends in nutrient concentrations in Latvian rivers and the response to the dramatic change in agriculture. Journal of Hydrology **283**, 184– 205.

Stockmarr, J. 2005: Groundwater quality monitoring in Denmark. Geological Survey of Denmark and Greenland Bulletin **7**, 33–36.

Authors' addresses

L.F.J. & E.G. (deceased), *Geological Survey of Denmark and Greenland, Øster Voldgade 10, DK-1350 Copenhagen K, Denmark.* E-mail: *lfj@geus.dk*

I.L., *Latvian Environment, Geology and Meteorology Agency (LEGMA), Maskavas Str. 165, LV-1019 Riga, Latvia.*

Bayesian belief networks as a tool for participatory integrated assessment and adaptive groundwater management: the Upper Guadiana Basin, Spain

Hans Jørgen Henriksen, Per Rasmussen, John Bromley, Africa de la Hera Portillo and M. Ramón Llamas

Las Tablas de Daimiel, together with other wetlands in La Mancha, Spain, situated in the Upper Guadiana Basin (Fig. 1), has been catalogued as a Biosphere Reserve Area since 1981 as part of the UNESCO *Man and the Biosphere* programme. Between the mid-1970s and late 1980s, over 150 000 hectares of new irrigation areas were established, mainly as a result of private initiative. The average recharge rate of groundwater in the western La Mancha aquifer in the Upper Guadiana Basin is estimated to be between 200 and 500 million m^3 per year, in dry and wet years respectively. Recharge also depends on the depth of the water table (Martínez-Cortina & Cruces 2003). Abstraction reached 600 million m^3 per year by the end of the 1980s. Up to this time a total of 3000–5000 million m^3 of the Upper Guadiana Basin aquifer's water reserves was withdrawn (Bromley *et al.* 2000; Lopéz-Geta *et al.* 2006). The intensive use of groundwater has been a main factor for the improvement of the social and economic situation in this region, with a population of about half a million people, and where the agricultural sector is very important (Llamas *et al.* 2006). Water-table drawdown due to the intensive abstraction of groundwater for irrigation has caused severe negative impacts on wetlands, streams and rivers, and has resulted in a lowering of groundwater levels by up to 50 m. The main conflicts in the area are between farmers and conservationists, between central, regional and local government water agencies, and between small farmers and big farmers. The conflicts began about three decades ago (Llamas 1988) and have not yet been settled. In 2001 the Spanish Parliament asked the Government to present a hydrological plan for the Upper Guadiana Basin within one year. More than 20 draft proposals have been presented, the last one in 2006 with a budget of almost four billion Euros. This proposal has been met with strong opposition from most farmer lobbies.

The Guadiana Basin is one of seven transboundary case studies of the EU NeWater research project (*New Approaches for Adaptive Water Management under Uncertainty*). The principal water-management issues in the project are addressed by adaptive and integrated water-resource management. This includes uncertainty and risk mitigation, governance, cross-sectoral integration, scale analysis, information management,

Fig. 1. Location of the Guadiana Basin in Spain. The Upper Guadiana Basin includes Las Tablas Daimiel and upstream areas in the Castilla-La Mancha region. Major rivers indicated.

stakeholder participation, financial aspects, system resilience and vulnerability. One work block in the NeWater project has the task of translating research outputs into tools for practitioners and end-users. As part of this effort, Bayesian belief networks (Bns) were selected as one possible tool to be developed as an aid to stakeholder participation in integrated assessment of gaps, being a suitable tool for dialogue in order to identify gaps in water-resource management functions, gaps to meet the goals of the EU Water Framework Directive and to analyse management potentials and constraints.

The purpose of this paper is to describe the testing of Bns as a tool for participatory integrated assessment and adaptive and integrated water-resource management in the Upper Guadiana Basin.

Participatory integrated assessment

Participatory integrated assessment can be considered a form of participatory policy analysis, which aims to support the policy process by designing and facilitating policy debate and argument. Assessment is integrated when it draws on a broader set of knowledge domains than are represented in the

research product of a single discipline. Assessment is distinguished from disciplinary research by its purpose: to inform policy and decision-making, rather than to advance knowledge for its intrinsic value (Hisschemöller *et al.* 2001).

A wide range of methods and techniques can be drawn from social psychology, policy sciences, decision analysis and anthropology (Hisschemöller *et al.* 2001) for high-level participatory integrated assessment. Some of these, like brainstorming or decision seminars, although well established, are of limited value for integrated water-resource management because a proper understanding of the spatial and temporal variation and the complexity within river basins requires a modelling approach (Croke *et al.* 2007). According to Jakeman & Letcher (2003) the tools for participatory integrated assessment must:

1. be problem-focussed, using an iterative, adaptive approach that links research to policy;
2. possess an interactive, transparent framework that enhances communication;
3. be enriched by stakeholder involvement and dedicated to adoption;
4. connect complexities between the natural and human environment, recognising spatial dependencies, feedbacks and impediments; and
5. attempt to recognise essential lacking knowledge.

Jakeman & Letcher (2003) list several tools for participatory integrated assessment, e.g. system dynamics, Bns, metamodels, risk assessment approaches, coupled component models, agent-based models and expert systems. Here Bns are in focus as a tool for adaptive and integrated water management in the Upper Guadiana Basin test case.

Bayesian belief networks

A Bayesian belief network (Bn) is a type of decision support system based on probability theory which implements Bayes' rule of probability (Jensen 2002; Bromley 2005). This rule shows mathematically how existing beliefs can be modified with the input of new evidence. Bns organise the body of knowledge in a given area by mapping out relationships among key variables and encoding them with numbers that represent the extent to which one variable is likely to affect another.

Bns have gained a reputation for being a powerful technique to model complex problems involving uncertain knowledge and uncertain impacts of causes. Ideally, Bns are a technique to assist decision-making that is especially helpful when there is scarcity and uncertainty in the data used in making the decision and the factors are highly interlinked, all of which makes the problem very complex. The graphical nature of Bns facilitates formal discussion of the structure of the proposed model. Furthermore, the ability of Bns to describe the uncertain relationships between variables is ideal to describe the relationship between events, which may not be well understood.

Bns help water managers, stakeholders and scientists (1) to visualise and recognise, in the face of complexity and uncertainty, the relationships between different actions and consequences; (2) to make learning about water-resource systems more efficient; and (3) to encourage the involvement of social and political values in water-resource management (e.g. Henriksen *et al.* 2007a, b). Furthermore, it has been judged that Bns are an excellent tool for integrating different domains, e.g. socio-economy, hydrology and groundwater quality data of different knowledge types (monitoring data, models and expert opinions; Henriksen *et al.* 2007a). Here the guidelines from the MERIT project (Bromley 2005) can help support a successful and efficient involvement of stakeholders in the participatory integrated assessment process, a process which is demanding to run due to multiple frames and opposing interests.

Design for testing the enhanced Bayesian belief network tool

A test of an enhanced Bn tool is being undertaken in the Upper Guadiana Basin as part of the NeWater project. The test involves the construction of a Bn to represent the management of groundwater levels in the region, taking into account the social, economic, hydrological and ecological consequences of alternative irrigation and groundwater management scenarios (Table 1).

In November 2006, an initial workshop was held at the Geological Survey of Spain (IGME) in Madrid with participants from the case study group. During this workshop a preliminary Bn for the Upper Guadiana Basin was developed by Bn experts from IGME, the University Complutense de Madrid, the Geological Survey of Denmark and Greenland, and the Centre of Ecology and Hydrology, Wallingford, UK,

Table 1. Management scenarios and impacts

Scenario	Agricultural output (mill. € per year)	Change in water level (m per year)	Recovery of wetlands (years)
A1	1000	–0.40	Never
A2	900	–0.08	Never
B1	510	+1.84	20–25
B2	490	+2.00	15–20

Scenarios A1 and A2 are based on business as usual (no recovery of wetlands). Scenarios B1 and B2 assume serious restrictions on the economic agricultural output, with technology as usual (resulting in recovery of wetlands).

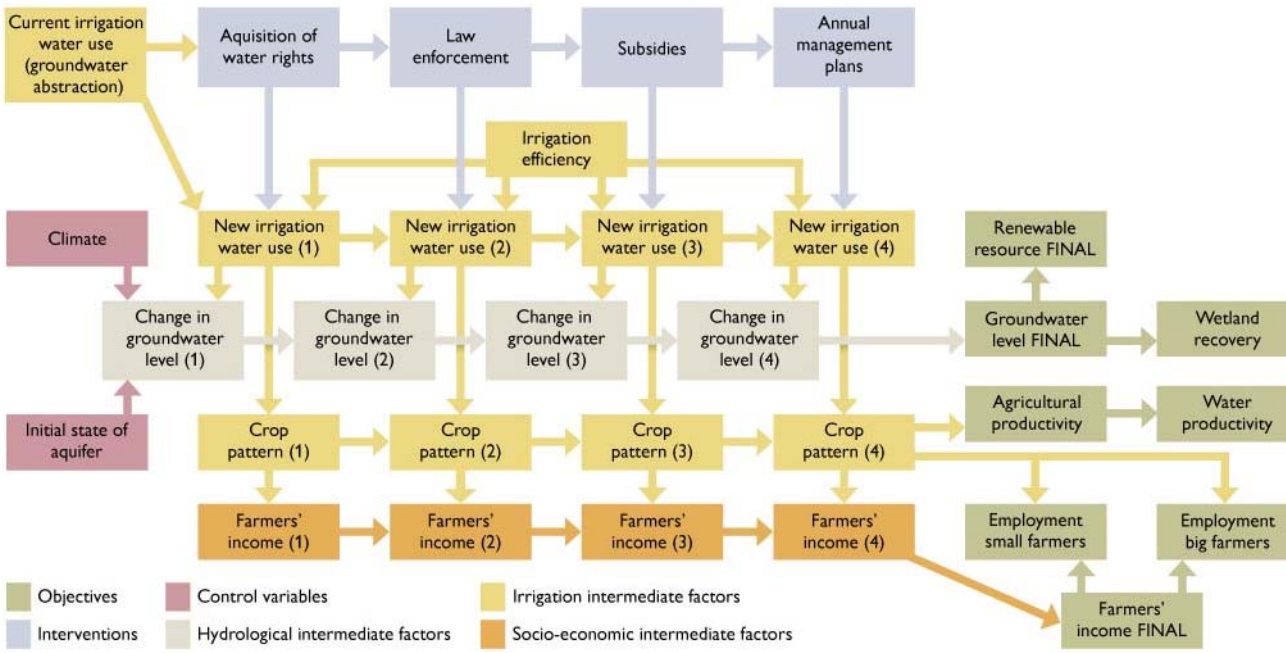

Fig. 2. Preliminary Bayesian network for the Upper Guadiana Basin. The objectives of the Bayesian network are to analyse the way in which different management actions will influence irrigation water use, change in groundwater level, crop pattern, farmers' income, wetland recovery, productivity and employment.

together with a representative of the water managers of the basin responsible for water planning in relation to implementation of the EU Water Framework Directive.

A joint workshop with all stakeholders to finalise the network has been planned for the first half of 2007. The process and method for constructing the Bn in the Upper Guadiana Basin test will follow the MERIT guidelines (Bromley 2005). In the following we present the preliminary Bn and the hypotheses relating to the use of the tool in participatory integrated assessment and adaptive management in the Guadiana Basin.

Results of testing Bayesian belief networks for adaptive water management

The initial step in network design was to establish the space and time boundaries of the system being modelled. It was agreed to restrict the model to the Upper Guadiana Basin, and a one-year time period for groundwater level and socio-economic consequences was decided. The pilot Bn for the Upper Guadiana Basin case which emerged from this process is shown in Fig. 2. The network deals with the way in which different management actions influence irrigation water use, groundwater level, crop pattern, farmers' income, wetland recovery, productivity and employment in the region (Fig. 2). Included among the potential actions that might be taken are: (1) acquisition of water rights; (2) law enforcement; (3) common agricultural programmes (CAP) subsidies; and (4) annual management plans. Climate and the initial state of the aquifer are included as control factors. The indicators (objectives) in the network include: (1) groundwater levels; (2) impact on wetland recovery; (3) agricultural productivity; (4) farmers' income; and (5) levels of employment in the region. When running the Bn, combinations of actions can be selected and calculated.

It is hypothesised that Bns fully support four of the five requirements proposed by Jakeman & Letcher (2003) for participatory integrated assessment (Table 2). One requirement, the representation of spatial dependencies, is only partly supported (e.g. input to the decision-making about which specific wetlands that will be recovered by a certain increase in groundwater level has to be evaluated using a groundwater model). However, as stated by Pascual (2005): "the beauty of Bns lies in their explanatory power: observations about any node generates knowledge about all other nodes, providing one with a tool to draw transparent, rational inferences in a probabilistic world". This illustrates that the tool can be used for diagnosis and social learning.

Bns allow targeted modelling, participatory integrated assessment and strong support for sense and decision-making in cases with multiple frames (e.g. when stakeholders perceive their environment differently, and frame and construct their world in different ways) that create ambiguous situations and conflicting interests hindering sustainable solutions for man-

Table 2. Hypotheses relating to the use of Bayesian belief networks as a tool for participatory integrated assessment and gap analysis within Integrated Water Resource Management (IWRM)

Requirement to tool for adaptive management and participatory integrated assessment*	Enhancement result	Comments: To be further tested for the Guadiana Basin
Being problem-focussed, using an iterative, adaptive approach that links research to policy	Yes	Bns allow flexible handling of complex systems, with clear overview of actions and indicators, and interferences. Flexible coupling of domains. Bns allow both hard and soft data.
Possessing an interactive, transparent framework that enhances communication	Yes	A good tool for a focussed dialogue. The tool enhances communication due to its flexibility and visual representation.
Being enriched by stakeholder involvement and dedicated to adoption	(Yes)	Easy to use with stakeholders for development of a shared conceptual understanding of the system. However, the conditional probability tables may be difficult to understand. Training is very important.
Connecting complexities between the natural and human environment, recognising spatial dependencies, feedback and impediments	Not fully	Spatial dependencies and feedback between variables cannot be handled fully. For such purposes coupled domain models are needed, but Bns can work on top of these models as a tool for coupling with other domains.
Attempting to recognise missing essential knowledge	Yes	Bns allow the exploration of complexity, uncertainty and multiple frames. A good tool for gap analysis within IWRM and subsequent negotiation and mutual understanding.

* Criteria according to Jakeman & Fletcher (2003).

agement of the environment. The tool and the probability tables (numbers) are not easily understood if not properly explained. Thus, training and introduction to the tool and the statistical background behind Bns is important (Table 2).

Acknowledgements

The work reported from the NeWater project has been financially supported by the European Commission under contract number 511179 (GOCE). Integrated project in Priority 6.3 Global Change and Ecosystems in the 6th EU Framework Programme.

References

Bromley, J. 2005: Guidelines for the use of Bayesian networks as a participatory tool for water resource management, 117 pp. Wallingford: Centre for Ecology and Hydrology.

Bromley, J., Cruces, J., Acreman, M., Martinez, L. & Llamas, M.R. 2000: Groundwater over-exploitation in the Upper Guadiana catchment, central Spain: the problems of sustainable groundwater resources management. International Water Resources Development **17**, 379–396.

Croke, B.F.W., Ticehurst, J.L., Letcher, R.A., Norton, J.P., Newham, T.T.H. & Jakeman, A.J. 2007: Integrated assessment of water resources: Australian experiences. Water Resource Management **21**, 351–373.

Henriksen, H.J., Rasmussen, P., Brandt, G., Bülow, D.v. & Jensen, F.V. 2007a: Engaging stakeholders in construction and validation of Bayesian belief network for groundwater protection. In: Castelletti, A.E.R. & Soncini-Sessa, R. (eds): Topics on system analysis and integrated water resource management, 49–72. Amsterdam: Elsevier.

Henriksen, H.J., Rasmussen, P., Brandt, G., Bülow, D.v. & Jensen, F.V. 2007b: Public participation modelling using Bayesian networks in management of groundwater contamination. Environmental Modelling & Software **22**, 1101–1113.

Hisschemöller, M., Tol, R.S.J. & Vellinga, P. 2001: The relevance of participatory approaches in integrated environmental assessment. Integrated Assessment **2**, 57–72.

Jakeman, A.J. & Letcher, R.A. 2003: Integrated assessment and modelling: features, principles and examples for catchment management. Environmental Modelling and Software **18**, 491–501.

Jensen, F. 2002: Bayesian networks and decision graphs: statistics for engineering and information science, 296 pp. New York: Springer-Verlag.

Llamas, M.R. 1988: Conflicts between wetland conservation and groundwater exploitation: two case histories in Spain. Environmental Geology and Water Sciences **11**, 241–251.

Llamas, M.R., Martínez-Santos, P. & Hera, A. de la 2006: Dimensions of sustainability in regard to groundwater resources: an overview. Proceedings of the International Symposium on Groundwater Sustainability, Alicante, Spain, 24–27 January 2006, 1–13. Madrid: Instituto Geológico y Minero de España.

López-Geta, J.A., Fornés, J.M., Ramos, G. & Villarroya, F. 2006: Groundwater. A natural underground resource, 107 pp. Madrid: Instituto Geológico y Minero de España, UNESCO and Fundación Marcelino Botín.

Martínez-Cortina, L. & Cruces, J. 2003: The analysis of the intensive use of groundwater in the Upper Guadiana Basin (Spain) using a numerical model. In: Llamas, M.R. & Custodio, E. (eds): Intensive use of groundwater, challenges and opportunities, 285–294. London: Taylor and Francis.

Pascual, P. 2005: Wresting environmental decisions from an uncertain world. Environmental Law Institute News and Analysis **8-2005**, 10539–10549.

Authors' addresses

H.J.H. & P.R., *Geological Survey of Denmark and Greenland, Øster Voldgade 10, DK-1350 Copenhagen K, Denmark.* E-mail: *hjh@geus.dk*

J.B., *Oxford University Centre for the Environment, South Parks Road, Oxford OX1 3QY, UK.*

A.d.l.H.P., *Geological Survey of Spain, 23 Rios Rosas, ITGE-E 28003 Madrid, Spain.*

M.R.L., *University of Complutense, Ciudad Universitaria, 28040 Madrid, Spain.*

Cenozoic evolution of the Vietnamese coastal margin

Michael B.W. Fyhn, Lars Henrik Nielsen and Lars Ole Boldreel

A series of Cenozoic basins fringes the Vietnamese coastal margin, often characterised by more than 10 km of sedimentary infill (Fig. 1). Greater parts of the margin are still in an early explorational state, although significant petroleum production has taken place in all but the southern Song Hong and the Phu Khanh Basins. This has increased the need for a fundamental understanding of the processes behind the formation of the basins, including analyses of potential source rocks.

The basins fringing the Indochina Block provide excellent evidence of the geological evolution of the region, and the basin geometries reflect the collision of India and Eurasia and the late Cenozoic uplift of south Indochina (Rangin *et al.* 1995a; Fyhn *et al.* in press). In addition, the basins provide evidence of regional Palaeogene rifting and subsequent Late Palaeogene through Early Neogene sea-floor spreading in the South China Sea. Apart from the regional Cenozoic tectonic record, the basins contain a high-resolution climatic record of South-East Asia due to the high depositional rates, changing depositional styles and large hinterland of the basin (Clift *et al.* 2004).

Background

Since 1995 the Geological Survey of Denmark and Greenland (GEUS) and the Department of Geography and Geology, University of Copenhagen, have operated jointly in Vietnam aiming to improve the local geoscientific capacity. The work is part of the ENRECA project (Enhancement of Research Capacity in Developing Countries), funded by the Danish International Development Agency (DANIDA). This part of the ENRECA project focuses on an assessment of the hydrocarbon potential of the Vietnamese continental margin, and has led to basin evaluations of the Song Hong and the Phu Khanh Basins (Fig. 1), and to a series of both Vietnamese and Danish M.Sc. projects (Nielsen *et al.* 1999; Nielsen & Abatzis 2004; Andersen *et al.* 2005; Boldreel *et al.* 2005; Fyhn *et al.* in press). The ongoing second phase of the project focuses both on training Vietnamese M.Sc. and Ph.D. students and on evaluating the hydrocarbon potential of the Vietnamese part of the Malay and Khmer Basins, as well as

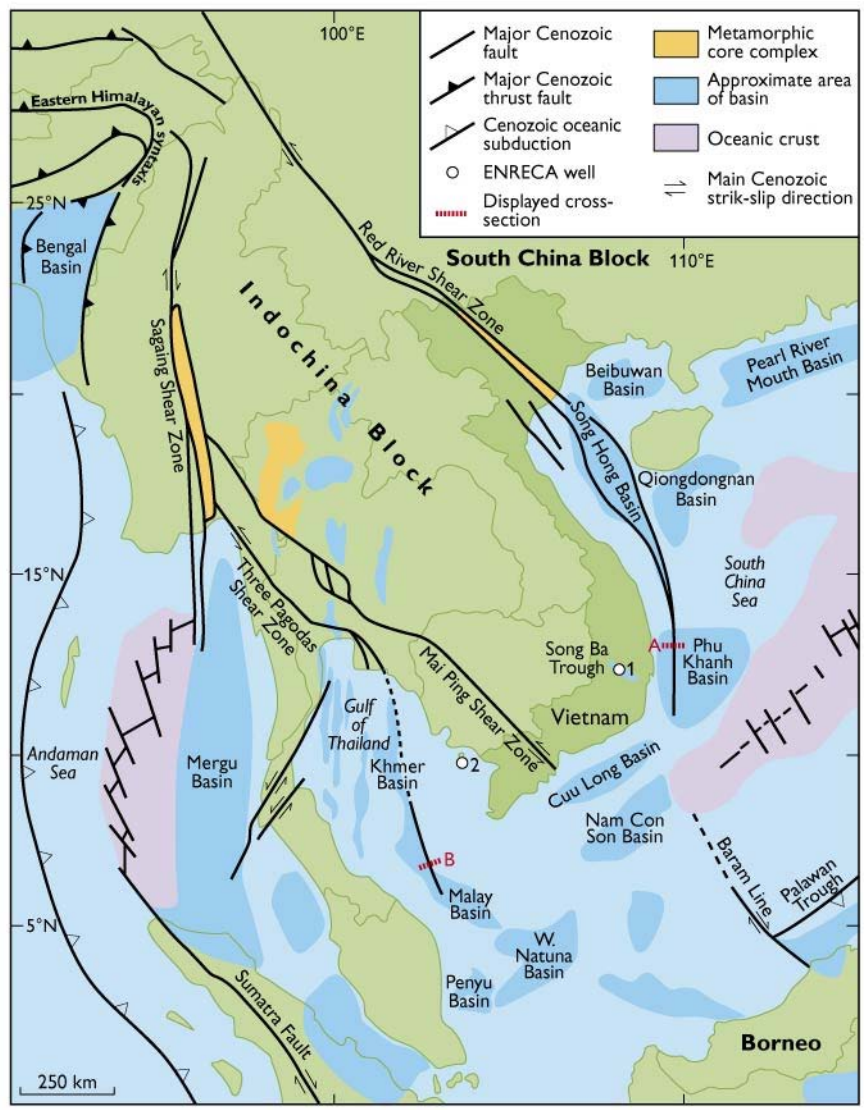

Fig. 1. Map showing major Cenozoic basins and oceanic crust and simplified Cenozoic structural features. **A**: cross-section shown in Fig. 3. **B**: cross-section shown in Fig. 4. Modified from Fyhn *et al.* (in press).

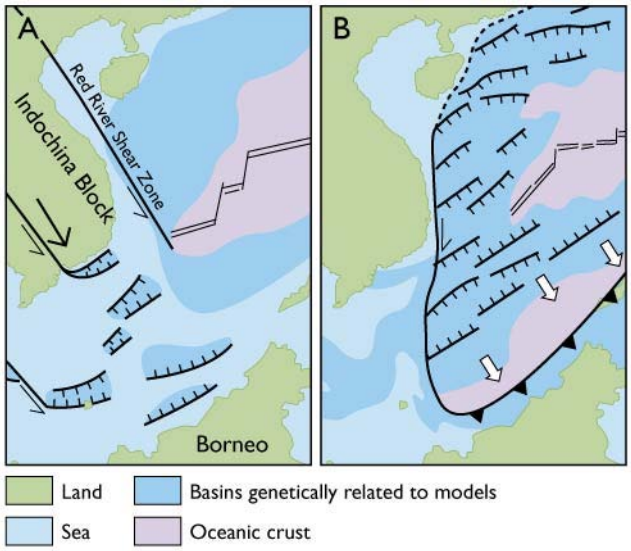

Fig. 2. Conceptual models of the two basic theories initially proposed for the formation of the South China Sea (Tapponier *et al.* 1982; Taylor & Hayes 1983). Later studies have suggested various integrations of the two models (Hall 2002; Morley 2002; Fyhn *et al.* in press). **A**: The pull-apart model suggests rifting and subsequent sea-floor spreading as a result of a complex left-lateral pull-apart mechanism. **B**: The subduction model suggests rifting and subsequent sea-floor spreading as a result of the subduction of old oceanic lithosphere beneath Borneo. Note that both models infer a transform zone along the central and south Vietnamese margin but with opposite relative sense of motion. Modified from Tapponier *et al.* (1982) and Taylor & Hayes (1983).

the Mesozoic strata underneath and shoreward of these basins. Sampling of source rocks and oil seeps and drilling of two 500 m deep, fully cored wells (ENRECA-1 and 2, Fig. 1) as well as acquisition of shallow seismic data have been carried out as part of the basin evaluations (Bojesen-Koefoed *et al.* 2005; Petersen *et al.* 2005). Furthermore, a broader analysis of the structure and stratigraphy of the entire Vietnamese margin is being carried out as a separate Ph.D. study funded by the University of Copenhagen.

Tectonic models

The Indochina Block is situated immediately south-east of the eastern Himalayan syntaxis. The Himalayan Orogeny thus had a major impact on the structural evolution of Indochina, leading to major north-west–south-east crustal shortening in the north and to significant lateral movements along shear zones transecting and bordering the Indochina Block (Fig. 1; Morley 2002). Some of the largest shear zones are the north-west-trending Red River, Mai Ping and Three Pagodas Shear Zones. South-eastward displacement and rotation of Indochina and adjacent areas produced a total left-lateral offset of several hundreds of kilometres along the three shear zones (Hall 2002). Tapponnier *et al.* (1982) suggested that the South China Sea and its marginal basins formed due to complex pull-apart mechanisms in response to these left-lateral displacements (Fig. 2A). Alternatively, Taylor & Hayes (1983) suggested that the formation of the South China Sea was a result of a southward subduction of ocean crust beneath Borneo (Fig. 2B). One of the major differences between the two models is that the subduction model predicts right-lateral displacement across a large part of the Vietnamese margin, whereas the pull-apart model is associated with a left-lateral transform along the margin.

The offshore Red River Shear Zone

The most extensive of the Indochinese left-lateral shear zones is the Red River Shear Zone that passes through South China and northern Vietnam into the Song Hong Basin. Seismic studies of the almost 20 km deep Song Hong Basin indicate that the basin formed in response to major Palaeogene left-lateral offset along the seaward continuation of the Red River Shear Zone (Rangin *et al.* 1995a; Nielsen *et al.* 1999; Andersen *et al.* 2005). Recent studies show that the shear zone continues along the Vietnamese coast in the Phu Khanh Basin further south (Fig. 1; Fyhn *et al.* in press). The shear zone runs along the western boundary of the Phu Khanh Basin

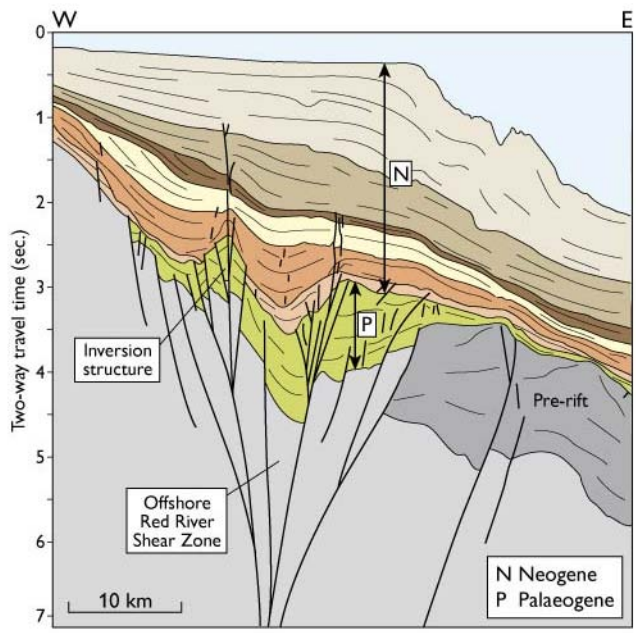

Fig. 3. Cross-section of the northern Phu Khanh Basin transecting the offshore continuation of the Red River Shear Zone. Timing of the deformations shows Palaeogene left-lateral movement followed by moderate right-lateral inversion during the early Neogene. The structural cut-off of the pre-rift sequence towards the shear zone is interpreted to be a result of the large left-lateral movement along the zone (see Fig. 1 for location).

forming a major rift structure filled by thick Palaeogene syn-rift deposits (Fig. 3). Left-lateral transtension ended during latest Oligocene time in the Phu Khanh Basin, but was followed by earliest Miocene structural inversion. This is interpreted to reflect a change from intense left-lateral transtension to modest right-lateral movements along the seaward extension in the Red River Shear Zone in the basin, corroborated by a study by Rangin *et al.* (1995b) showing that left-lateral, coast-parallel wrench faults onshore have been inverted by right-lateral movements. The latest Palaeogene termination of left-lateral movement along the offshore part of the Red River Shear Zone in the Phu Khanh Basin does not support Neogene sea-floor spreading in the South China Sea as a result of left-lateral pull-apart. Consequently, Neogene sea-floor spreading cannot have been caused by left-lateral pull-apart, but was probably forced by subduction of older oceanic crust beneath Borneo. Palaeogene rifting along the Vietnamese margin was, on the other hand, greatly influenced by left-lateral transtension.

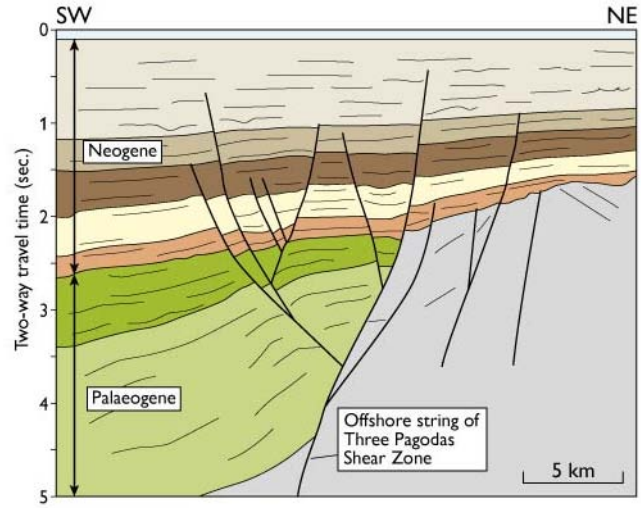

Fig. 4. Cross-section of the Vietnamese part of the Malay Basin which transects a fault strand of the seaward continuation of the Three Pagodas Shear Zone. The main offset along the major fault occurred during Palaeogene times as left-lateral transtension forced by the indentation of India into Eurasia (see Fig. 1 for location).

The offshore Three Pagodas Shear Zone

Rifting in the Malay and Khmer Basins south-west of Vietnam was originally linked to left-lateral transtension across a seaward extension of the Three Pagodas Shear Zone (Fig. 1; Tapponnier *et al.* 1982). Later models suggested right-lateral faulting along the fault zone as the forcing mechanism (Polachan & Sattayarak 1989), or a combination of forces related to the Indochina extrusion and extension caused by subduction roll-back (Morley 2001), or mantle plume emplacement (Ngah *et al.* 1996).

Seismic structural analysis of the Vietnamese part of the Malay and Khmer Basins indicates that rifting mainly took place during the Palaeogene, and was controlled by a steep, north-north-west-trending, downward steeping master fault, which is flanked by smaller north-west-trending conjugate normal faults (Fig. 4). The master fault offsets the basement with up to more than 2 sec. TWT and transects the entire study region striking towards the point at which the Three Pagodas Shear Zone enters the Gulf of Thailand. The master fault is therefore interpreted as an offshore fault strand of the Three Pagodas Shear Zone. The fault characteristics indicate Palaeogene left-lateral transtension and thus support a close relation between extrusion of Indochina and rifting in the two basins.

Depositional trends

Sea-floor spreading in the South China Sea did not start until the middle Oligocene, and Palaeogene syn-rift sedimentation was therefore dominated by alluvial and lacustrine deposition. In the Song Hong Basin a gradual marine transgression of the margin started after the onset of sea-floor spreading. During initial transgression siliciclastic deposition in estuaries and narrow marine pathways dominated larger parts of the basins, and carbonate growth took place on inundated highs. Open marine conditions prevailed in most basins during Neogene times as sea-floor spreading propagated to its maximum south-western extension. Extensive carbonate growth took place on many intra- and interbasinal highs south of and along the Vietnamese margin up to *c.* 16°N during the Neogene, favoured by the open marine environment and climatic conditions. In contrast, sediment supply kept pace with subsidence in most parts of the Malay and Song Hong Basins, preventing long-lasting periods of open marine sedimentation.

During Late Neogene time, central and southern Indochina were thermally uplifted, thus significantly increasing the siliciclastic input to the marginal basins. The increased terrigenous sediment supply inhibited widespread carbonate growth off southern and central Vietnam and resulted in the progradation of a distinct shelf slope, which has led to the present outline of the margin.

Source rocks

One of the main risk factors regarding petroleum exploration in the Vietnamese offshore basins is the presence of adequate source rock intervals. Onshore data from the ENRECA-1 core through the Song Ba Trough in central Vietnam show, however, that thick intervals of excellent oil- and gas-prone lacustrine mudstone and humic coals may develop even in

small basins characterised by high sediment input. Although the Song Ba Trough is an order of magnitude smaller than the Vietnamese offshore basins, seismic data in the latter show apparent depositional similarities suggesting the presence of similar high-quality source rocks in the offshore basins (Nielsen *et al.* 2007; Fyhn *et al.* in press). In addition, seismic facies analysis as well as oil and gas compositions indicate that other source rock types, such as Neogene fluvio-deltaic coals, carbonaceous shales and fore-reef marls are present in some of the basins and thus testify to the great petroleum potential of the Vietnamese margin (Bojesen-Koefoed *et al.* 2005; Fyhn *et al.* in press).

Acknowledgements

This study is a Ph.D. project funded by the Faculty of Natural Science at the University of Copenhagen to the first author. Funding to the ENRECA project was given by the Danish Ministry of Foreign Affairs through DANIDA. Vietnam Petroleum Institute (PetroVietnam) is thanked for providing the seismic reflection and well data and giving permission to publish these.

References

Andersen, C., Mathiesen, A., Nielsen, L.H., Tiem, P.V., Petersen, H.I. & Diem, P.T. 2005: Evaluation of petroleum systems in the northern part of the Cenozoic Song Hong basin (Gulf of Tonkin), Vietnam. Journal of Petroleum Geology **28**, 167–184.

Bojesen-Koefoed, J.A., Nielsen, L.H., Nytoft, H.P., Petersen, H.I., Dau, N.T., Hien, L.V., Duc, N.A. & Quy, N.H. 2005: Geochemical characteristics of oil seepages from Dam Thi Nai, central Vietnam: implications for exploration in the offshore Phu Khanh Basin. Journal of Petroleum Geology **28**, 3–18.

Boldreel, L.O. *et al.* 2005: The Phu Khanh Basin – aspects of structural evolution and hydrocarbon potential. Science-technology conference: 30 years Vietnam petroleum industry – new challenges and opportunities, 24–25 August 2005. Hanoi, Vietnam: PetroVietnam (CD-ROM).

Clift, P.D., Layne, G.D. & Blusztajn, J. 2004: Marine sedimentary evidence for Monsoon strengthening, Tibetian uplift and drainage evolution in East Asia. In: Clift, P.D. *et al.* (eds): Continent–ocean interactions within East Asian marginal seas. Geophysical Monograph Series **149**, 235–254.

Fyhn, M.B.W. *et al.* in press: Geological evolution, regional perspectives and hydrocarbon potential of the northwest Phu Khanh Basin, offshore central Vietnam. Marine and Petroleum Geology.

Hall, R. 2002: Cenozoic geological and plate tectonic evolution of SE Asia and the SW Pacific: Computer-based reconstructions, model and animations. Journal of Asian Earth Sciences **20**, 353–431.

Morley, C.K. 2001: Combined escape tectonics and subduction roll-back–back arc extension: a model for the evolution of Tertiary rift basins in Thailand, Malaysia and Laos. Journal of the Geological Society (London) **158**, 461–474.

Morley, C.K. 2002: A tectonic model for the Tertiary evolution of strike-slip faults and rift basins in SE Asia. Tectonophysics **347**, 189–215.

Ngah, K., Madon, M. & Tjia, H.D. 1996: Role of pre-Tertiary fractures in formation and development of the Malay and Penyu Basins. In: Hall, R. & Blundell, D. (eds): Tectonic evolution of Southeast Asia. Geological Society Special Publication (London) **106**, 281–289.

Nielsen, L.H. & Abatzis, I. 2004: Petroleum potential of sedimentary basins in Vietnam: long-term geoscientific co-operation with the Vietnam Petroleum Institute. Geological Survey of Denmark and Greenland Bulletin **4**, 97–100.

Nielsen, L.H., Mathiesen, A., Bidstrup, T., Vejbæk, O.V., Dien, P.T. & Tiem, P.V. 1999: Modeling the hydrocarbon generation in the Cenozoic Song Hong basin, Vietnam: a highly prospective basin. Journal of Asian Earth Sciences **17**, 269–294.

Nielsen, L.H., Petersen, H.I., Thai, N.D., Duc, N.A., Fyhn, M.B.W., Boldreel, L.O., Tuan, H.A., Lindstöm, S. & Hien, L.V. 2007: A Middle–Upper Miocene fluvial-lacustrine rift sequence in the Song Ba Rift, Vietnam: an analogue to oil-prone, small-scale continental rift basins. Petroleum Geoscience **13**, 145–168.

Petersen, H.I., Tru, V., Nielsen, L.H., Duc, N.A. & Nytoft, H.P. 2005: Source rock properties of lacustrine mudstones and coals (Oligocene Dong Ho Formation), onshore Song Hong Basin, northern Vietnam. Journal of Petroleum Geology **28**, 19–38.

Polachan, S. & Sattayarak, N. 1989: Strike-slip tectonics and the development of Tertiary basins in Thailand. In: Thanasuthipitak, T. (ed.): Proceeding of the international symposium on intermountain basins: geology and resources, 243–253. Chiang Mai, Thailand: University Press.

Rangin, C., Klein, M., Roques, D., Le Pichon, X. & Trong, L.V. 1995a: The Red River fault system in the Tonkin Gulf, Vietnam. Tectonophysics **243**, 209–222.

Rangin, C., Huchon, P., Le Pichon, X., Bellon, H., Lepvrier, C., Roques, D., Hoe, N.D. & Quynh, P.V. 1995b: Cenozoic deformation of central and south Vietnam. Tectonophysics **235**, 179–196.

Tapponier, P., Peltzer, G., Le Dain, A.Y., Armijo, R. & Cobbold, P. 1982: Propagating extrusion tectonics in Asia: new insights from simple experiments with plasticine. Geology **10**, 611–616.

Taylor, B. & Hayes, D.E. 1983: Origin and history of the South China Sea Basin. In: Hayes, D.E. (ed.): The tectonic and geologic evolution of Southeast Asian seas and islands **2**. Geophysical Monograph Series **27**, 23–56.

Authors' addresses

M.B.W.F. & L.O.B., *Department of Geography and Geology, University of Copenhagen, Øster Voldgade 10, DK-1350 Copenhagen K, Denmark.*

E-mail: *fyhn@geol.ku.dk*

L.H.N., *Geological Survey of Denmark and Greenland, Øster Voldgade 10, DK-1350 Copenhagen K, Denmark.*

De Nationale Geologiske Undersøgelser for Danmark og Grønland (GEUS)

Geological Survey of Denmark and Greenland
Øster Voldgade 10, DK-1350 Copenhagen K
Denmark

The series *Geological Survey of Denmark and Greenland Bulletin* started in 2003 and replaced the two former bulletin series of the Survey, viz. *Geology of Greenland Survey Bulletin* and *Geology of Denmark Survey Bulletin*. Some of the twenty-one volumes published since 1997 in those two series are listed on the facing page. The present series, together with *Geological Survey of Denmark and Greenland Map Series*, now form the peer-reviewed scientific series of the Survey.

Geological Survey of Denmark and Greenland Bulletin

1	The Jurassic of Denmark and Greenland, 948 pp. (28 articles), 2003. *Edited by* J.R. Ineson & F. Surlyk.	500.00
2	Fish otoliths from the Paleocene of Denmark, 94 pp., 2003. *By* W. Schwarzhans.	100.00
3	Late Quaternary environmental changes recorded in the Danish marine molluscan faunas, 268 pp., 2004. *By* K.S. Pedersen.	200.00
4	Review of Survey activities 2003, 100 pp. (24 articles), 2004. *Edited by* M. Sønderholm & A.K. Higgins.	180.00
5	The Jurassic of North-East Greenland, 112 pp. (7 articles), 2004. *Edited by* L. Stemmerik & S. Stouge.	160.00
6	East Greenland Caledonides: stratigraphy, structure and geochronology, 93 pp. (6 articles), 2004. *Edited by* A.K. Higgins and F. Kalsbeek.	160.00
7	Review of Survey activities 2004, 80 pp. (19 articles), 2005. *Edited by* M. Sønderholm & A.K. Higgins.	180.00
8	Structural analysis of the Rubjerg Knude Glaciotectonic Complex, Vendsyssel, northern Denmark, 192 pp., 2005. *By* S.A.S. Pedersen.	300.00
9	Scientific results from the deepened Lopra-1 borehole, Faroe Islands, 156 pp. (11 articles), 2006. *Edited by* J.A. Chalmers & R. Waagstein.	240.00
10	Review of Survey activities 2005, 68 pp. (15 articles), 2006. *Edited by* M. Sønderholm & A.K. Higgins.	180.00
11	Precambrian crustal evolution and Cretaceous–Palaeogene faulting in West Greenland, 204 pp. (12 articles), 2006. *Edited by* A.A. Garde & F. Kalsbeek.	240.00
12	Lithostratigraphy of the Palaeogene – Lower Neogene succession of the Danish North Sea, 77 pp., 2007. *By* P. Schiøler, J. Andsbjerg, O.R. Clausen, G. Dam, K. Dybkjær, L. Hamberg, C. Heilmann-Clausen, E.P. Johannessen, L.E. Kristensen, I. Prince & J.A. Rasmussen.	240.00
13	Review of Survey activities 2006, 76 pp. (17 articles), 2007. *Edited by* M. Sønderholm & A.K. Higgins.	

Geological Survey of Denmark and Greenland Map Series

1	Explanatory notes to the Geological map of Greenland, 1:500 000, Humboldt Gletscher, Sheet 6, 48 pp., 2004. *By* P.R. Dawes	280.00
2	Explanatory notes to the Geological map of Greenland, 1:500 000, Thule, Sheet 5 (1991), 97 pp. + map, 2006. *By* P.R. Dawes.	300.00
3	Explanatory notes to the Geological map of Greenland, 1:100 000, Ussuit 67 V.2 Nord, 40 pp. + map, 2007. *By* J.A.M. van Gool & M. Marker.	280.00

Geology of Greenland Survey Bulletin (discontinued)

175 Stratigraphy of the Neill Klinter Group; a Lower – lower Middle Jurassic tidal embayment succession, Jameson Land, East Greenland, 80 pp., 1998. *By* G. Dam & F. Surlyk. 250.00

176 Review of Greenland activities 1996, 112 pp. (18 articles), 1997. *Edited by* A.K. Higgins & J.R. Ineson. 200.00

177 Accretion and evolution of an Archaean high-grade grey gneiss – amphibolite complex: the Fiskefjord area, southern West Greenland, 115 pp., 1997. *By* A.A. Garde. 200.00

178 Lithostratigraphy, sedimentary evolution and sequence stratigraphy of the Upper Proterozoic Lyell Land Group (Eleonore Bay Supergroup) of East and North-East Greenland, 60 pp., 1997. *By* H. Tirsgaard & M. Sønderholm. 200.00

179 The Citronen Fjord massive sulphide deposit, Peary Land, North Greenland: discovery, stratigraphy, mineralization and structural setting, 40 pp., 1998. *By* F.W. van der Stijl & G.Z. Mosher. 200.00

180 Review of Greenland activities 1997, 176 pp. (26 articles), 1998. *Edited by* A.K. Higgins & W.S. Watt. 200.00

181 Precambrian geology of the Disko Bugt region, West Greenland, 179 pp. (15 articles), 1999. *Edited by* F. Kalsbeek. 240.00

182 Vertebrate remains from Upper Silurian – Lower Devonian beds of Hall Land, North Greenland, 80 pp., 1999. *By* H. Blom. 120.00

183 Review of Greenland activities 1998, 81 pp. (10 articles), 1999. *Edited by* A.K. Higgins & W.S. Watt. 200.00

184 Collected research papers: palaeontology, geochronology, geochemistry, 62 pp. (6 articles), 1999. 150.00

185 Greenland from Archaean to Quaternary. Descriptive text to the Geological map of Greenland, 1:2 500 000, 93 pp., 2000. *By* N. Henriksen, A.K. Higgins, F. Kalsbeek & T.C.R. Pulvertaft. 225.00

186 Review of Greenland activities 1999, 105 pp. (13 articles), 2000. *Edited by* P.R. Dawes & A.K. Higgins. 225.00

187 Palynology and deposition in the Wandel Sea Basin, eastern North Greenland, 101 pp. (6 articles), 2000. *Edited by* L. Stemmerik. 160.00

188 The structure of the Cretaceous–Palaeogene sedimentary-volcanic area of Svartenhuk Halvø, central West Greenland, 40 pp., 2000. *By* J. Gutzon Larsen & T.C.R. Pulvertaft. 130.00

189 Review of Greenland activities 2000, 131 pp. (17 articles), 2001. *Edited by* A.K. Higgins & K. Secher. 160.00

190 The Ilímaussaq alkaline complex, South Greenland: status of mineralogical research with new results, 167 pp. (19 articles), 2001. *Edited by* H. Sørensen. 160.00

191 Review of Greenland activities 2001, 161 pp. (20 articles), 2002. *Edited by* A.K. Higgins, K. Secher & M. Sønderholm. 200.00

Geology of Denmark Survey Bulletin (discontinued)

36 Petroleum potential and depositional environments of Middle Jurassic coals and non-marine deposits, Danish Central Graben, with special reference to the Søgne Basin, 78 pp., 1998. *By* H.I. Petersen, J. Andsbjerg, J.A. Bojesen-Koefoed, H.P. Nytoft & P. Rosenberg. 250.00

37 The Selandian (Paleocene) mollusc fauna from Copenhagen, Denmark: the Poul Harder 1920 collection, 85 pp., 2001. *By* K.I. Schnetler. 150.00

Prices are in Danish kroner exclusive of local taxes, postage and handling

Note that information on the publications of the former Geological Survey of Denmark and the former Geological Survey of Greenland (amalgamated in 1995 to form the present Geological Survey of Denmark and Greenland) can be found on the Survey's website: *www.geus.dk*